THE UNIVERSITY OF ALBERTA

A STUDY OF THE NORTH AMERICAN CENTRAL PLAINS CONDUCTIVITY ANOMALY

by

[illegible]

A THESIS

[illegible]

IN PARTIAL FULFILLMENT OF THE REQUIREMENTS FOR THE DEGREE

OF DOCTOR OF PHILOSOPHY

DEPARTMENT OF PHYSICS

EDMONTON, ALBERTA.

FALL, 1970

THE UNIVERSITY OF ALBERTA

FACULTY OF GRADUATE STUDIES AND RESEARCH

The undersigned certify that they have read, and recommend to the Faculty of Graduate Studies and Research for acceptance, a thesis entitled "A Study of the North American Central Plains Conductivity Anomaly," submitted by Adeniyi Olurami Alabi in partial fulfilment of the requirements for the degree of Doctor of Philosophy in Geophysics.

Supervisor

External Examiner

Date [illegible]

ABSTRACT

A two-dimensional array of 42 magnetometers were operated in the summer of 1972, jointly by the University of Alberta and the Earth Physics Branch of the Department of Energy, Mines and Resources, Government of Canada in the North American Central Plains. The array of 34 Gough-Reitzel magnetometers and 17 three-component fluxgate magnetometers was designed to secure an improved knowledge of the narrow conducting zone observed near the eastern edge of a previous magnetometer array study in 1969. The magnetograms from the 34 Gough-Reitzel magnetometers were digitized on a flying-spot optical scanner designed and built in the University of Alberta. The production of the editing computer programs was a contribution of the writer. These programs were used in processing the data from the present array study.

Four polar substorm events and two worldwide events have been analyzed for detailed study. Visual examination of magnetograms has revealed the presence of a linear conductive body extending from latitude 52°N to about 50°N for the substorm events and as far north as 54°N for the worldwide magnetic disturbances. The large amplitude of the eastward horizontal fields and the Pegish southward decay of the northward component of the substorm fields were consistent with a three-dimensional source field in which the disturbed field signal currents are mainly responsible for the eastward field. Fourier

transforms of the events yield coefficients of adequate amplitudes in the period range 11 to 170 minutes. Maps of the horizontal polarization ellipses at the stations of the array give a clear distinction between the more uniform source fields of world-wide disturbances and the localized substorm fields near the auroral zone. Fourier maps at eight periods provide more precise definition of the linear conductive body especially in the eastward horizontal and vertical amplitude maps and I phase maps. North of latitude 69°N the use of a form of residual Fourier maps was found effective in isolating the induction anomaly from the masking effect of the substorm source fields. Transfer functions plotted as induction arrows on the array map show evidence of the anomaly extending across the whole length of the array in the quadrature-phase induction arrows at period 68 minutes near midnight in the substorm/aurora. Amplitude profiles of normalized transfer functions eastward and vertical fields show peaks in excess of those that can be accounted for by the induction generated alone. This requires the channelling of increased induced in conductive regions outside the array.

The major fields in the eastward component of the vertical transfer function should lie in line with the conductive body, and this suggests an association of the conductive sink feeding in the basement under the Paleozoic sediments. These earth-motion have occurred in a generally easterly region of southern Saskatchewan since 1969, with epicentres near the conductive

body. It is possible that the basement faults are still active. The actual nature of the conductor could be a graphite schist in a metamorphic belt preserved between faults, or intrusives of hydrated ultramafic rocks along the fault zone may be responsible.

Southwest of the Black Hills the North American Central Plains magnetic variation anomaly overlaps that due to the upper mantle conductor under the Southern Rockies. It is probable that a nearly vertical link through the lower crust here joins the crustal, compositional conductor and the upper mantle partial-melting thermal conductor.

ACKNOWLEDGEMENTS

I must thank first and foremost my thesis supervisor, Professor D. I. Gough for his guidance and encouragement at all phases of this research. Studying under him has not only been very inspiring but has also given me the rare opportunity of participating in observational studies of various other regions of the world. I am indeed grateful for these.

I owe many thanks to my partner in this project, Dr. F. W. Camfield of the Earth Physics Branch EMR Ottawa. On several occasions he has been kind enough to keep me from deviating from the correct paths on critical phases of this work.

I happy to thank Dr. Don Kiyan and Dr. D. Thomson of the Physics Department, University of Alberta. The former for useful discussions on the nature of the sources of geomagnetic variations and the latter for discussion on induction problems and for the use of his program of a line-current model of the auroral electrojet. Dr. Rosemary Hutton of the University of Edinburgh introduced me to induction studies and has given me continuing encouragement since. I am deeply grateful.

My further thanks go to those who assisted at various stages of the work. To Messrs. John Davies and Johan de Beer and to Dr. W. G. Fraser for sharing the driving and assisting in other ways during the field trips.

This project has been funded by the National Research Council and the Department of Energy, Mines and Resources of the Government of Canada. Additional thanks are due to the University of Alberta for supporting me financially through a Graduate Teaching assistantship.

I dearly thank my wife for her patience and understanding for my absence during most of the period this work was done.

The excellent typing of Mrs. M. Mahl is appreciated with many thanks.

TABLE OF CONTENTS

	PAGE
ABSTRACT	iv
ACKNOWLEDGEMENTS	vii
LIST OF TABLES	xii
LIST OF FIGURES	xiii
CHAPTER I GEOMAGNETIC DEPTH SOUNDING AND MAGNETOMETER ARRAY STUDIES	1
1.1 Introduction	1
1.2 Radial Distribution of Electrical Conductivity	4
1.3 Electromagnetic Induction in a Stratified Plane Conductor	7
1.4 Electrical Conductivity Anomalies	16
1.5 Geomagnetic Depth Sounding: Linear Array Method	17
1.6 Transfer Functions and Induction Arrows	20
1.7 Two-Dimensional Array Studies	25
CHAPTER II A CONTRIBUTION IN PROCESSING MAGNETOMETER ARRAY DATA	35
2.1 Introduction	35
2.2 The Film Scanner	39
2.3 The Film Scanner/PDP-11 System	42
2.4 An Introduction to the Editing Programmes	46
2.5 The Programme Package: AUTO-EDIT	49

PAGE

2.6 The Programme Package: SEMI-AUTO 56

2.7 Comments on the Present System 67

CHAPTER III THE NORTH AMERICAN CENTRAL PLAINS ANOMALY 68

. . . . . .

3.1 The 1967 Magnetometer Array Study . . . 68

3.2 The 1969 Magnetometer Array Study . . . 77

CHAPTER IV THE ARRAY STUDY OF 1972 88

4.1 The Observations 88

4.2 Magnetograms 91

4.2.1 The Event of August 28, 1972 94

4.2.2 The Event of August 30, 1972 104

4.2.3 The Event of August 31, 1972 114

4.2.4 The Event of September 08, 1972 . . . 123

4.2.5 The Event of September 12, 1972 . . . 133

4.2.6 The Event of September 13, 1972 . . . 146

4.3.1 The Fourier Spectra 153

4.3.2 The Polarization of the Horizontal Field 163

4.3.3 The Fourier Transform Maps 171

4.3.4 Residual Fourier Coefficient Maps . . 191

4.4 Transfer Functions 202

CHAPTER V THE NATURE OF THE CONDUCTIVE ZONE UNDER THE NORTH AMERICAN CENTRAL PLAINS 209

5.1 Depth Estimates for the Conducting Zone Under the Central Plains 209

PAGE

5.2 Possible Association of N.A.C.P. Anomaly with other Geophysical Observations . . 222

5.3 Suggestions for Future Array Studies . 228

REFERENCES 231

APPENDICES 240

APPENDIX A: Locations and the Names of the Magnetometer Stations 241

B: The Source of Polar Magnetic Substorm Fields 245

LIST OF TABLES

TABLE		PAGE
4.1	The dates, times of occurrence and types of disturbance events	92
4.2	The positions of the Stations whose amplitude spectra are illustrated in Figs. 4.9-4.11. . .	161
4.3	Periods at which the spectral peaks for the events occur	162
5.1	Maximum depths to the line current and the locations of its axis at various latitudes . .	220

LIST OF FIGURES

FIGURE		PAGE
1.1	An N-layered earth model	10
2.1	A section of Gough-Reitzel magnetometer record	37
2.2	The basic hardware components of the optical flying-spot scanner	41
2.3	Block diagram illustrating the operation of the scanning system	45
2.4	Records that can be edited with the programme AUTO-EDIT	48
2.5	Samples of records in which traces tangle and cross-over	51
2.6	A flow diagram showing the processing steps involved in programme AUTO-EDIT	53
2.7	The flow diagram of programme SEMI-AUTO . . .	59
2.8	The division of the graphic terminal screen into zones anda sample of designated points on a trace	64
3.1	The stations of 1967 and 1969 studies	70
3.2	The amplitude and phase maps of the unseparated field of a substorm at 30 minutes period . . .	73
3.3	Conductive models which fit normalized anomalous fields recorded by the 1967 array	76
3.4	The location of stations operated in the 1969 array plotted on simplified tectonic map . . .	79
3.5	Fourier spectral maps at period 47.6 minutes .	82
3.6	Profiles of the normalized anomalous fields across the Black Hills uplift	85
4.1	The location of the stations in the 1972 array drawn on a simplified tectonic map	90

FIGURE		PAGE
4.3a	Magnetograms for the substorm of August 30, 1972, lines 1 and 2	98
4.3b	Magnetograms for the substorm of August 30, 1972, lines 3 and 4	98
4.3c	Magnetograms for the substorm of August 30, 1972, lines 5 and 6	100
4.3d	Magnetograms for the substorm of August 30, 1972, lines 7 and 8	102
4.3a	Magnetograms for the substorm of August 30, 1972, lines 1 and 2	106
4.3b	Magnetograms for the substorm of August 30, 1972, lines 3 and 4	108
4.3c	Magnetograms for the substorm of August 30, 1972, lines 5 and 6	110
4.3d	Magnetograms for the substorm of August 30, 1972, lines 7 and 8	112
4.4a	Magnetograms for the substorm of August 31, 1972, lines 1 and 2	116
4.4b	Magnetograms for the substorm of August 31, 1972, lines 3 and 4	118
4.4c	Magnetograms for the substorm of August 31, 1972, lines 5 and 6	120
4.4d	Magnetograms for the substorms of August 31, 1972, lines 7 and 8	122
4.5a	Magnetograms for the pulsation of September 08, 1972, lines 1 and 2	125
4.5b	Magnetograms for the pulsation of September 08, 1972, lines 3 and 4	127
4.5c	Magnetograms for the pulsation of September 08, 1972, lines 5 and 6	129
4.5d	Magnetograms for the pulsation of September 08, 1972, lines 7 and 8	131

FIGURE		PAGE
4.6a	Magnetograms for the substorm of September 12, 1972, lines 1 and 2	135
4.6b	Magnetograms for the substorm of September 12, 1972, lines 3 and 4	137
4.6c	Magnetograms for the substorm of September 12, 1972, lines 5 and 6	139
4.6d	Magnetograms for the substorm of September 12, 1972, lines 7 and 8	141
4.7a	Magnetograms for the disturbance event of September 13, 1972, lines 1 and 2	144
4.7b	Magnetograms for the disturbance event of September 13, 1972, lines 3 and 4	146
4.7c	Magnetograms for the disturbance event of September 13, 1972, lines 5 and 6	148
4.7d	Magnetograms for the disturbance event of September 13, 1972, lines 7 and 8	150
4.8	The approximate location of the North American Central Plains conductor	152
4.9	Fourier amplitude spectra in the period range 20-180 minutes for the substorm of August 28, 1972 for four normal stations	155
4.10	Fourier amplitude spectra in the period range 20-180 minutes for the substorm of August 30, 1972 for four normal stations	157
4.11	Fourier amplitude spectra in the period range 20-120 minutes for the event of September 13, 1972 for four normal stations	159
4.12	Horizontal polarization ellipses for the substorm events	167
4.13	Horizontal polarization ellipses for the world-wide magnetic disturbances	169
4.14	Fourier amplitudes (in gammas) and phases (in minutes) at period 26.6 minutes from the magnetic polar substorm of September 12, 1972.	174

FIGURE		PAGE
4.13	Fourier amplitudes (in gammas) and phases (in minutes) at period 68.3 minutes from the magnetic polar substorm of August 28, 1972.	178
4.14	Fourier amplitudes (in gammas) and phases (in minutes) at period 78.8 minutes from the magnetic polar substorm of August 30, 1972.	180
4.15	Fourier amplitude (in gammas) and phases (in minutes) at period 170.7 minutes from the magnetic polar substorm of August 31, 1972.	182
4.16	Fourier amplitudes (in gammas) and phases (in minutes) at period 13.3 minutes from the pulsation event of September 08, 1972.	183
4.19	Fourier amplitudes (in gammas) and phases (in minutes) at period 25.6 minutes from the magnetic disturbance event of September 13, 1972.	184
4.20	Fourier amplitudes (in gammas) and phases (in minutes) at period 31.5 minutes from the pulsation event of September 08, 1972.	186
4.21	Fourier amplitudes (in gammas) and phases (in minutes) at period 36.6 minutes from the magnetic disturbance event of September 13, 1972.	188
4.22	Residual Fourier coefficient maps at period 26.6 min.	194
4.23	Residual Fourier coefficient maps at period 68.3 min.	196
4.24	Residual Fourier coefficient maps at period 170.7 min.	198
4.25	The location of N.A.C.P. conductive body.	201
4.26	The induction arrows at period 68.3 min. as in-phase and quadrature phase components.	204
4.27	The induction arrows at period 78.8 min. as in-phase and quadrature phase components.	206
5.1	Normalized anomalous eastward (Y_a/Y_n) and vertical (Z_a/Y_n) amplitude profiles at latitude 43.8°N.	212

FIGURE		PAGE
3.3	Normalised anomalous eastward (T_A/T_n) and vertical (Z_A/T_n) amplitude profiles at latitude 46.6°N.	214
3.4	Normalised anomalous eastward (T_A/T_n) and vertical (Z_A/T_n) amplitude profiles at 41.8°N.	216
3.5	Normalised anomalous eastward (T_A/T_n) and vertical (Z_A/T_n) amplitude profiles at latitude 48°N.	218
3.6	Map of Saskatchewan showing the M.A.C.P. conductive body and the epicentres of the 3 earthquakes recorded in this region.	227
B-1	An illustration of a three-dimensional current system responsible for the polar substorm fields.	247
B-2	The standard observatories whose magnetograms were examined for the classification of the six magnetic events.	250

CHAPTER 1

GEOMAGNETIC DEPTH SOUNDING AND MAGNETOMETER ARRAY STUDIES

1.1 Introduction

Geomagnetic depth sounding uses mapping of three orthogonal components of the time-varying part of the geomagnetic field to obtain information about conductivity distribution in the earth. The time varying magnetic fields have primary sources outside the earth. The fields diffuse through the Earth which is more or less a conductor to induce currents and produce secondary fields. The basic equations for geomagnetic depth sounding theory are the four Maxwell's equations. In MKSA units these are:

$$\text{Curl } \vec{H} = \vec{J} + \partial\vec{D}/\partial t \qquad (1.1a)$$

$$\text{Curl } \vec{E} = -\partial\vec{B}/\partial t \qquad (1.1b)$$

$$\text{Div } \vec{B} = 0 \qquad (1.1c)$$

$$\text{Div } \vec{E} = \rho \qquad (1.1d)$$

where

$\vec{H}$ is the magnetic field

$\vec{J}$ is the current density

$\vec{D}$ is the electric induction

$\vec{B}$ is the magnetic induction

ρ is the electric charge density

In an isotropic medium the following constitutive relations hold

$$\vec{D} = \epsilon \vec{E} \tag{1.2a}$$

$$\vec{B} = \mu \vec{H} \tag{1.2b}$$

$$\vec{J} = \sigma \vec{E} \tag{1.2c}$$

where

ϵ is the dielectric constant

μ is the magnetic permeability

σ is the electric conductivity

For the slowly-varying fields of periods approximately 100 seconds used in geomagnetic depth sounding, the displacement current $\frac{\partial \vec{D}}{\partial t}$ in (1.1a) is negligible compared with $\vec{J}$. By taking the curl of (1.1a) and using (1.1b) and the constitutive relations (1.2a), (1.2b) and (1.2c) to eliminate $\vec{E}$ Maxwell's equations reduce to the diffusion (or induction) equation

$$\nabla^2 \vec{H} = \sigma \mu \frac{\partial \vec{H}}{\partial t} \tag{1.3a}$$

Similarly by taking curl of (1.1b) and using (1.1a), (1.2a), (1.2b) and (1.2c) to eliminate $\vec{H}$, the diffusion equation is then

$$\nabla^2 \vec{E} = \sigma \mu \frac{\partial \vec{E}}{\partial t} \tag{1.3b}$$

Tozer (1959) showed that deep in the ground μ is close to μ_o ($= 4\pi.10^{-7}$H/m). Therefore, the diffusion equation

is dependent only on the period of the field and the electrical conductivity.

Outside the Earth, the conductivity of air is negligible so that

$$\nabla^2 \vec{H} = 0 \tag{1.4}$$

This implies that $\vec{H}$ is derivable from a scalar potential Ω which satisfies Laplace's equation.

$$\nabla^2 \Omega = 0 \tag{1.5}$$

and

$$\vec{H} = -\text{grad } \Omega \tag{1.6}$$

The diffusion of the primary field into the Earth is controlled by skin depth given by

$$\delta = \sqrt{\frac{2}{\omega \mu_o \sigma}} \tag{1.7}$$

where ω is the frequency of the inducing field.

This defines the depth beneath the plane surface of a uniform conducting half-space where the amplitude of the primary field falls to 1/e of its surface value. The skin depth decreases as the conductivity increases and as the period decreases. Skin depths of geophysical relevance vary from 10km for a field of period 5 minutes incident on saline sediments of conductivity 1 $(\text{ohm m})^{-1}$, to > 4,000 km for period 24 hours and conductivity 10^{-3} $(\text{ohm m})^{-1}$ (dry crystalline rocks at crustal temperatures). However, in the

depth range 400 - 700 km the conductivity rises steeply to values in excess of 1 (ohm m)$^{-1}$, so that even storm-time fields which include periods of several days do not reach 1,000 km depth with significant amplitude. This limits geomagnetic depth sounding to depths less than 1,000 km.

1.2 Radial Distribution of Electrical Conductivity

In a conducting medium use can be made of the magnetic vector potential $\vec{A}$ such that

$$\vec{B} = \text{curl } \vec{A} \tag{1.8}$$

and

$$\text{Div } \vec{A} = 0 \tag{1.9}$$

If one takes the curl of (1.8) and uses (1.2b) and (1.9) and the fact that

$$\vec{E} = -\frac{\partial \vec{A}}{\partial t} \tag{1.10}$$

together with the assumption that free charges are not present within the conductor, one finds

$$\nabla^2 \vec{A} = \sigma \mu \frac{\partial \vec{A}}{\partial t} \tag{1.11}$$

In the air, the magnetic potential Ω satisfies $\nabla^2 \Omega = 0$. It can be represented in terms of spherical harmonics which are solutions of Laplace's equation. The harmonic of degree n and order m is given by

$$\Omega_n^m = \left\{ e_n^m \left(\frac{r}{R}\right)^n + i_n^m \left(\frac{r}{R}\right)^{-n-1} \right\} P_n^m (\cos \theta)\, e^{im\phi} \tag{1.12}$$

where

θ is the colatitude

ϕ is the longitude

R is the earth's radius

e_n^m and i_n^m are functions of time only. They are amplitudes of the external and internal fields respectively. $P_n^m(\cos\theta)$ is the associated Legendre function of degree n order m.

Inside the conductor, solution of (1.11) is the sum of such terms as

$$\vec{A}_n^m = R(\vec{r} \times \text{grad } P_n^m(\cos\theta)\, e^{im\phi})\, f_n^m(r) \qquad (1.13)$$

$\vec{r}$ denotes the vector from origin of a sphere to point (r,θ,ϕ) in spherical coordinates.

$f_n^m(r)$ satisfies the radial induction equation

$$\frac{\partial}{\partial r}\left(r^2 \frac{df_n^m(r)}{\partial r}\right) = n(n+1)f_n^m(r) + \mu_o\sigma(r)\, r^2 \frac{\partial f_n^m(r)}{\partial t} \qquad (1.14)$$

Equation (1.14) is solved for $f_n^m(r)$. By using the boundary conditions that the tangential components of $\vec{E}$ and $\vec{H}$ are continuous at the surface of the sphere, the response function S_n^m is obtained. It is assumed that in the earth, conductivity varies only radially. The response function defined as

$$S_n^m = i_n^m / e_n^m \qquad (1.15)$$

gives the surface ratio of internal to external fields for

the assumed model. This is compared with internal to external fields ratio obtained from observational data.

Schuster (1889) used the concepts outlined above to show that about 1/3 of the observed field of quiet time daily variation (S_q) is due to induction in the solid earth.

Chapman and Whitehead (1923) computed the response functions for the earth's model containing a uniformly conducting core surrounded by an insulating layer of thickness about 250 km, the insulating layer itself being covered by a highly conducting ocean everywhere of thickness about 1/4 km. The response functions fitted very well for the observed surface ratio of internal to external parts of the S_q field. Chapman and Price (1930) computed response functions of similar models for magnetic storm data.

Lahiri and Price (1939) obtained an analytic solution for equation (1.14) for a model in which the electrical conductivity is an arbitrary power of the radius. They fitted the reponse function to storm time and quiet time variation fields. The major features of their model are as follows:

(1) The electrical conductivity varies slowly from a value of 0.001 $(\text{ohm m})^{-1}$ near the earth's surface to about 0.2 $(\text{ohm m})^{-1}$ at a depth of about 400 km.

(2) Between 400 and 800 km, the conductivity increases rapidly with depth.

Rikitake (1950a,b) employed spherical harmonic methods to fit response functions to short period magnetic field data

such as the bay and s.f.e. He found that the first 400 km layer of the earth is far from being electrically homogeneous.

The steep rise, at depth between 400 and 800 km, in the electrical conductivity is consistent with other geophysical data and laboratory experiments on ultrabasic silicates at high temperatures and pressures. At a depth of 400 km, there is a rapid rise in seismic wave velocities often associated with a phase change to a spinel form of olivine. A second seismic-velocity discontinuity near 650 km may be associated with further phase changes to close-packed oxides (Anderson, 1967).

The spherical harmonic methods outlined above are not suitable for the study of the electrical conductivity distribution with position on the earth in a limited region. Too many harmonics would be needed to represent the field. For regional studies, the earth is usually considered as a half-space of variable conductivity. In the next section, the case of a plane layered earth is considered.

1.3 Electromagnetic Induction in a Stratified Plane Conductor

The theory of electromagnetic induction as developed by Price (1950, 1962) makes it possible to compute the ratio (normal/tangential) magnetic field components at the plane surface of an N-layered conductor. Starting from Maxwell's field equations and the diffusion equation a recurrence relation is derived by a method given by Price (1962). The nature of

the problems involved in such induction studies will be demonstrated for the case of a simple two-layered earth model.

Consider an N-layered conductor in which the conductivity and the thickness of the n^{th} layer are σ_n and h_n respectively (see Fig. 1.1). Consider a periodic primary field with $\exp(i\omega t)$ time dependence. All the equations are expressed in Cartesian coordinates (x,y,z) with z downward positive.

Price (1962) showed that a solution of the diffusion equation (1.3b) is of the form

$$\vec{E} = e^{i\omega t} Z(z) \vec{F}(x,y) \tag{1.16}$$

where

$$\vec{F}(x,y) = \left(\frac{\partial P}{\partial y}, -\frac{\partial P}{\partial x}, 0\right) \tag{1.17}$$

and $P(x,y)$ satisfies the equation

$$\frac{\partial^2 P}{\partial x^2} + \frac{\partial^2 P}{\partial y^2} + \nu^2 P = 0 \tag{1.18}$$

The parameter ν is a measure of the non-uniformity of the primary field. It is given by

$$\nu = 2\pi/\lambda \tag{1.19}$$

where λ is a linear dimension of the source field. Thus, $\nu = 0$ implies a uniform source. For regional study λ may range between 400 and 40,000 km. The diffusion equation for

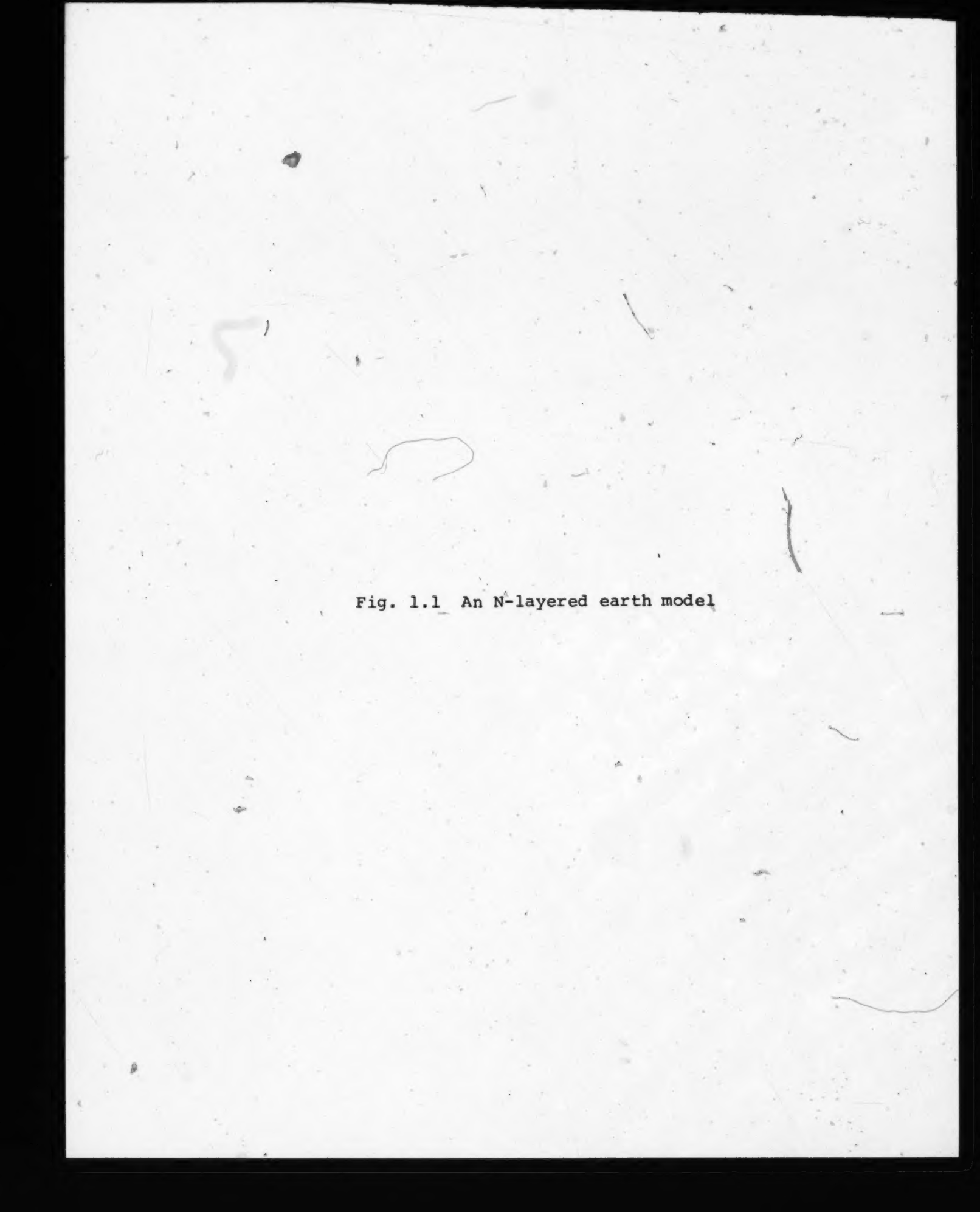

Fig. 1.1 An N-layered earth model

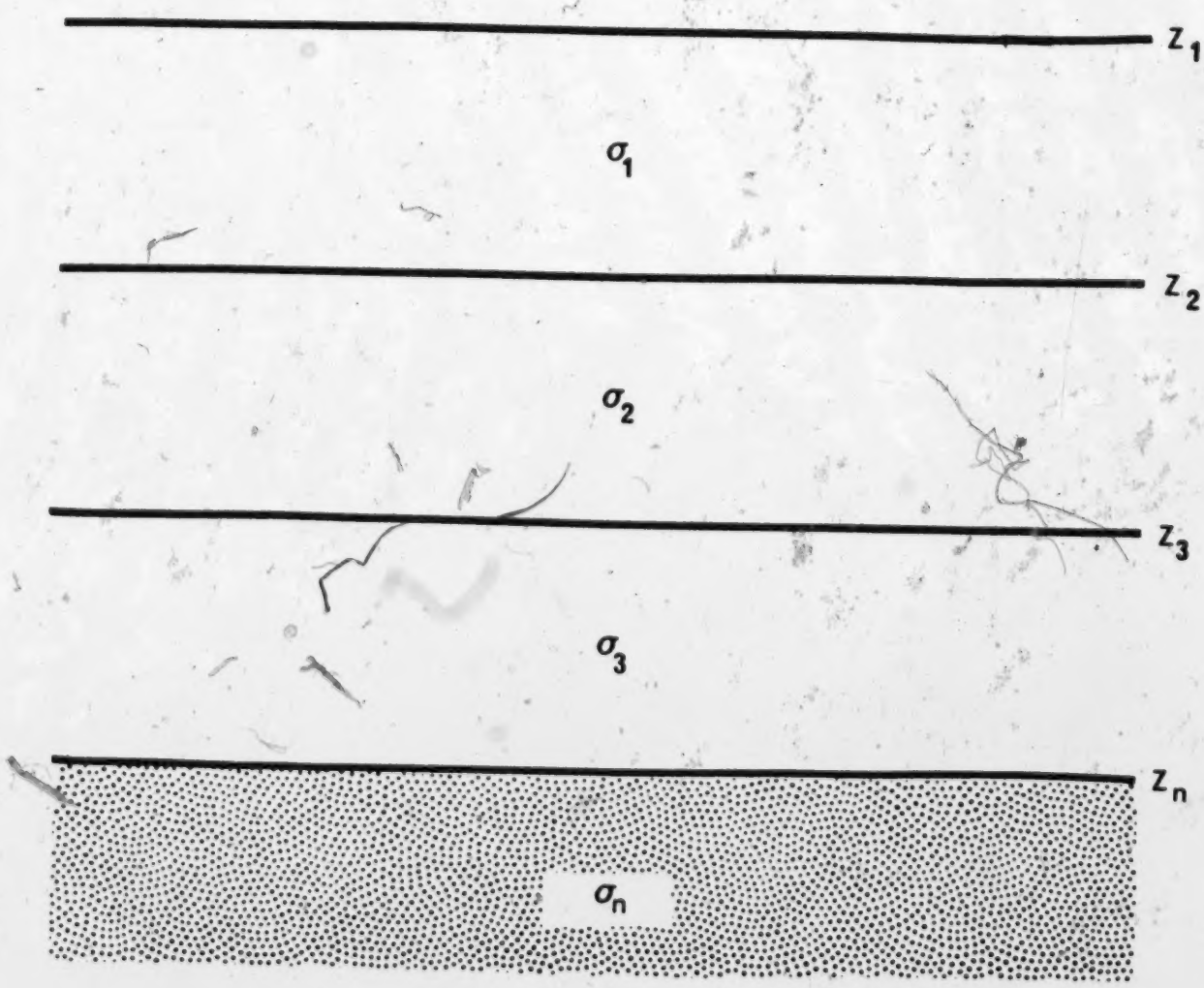
z_1
σ_1
z_2
σ_2
z_3
σ_3
z_n
σ_n

Z is

$$\frac{d^2Z}{dz^2} = \{\nu^2 + i\omega\mu_o\sigma\} Z \qquad (1.20)$$

or

$$\frac{d^2Z}{dz^2} = \beta^2 Z \qquad (1.21)$$

where

$$\beta^2 = \nu^2 + i\omega\mu_o\sigma$$

and

$$\beta = \frac{1}{2}\left[\left\{(\alpha^4 + \nu^4)^{\frac{1}{2}} + \nu^2\right\}^{\frac{1}{2}} + i\left\{ (\alpha^4 + \nu^4)^{\frac{1}{2}} - \nu^2 \right\}^{\frac{1}{2}} \right]^{\frac{1}{2}} \qquad (1.22)$$

writing

$$\alpha^2 = \omega\mu_o\sigma \qquad (1.23)$$

The magnetic field can be obtained from Curl $\vec{E} = -\partial\vec{B}/\partial t$ and is given by

$$i\omega\vec{H} = -\left\{ \frac{\partial Z}{\partial z} \frac{\partial P}{\partial x}, \frac{\partial Z}{\partial z} \frac{\partial P}{\partial y}, \nu^2 ZP \right\} \qquad (1.24)$$

In the n^{th} layer, the solution of equation (1.21) is

$$Z_n = A_n e^{-\beta_n z} + B_n e^{\beta_n z} \qquad (1.25)$$

and

$$\frac{dZ_n}{dz} = -\beta_n\left\{ A_n e^{-\beta_n z} - B_n e^{\beta_n z} \right\} \qquad (1.26)$$

At any interface between layers, the tangential magnetic and electric field intensities are continuous. This implies

$$Z_{n+1}\,(z_{n+1}) = Z_n\,(z_{n+1}) \tag{1.27a}$$

and

$$\frac{dZ_{n+1}}{dz}\,(z_{n+1}) = \frac{dZ_n}{dz}\,(z_{n+1}) \tag{1.27b}$$

Schmucker (1970) defined a vertical function $G_n(z)$ as

$$G_n\,(z) = \frac{A_n e^{-\beta_n z} - B_n e^{\beta_n z}}{A_n e^{-\beta_n z} + B_n e^{\beta_n z}} \tag{1.28}$$

The continuity conditions (1.27a) and (1.27b) for the interface between the n^{th} and $(n+1)^{th}$ layer imply

$$\beta_n\, G_n\,(z_{n+1}) = \beta_{n+1}\, G_{n+1}\,(z_{n+1}) \tag{1.29}$$

By eliminating A_n and B_n from $G_n\,(z)$ and using (1.25) and (1.26) we have

$$G_n(z) = \frac{G_n(z_n) - \tanh \beta_n\,(z-z_n)}{1 + G_n\,(z_n)\ \tanh \beta_n\,(z - z_n)} \tag{1.30}$$

where

$$z_n \leq z \leq z_{n+1}$$

If we set $z = z_{n+1}$ then

$$G_n(z) = \frac{c_{n+1} - \beta_n \tanh\,(\beta_n h_n)}{\beta_n + c_{n+1} \tanh\ \beta_n h_n} \tag{1.31}$$

where

$$c_{n+1} = \beta_{n+1} G_{n+1} (z_{n+1}) \qquad (1.32)$$

Starting form the bottom (N^{th}) layer with $G_N (z_N) = 1$, the recurrence relation (1.31) is used for successive substitution ending with a value of G_1 ($z_1 = 0$). In this way the surface values for an N-layered earth can be obtained.

To gain some insight into the general features of electromagnetic induction, a two-layered earth model is considered here. It consists of a non-conducting top layer of thickness h underlain by a conducting layer with conductivity σ.

The two layered earth model. The surface ratio $(Z/\sqrt{X^2 + Y^2})$ of the vertical component to the horizontal field is denoted by Z/H. From (1.24) this is given by

$$Z/H + = (\nu^2 Z/\frac{\partial Z}{\partial z}) \; P(x,y,\nu) \left[\left\{ \frac{\partial P(x,y,\nu)}{\partial x} \right\}^2 + \left\{ \frac{\partial P(x,y,\nu)}{\partial y} \right\}^2 \right]^{-1/2} \qquad (1.33)$$

which from the definition of vertical function (1.28), (1.25) and (1.26) becomes

$$Z/H = - \nu^2 \frac{1}{\beta, G, (z,)} \Phi (x,y, \nu) \qquad (1.34)$$

where

$$\Phi (x,y,\nu) = P(x,y,\nu) \left[\left\{ \frac{\partial P(x,y,\nu)}{\partial x} \right\}^2 + \left\{ \frac{\partial P(x,y,\nu)}{\partial y} \right\}^2 \right]^{-\frac{1}{2}} \qquad (1.35)$$

For two-layered model in which the first layer has a thickness smaller than spatial wavelength of the source field in which the skin depth in the second layer is small compared with its thickness, Schmucker (1970) showed the surface function to be

$$G_1(z_1) = \frac{\beta_2}{\nu(1+\beta_2 h)} \tag{1.36}$$

and β_2 to be

$$\beta_2 \simeq (1 + i)/\delta_2 \tag{1.37}$$

where δ_2 is the skin depth in the second layer. By substituting (1.36) and (1.37) into (1.34), we have

$$\frac{Z}{H} = -\nu^2\left\{(h + \frac{1}{2}\delta_2) - i\,\frac{1}{2}\delta_2\right\}\Phi(x,y,\nu) \tag{1.38}$$

where the parameter

$$\delta_2 = \sqrt{\frac{2}{\omega\mu_o\sigma}} \tag{1.39}$$

In geomagnetic depth sounding Z/H forms an important diagnostic parameter. The effects of the source field distribution and source field non-uniformity on this ratio are implied in equation (1.38). The following features of Z/H are demonstrated by (1.38).

(1) The wave number ν of the source field affects Z/H.

(2) The amplitude and phase of Z/H depend on the depth h of the conducting layer and on the conductivity of the bottom layer. When the bottom layer is a super conductor ($\sigma \to \infty$) and close to the surface $Z/H \to 0$. In the limit the induced vertical field cancels out the inducing field. Price (1950) showed that for this case, the induced horizontal field enhances the inducing horizontal field and doubles it in the limit.

(3) The expression (1.38) shows that to use the surface ratio Z/H, a knowledge of the source function $P(x,y, \nu)$ and its gradient is required.

Various workers have used different methods to approximate $P(x,y, \nu)$ from assumed morphology of the source field. Hutton (1969) by assuming a simple cosine function of latitude for $P(x,y, \nu)$ in the equatorial electrojet region, obtained estimates of the layered conductivity distribution suitable for this region. Oni and Alabi (1972) working in the same region, evaluated $P(x,y, \nu)$ from observed time-varying telluric and magnetic measurements. Peltier and Hermance (1971) obtained integral expressions for the magneto-telluric fields of a Gaussian electrojet. This is applicable to studies in both the equatorial and auroral electrojet regions. Weaver (1973) outlined the use of magnetic and electric Hertz potentials for computing surface magnetic field ratios for any layered earth model.

The use of the 'array' methods to some extent eases the problem of finding the field function $P(x,y,\nu)$ for the fitting of layered structure to 'normal' Z/H ratios (Schmucker, 1970). However, the principal use of an array is to study lateral variations in conductivity.

In an array, a number of magnetometers are operated simultaneously. The type of variation events used are polar magnetic substorms and other disturbance variations. These are known to have long spatial wavelength λ in midlatitudes, with mainly latitudinal variation. If the magnetometers of an array are arranged on east-west profiles, the stations of a profile may show little variability in amplitude or phase. Any significant variability is then usually associated with a conductivity anomaly in the Earth below the region of the array. Two types of array, 'linear' and 'two-dimensional' arrays may be distinguished. Through array studies a number of inhomogeneities in the local distribution of the electrical conductivity have been located in different parts of the world. Some observed types of conductivity anomalies will be briefly described and array methods will then be considered.

1.4 Electrical Conductivity Anomalies

Schmucker (1964) classified conductivity anomalies into surface anomalies, intermediate anomalies and deep anomalies. Surface anomalies are often associated with saline water in the top few kilometres of porous rock, and deep anomalies with thermal and/or melting effects in the upper

mantle. Studies such as those of Whitham (1964) and Camfield, Gough and Porath (1971) have discussed anomalies best explained in terms of current concentration under the anomaly by a conductive body joining regions of induction elsewhere (Whitham, 1964; Dyck and Garland, 1969; Gough 1973). It is convenient to regard such current channelling effects as a fourth type of anomaly. Such anomalies may be associated with conductive bodies up to several thousands of kilometres in dimension.

The observed time-varying geogmagnetic field $\vec{H}(t)$ at a particular point may be regarded as being made up of a normal part $\vec{H}_n(t)$ and anomalous part $\vec{H}_a(t)$. For dealing with local anomalies it is convenient to define $\vec{H}_n(t)$ as due to the source field and the field of currents induced in the 'normal' stratified conductive earth. The anomalous part is due to induction and current concentration in a local conductive body

$$\vec{H}(t) = \vec{H}_n(t) + \vec{H}_a(t) \qquad (1.40)$$

1.5 Geomagnetic Depth Sounding: Linear Array Method

In a linear array, seven magnetometers or less may be operated simultaneously conveniently on a profile. Schmucker (1964) and later Caner et al. (1967) used this method to locate some conductivity anomalies in the Midwestern United States.

Magnetic disturbances having periods $\simeq$ 1 hour, some of them associated with polar magnetic substorms are commonly used. Qualitative interpretation starts with the visual examination of magnetograms. Any significant differences in the amplitudes or phases may give an approximate location of a conductivity anomaly.

The next step may involve Fourier transformation of the data. The magnetic record is sampled at some constant time interval Δt to obtain time series $(x_0, x_1, \ldots\ldots x_{N-1})$. An event of time duration T gives rise to N data points where $N - 1 = T/\Delta T$. The disturbance events are transient signals and can therefore be Fourier transformed in the finite interval $(-T/2, T/2)$. The discrete Fourier coefficients of the time series may be obtained from

$$x_i = a_o + \sum_{k=1}^{N-1} \left\{ a_k \cos \frac{\pi jk}{N} + b_k \sin \frac{\pi jk}{N} \right\} \quad (1.41)$$

where $j = 0, 1, \ldots\ldots, N-1$. The Fourier cosine and sine amplitude coefficients series are $\{a_0, a_1, \ldots\ldots a_{N-1}\}$ and $\{b_0, b_1, \ldots\ldots, b_{N-1}\}$ respectively.

The magnitude of amplitude A_k and the phase θ_k of the k^{th} component of the Fourier spectra are given respectively by

$$A_k = a_k^2 + b_k^2 \quad (1.42)$$

and

$$\theta_k = \tan^{-1} \left(\frac{b_k}{a_k}\right) \quad (1.43)$$

In the complex number notation the k^{th} component of the Fourier spectra is written as

$$C(k) = a_k + i\, b_k \qquad (1.44)$$

The distribution on the Earth's surface of $C_Z(k)/C_H(k)$ (ratio of Fourier amplitude of the vertical field to the Fourier amplitude of the horizontal field at a frequency k) is an important parameter for investigating lateral variation in the subsurface conductivity. The lower the frequency component, the greater is the depth being probed.

Schmucker (1964, 1970) employed linear magnetometer arrays to locate a number of conductivity anomalies in Midwestern United States. The Rio Grande anomaly near the Mexican border is an example. The well studied Japanese anomaly (Rikitake (1966), Rikitake and Honkura (1973)) and the conductivity anomaly under the Peruvian Andes (Schmucker et al. (1967)) are further examples of anomalies located by linear arrays.

By the use of transfer functions, magnetic variation events (1,2, ..., n) recorded at locations (1,2,....., m) can be combined with events (n+1, ...) recorded at sites (m+1, ...) in the study of conductivity structure. The use of transfer functions will next be outlined.

1.6 Transfer Functions and Induction Arrows

Schmucker (1964, 1970) and Everett and Hyndman (1967) applied the theory of transfer functions to geomagnetic depth sounding. The basic idea is that the anomalous parts of the observed fields are expressible as linear functions of the normal parts. This is a consequence of the linear character of Maxwell's field equations. If the Fourier spectra of X(t), Y(t) and Z(t) are denoted by C(X), C(Y) and C(Z) respectively the transfer functions are given as

$$\begin{bmatrix} C(X_a) \\ C(Y_a) \\ C(Z_a) \end{bmatrix} = \begin{bmatrix} X_x & X_y & X_z \\ Y_x & Y_y & Y_z \\ Z_x & Z_y & Z_z \end{bmatrix} \begin{bmatrix} c(X_n) \\ c(Y_n) \\ c(Z_n) \end{bmatrix} + \begin{bmatrix} C(\delta X) \\ C(\delta Y) \\ C(\delta Z) \end{bmatrix} \qquad (1.45)$$

The 3 x 3 matrix is the transfer functions matrix. Each element of the matrix is a complex number for example, z_x is expressible as

$$z_x = z_x(u) + iz_x(v) \qquad (1.46)$$

where $z_x(u)$ is the real part of z_x and $z_x(v)$ the imaginary part. The last column matrix contains the Fourier spectra of the uncorrelated part (residual) of each field component. The matrix of transfer functions must be determined such that the powers of the residuals S(δX), S(δY) and S(δZ) are minimum. The powers of residuals are defined for example as

$$S(\delta x) = C(\delta X)\, C^{*}(\delta X) \tag{1.47}$$

The asterisk denotes the complex conjugate. Let us consider the third row of (1.45) which can be written as

$$C(\delta Z) = C(Z_a) - z_x C(X_n) - z_y C(Y_n) - z_n C(Z_n) \tag{1.48}$$

If we form the power spectra of residual C(Z) as given in (1.47) and differentiate with respect to the complex transfer function z_x we have

$$\frac{\partial S(\delta Z)}{\partial z_x(u)} = -\left\{C(\delta Z)\, C^{*}(X_n) + C^{*}(\delta Z)\, C(X_n)\right\} \tag{1.49}$$

$$\frac{\partial S(\delta Z)}{\partial z_x(v)} = i\left\{C(\delta Z)\, C^{*}(X_n) - C^{*}(\delta Z)\, C(X_n)\right\} \tag{1.50}$$

The power of the residual being minimal implies

$\frac{\partial S(\delta Z)}{\partial z_x(u)}$ and $\frac{\partial S(\delta Z)}{\partial z_x(v)}$ are both zero.

Hence

$$S(\delta Z X_n) = S(\delta Z Y_n) = S(\delta Z Z_n) = 0 \tag{1.51}$$

This means that the cross-spectra between the residuals and the normal parts X_n, Y_n and Z_n vanish. We define the power S(x) of X(t) and the cross-power S(XY) of X(t) and Z(t) as

$$S(X) = C(x)\, C^{*}(X)/T_o \tag{1.52}$$

$$S(XZ) = S^{*}(ZX) = C(X)\, C^{*}(Z)/T_o \tag{1.53}$$

where T_o is the length of the time series from which the Fourier spectra are computed.

If we form the cross spectra of $C(\delta Z)$ with $C(X_n)$, $C(Y_n)$ and $C(Z_n)$ respectively using the condition given in (1.51) we have

$$\begin{bmatrix} S(Z_a X_n) \\ S(Z_a Y_n) \\ S(Z_a Z_n) \end{bmatrix} = \begin{bmatrix} S(X_n) & S(Y_n X_n) & S(Z_n X_n) \\ S(X_n Y_n) & S(Y_n) & S(Z_n Y_n) \\ S(X_n Z_n) & S(Y_n Z_n) & S(Z_n) \end{bmatrix} \begin{bmatrix} z_x \\ z_y \\ z_z \end{bmatrix} \tag{1.54}$$

by matrix inversion we can find the vertical transfer functions z_x, z_y, and z_z at a particular frequency. This general form of transfer functions (1.54) has hardly been used in geomagnetic depth sounding because in practice it is not usually possible to separate the normal and anomalous fields. Similarly, the horizontal transfer functions x_x, x_y, x_z and y_x, y_y, y_z can be obtained by forming the cross-spectra of $C(\delta X)$ and $C(\delta Y)$ with $C(X_n)$, $C(Y_n)$ and $C(Z_n)$ respectively and by using conditions given in (1.51). Cochrane and Hyndman (1970) however reported difficulties in finding stable horizontal transfer function components. $C(X_a)$ and $C(Y_a)$ are even more difficult to estimate than $C(Z_a)$.

As in other methods of interpretation of the data from arrays of magnetometers, the major problem in computing transfer functions is in making fair estimates of the normal

and anomalous fields. At a normal magnetometer station the vertical component must show no persistent correlation with either X or Y fields. Reliable estimates of transfer functions require the use of a number of events of various polarizations and if possible due to various current sources, which are averaged in obtaining the power and cross-power spectra. Schmucker (1970) showed that when M events are used, the residuals cannot exceed $\{(M-5)/(M-3)\}^{\frac{1}{2}}$. Hence power and cross spectra must be obtained from not less than five events.

Most workers make some simplifying assumptions in computing transfer functions. Firstly, the normal Z_n is assumed to bear no correlation with either X_n or Y_n. Secondly, X_n and Y_n can be replaced by X and Y observed at some stations regarded as normal. These two assumptions may be roughly true in midlatitudes and at normal stations. Hence, approximately, under these assumptions,

$$C(Z_a) = z_x C(X_n) + z_y C(Y_n) + C(\delta Z) \qquad (1.55)$$

at some frequency k. By minimizing $C(\delta Z)$ using the condition given in (1.51) we obtain the vertical transfer functions in the explicit relations

$$z_x = \frac{S(Z_a Y_n)S(Y_n) - S(Z_a Y_n)S(Y_n X_n)}{S(X_n)S(Y_n) - S(Y_n X_n)^2} \qquad (1.56a)$$

$$z_y = \frac{S(Z_a Y_n)S(X_n) - S(Z_a X_n)S(X_n Y_n)}{S(X_n)S(Y_n) - S(Y_n X_n)^2} \qquad (1.56b)$$

Parkinson (1959, 1962) and Wiese (1962) introduced the use of arrows as a convenient method of displaying the anomalous behaviour of the vertical magnetic field with position. Induction arrows form a similarly convenient display of the information contained in computed transfer functions. If we choose $\vec{j}$ and $\vec{k}$ as unit vectors towards geographic north and geographic east at a particular station, the induction arrows are given at any particular frequency as

$$\vec{w}_u = -z_x(u)\vec{j} - z_y(u)\vec{k} \quad \text{(in phase)} \tag{1.57a}$$

$$\vec{w}_v = -z_x(v)\vec{j} - z_y(v)\vec{k} \quad \text{(quadrature phase)} \tag{1.57b}$$

The in-phase arrow is the negative of the vector sum of the real parts of the transfer functions and the quadrature phase arrow is the negative of the vector sum of the imaginary parts of the transfer functions. When the induction arrows are plotted according to the scheme outlined above, the in-phase arrow points towards a conductor in which the current flows in-phase with the normal field. The quadrature arrow points toward a conductor in which the induced current flows in quadrature phase with the normal field. In practice, induced currents will flow at a phase angle between 0 and $\pi/2$ with the normal field, and a given conductor will contribute to both induction vectors.

Schmucker (1970) showed that the degree of statistical significance of the induction vectors can be displayed by a circle of confidence whose radius r is given by

$$r = C(\delta Z)\left[\left|c_u\right|^2 + \left|c_v\right|^2\right]^{\frac{1}{2}} \qquad (1.58)$$

where

$$c(\delta Z) = \left[1 - \frac{z_x S(Z_n X_n) + z_y S(Z_n Y_n)}{S(Z_n)}\right]^{\frac{1}{2}} \qquad (1.59)$$

Schmucker (1964, 1970) made use of transfer functions to obtain first order quantitative interpretations of the anomalies which he observed in the south western United States Rikitake and Honkura (1973) employed transfer functions in similar quantitative interpretation of the Japanese anomaly.

Lilley and Bennett (1973) warned that induction arrows may yield erroneous results when employed in a region where there is ". . . extensive current channelling". This caveat is probably well based but has yet to be tested against an adequate amount of observational data. Some results for the North American Central Plains anomaly, which involves current channelling (Porath et al., 1971) are given later in this thesis.

1.7 Two-Dimensional Array Studies

Gough and Reitzel (1967) developed an inexpensive three-component portable magnetometer which opened the way for simultaneous recording of magnetic variation fields over an area of the order of 10^6 km^2. The array of magnetometers is usually arranged along three or four lines perpendicular to the strike of suspected conductive structures. The spacing

between stations in a line may range between 100 and 250 km if the upper mantle structure is the object of investigation. The spacing between lines may range from 150 km to 250 km. In the existing array studies between 25 and 46 instruments have been operated over a period of several weeks to record a sufficient number of magnetic variation events. Active portions of the magnetic records are selected for analysis and interpretation. The first two-dimensional array studies were made in western North America by the University of Texas at Dallas and the University of Alberta (Reitzel, Gough and Porath, 1970; Porath, Oldenburg and Gough, 1970; Camfield, Gough and Porath, 1971) in the central United States (Porath and Dziewonski 1971) and have been followed by studies in Australia (Lilley and Bennett, 1972; Gough, Lilley and McElhinny, 1972) and in South Africa (Gough, de Beer and van Zijl, 1973).

Quantitative interpretation begins with a visual examination of magnetograms plotted in stacks. Regional conductivity anomalies are exhibited as variation in amplitude or phase for magnetograms observed along a line of stations crossing the anomaly. Maps of Fourier spectral parameters were introduced by Reitzel et al., (1970) as a new form of geophysical anomaly for subsequent interpretation. The selected magnetic variation events are Fourier transformed and amplitudes and phases of the Fourier spectra are selected at periods where the amplitude spectra of the horizontal components

show maximum energy over the whole array. Contour maps are produced for amplitudes and phases or for sine and cosine coefficients of the transforms of field components X, Y, Z. A set of six contour maps is required to represent the field of one variation event at one period.

The Fourier maps represent the vector sum of the normal field and the anomalous field. Before a more refined interpretation of the anomaly can be made, the observed field must be decomposed into normal and anomalous parts.

In regions away from local anomalies, where one dimensional models can be fitted, an estimate of the spatial wave number is required (section 1.3). The amplitude provide such an estimate from the gradients $\frac{\partial X}{\partial x}$ and $\frac{\partial Y}{\partial y}$ which can be read from the maps (Schmucker, 1970; p. 92). As an array covers a small portion of earth, the estimates of the spatial field gradients have limited accuracy, but at least an estimate replaces a guess when an array is used.

Separation of fields into external and internal parts. Magnetic fields observed over part of the Earth are separable into external and internal parts by use of surface integrals. Oldenburg (1969) and Porath, Oldenburg and Gough (1970) used surface integrals to separate fields obtained with two-dimensional magnetometer arrays. The separation formulae follow for the point (x_o, y_o) on the plane.

For the X-component;

$$2\pi\ (X_e - X_i)\Big|_o = -\int_{-\infty}^{\infty}\int_{-\infty}^{\infty} \frac{(x-x_o)Z(x,y)}{\{(x-x_o)^2 + (y-y_o)^2\}^{\frac{3}{2}}}\ dxdy \qquad (1.60)$$

For the Y-component;

$$2\pi\ (Y_e - Y_i)\Big|_o = -\int_{-\infty}^{\infty}\int_{-\infty}^{\infty} \frac{(y-y_o)Z(x,y)}{\{(x-x_o)^2 + (y-y_o)^2\}^{\frac{3}{2}}}\ dxdy \qquad (1.61)$$

For the Z-component;

$$2\pi\ (Z_e - Z)\Big|_o = \int_{-\infty}^{\infty}\int_{-\infty}^{\infty} \frac{(x-x_o)X(x,y) + (y-y_o)Y(x,y)}{\{(x-x_o)^2 + (y-y_o)^2\}^{\frac{3}{2}}}\ dxdy \qquad (1.62)$$

where the observed fields $X = X_e + X_i$, etc. The subscript "e" denotes the external part, "i" the internal part.

The separation can be done for instantaneous fields in the time domain or for a given period in the period domain (Oldenburg (1969), Porath et al., (1970)). The integrations given above are numerically approximated over a square 'summation window' centered at the point (x_o, y_o) where the fields are to be separated. Separation in the period domain is preferable to separation in the time domain as this provides information about the contribution of the induced currents at different periods. Maps of sine and cosine coefficients of the Fourier

spectra are drawn for each magnetic field component. The X- and Y- maps are drawn with interpolation aided by application of the 'curl-free' condition. The separation formulas above are then applied. Near the point of separation the eqns. (1.60) through (1.62) give indeterminate values. Contributions from a small square of side 2a centered at (x_o, y_o) are

$$2\pi (X_e - X_i)_{2a} = -2a \ln \left[\frac{\sqrt{2}+1}{\sqrt{2}-1}\right] \left[\frac{\partial Z}{\partial x}\bigg|_o\right] \tag{1.63}$$

$$2\pi (Y_e - Y_i)_{2a} = -2a \ln \left[\frac{\sqrt{2}+1}{\sqrt{2}-1}\right] \left[\frac{\partial Z}{\partial y}\bigg|_o\right] \tag{1.64}$$

$$2\pi (Z_e - Z_i)_{2a} = -2a \ln \left[\frac{\sqrt{2}+1}{\sqrt{2}-1}\right] \left[\frac{\partial X}{\partial x}\bigg|_o + \frac{\partial Y}{\partial y}\bigg|_o\right] \tag{1.65}$$

Separation of variation fields over a limited portion of the earth has some short-comings. Near the boundaries of the array, separation is less reliable because the fields must be extrapolated outside the array in order to perform the surface integration over the summation window. Further, fields whose dimensions are larger than the dimension of the array are not separable by this method. In the middle latitudes the source fields have dimensions that are larger than the array dimensions and cannot be separated. The

investigator must use personal judgement to divide such unseparated normal fields between the internal and external parts.

Modelling of conductivity anomalies. More quantitative interpretation of conductivity anomalies involve fitting models of conductive structures to the normalized anomalous fields. This can be done by numerical methods. Also analogue models (Dosso, 1966; Dosso and Jacobs, 1968; Hermance, 1968) have been used to gain quantitative knowledge of conductivity structure. In two-dimensional cases it is useful to consider anomalous fields which are E-polarized or H-polarized. In the E-polarized field, the induced currents flow parallel to the infinitely long dimension of the structure. The induced field is also E-polarized. The induced currents of the H-polarized field flow at right angles to the long dimension of the structure and their magnetic fields are not observable at the earth's surface.

Analytic methods of modelling deal with conductors of simple geometrical shapes. d'Erceville and Kunetz (1962) obtained exact solutions for a semi-infinite conductor with a vertical plane of discontinuity. Rankin (1962) solved the problem of a model of a dyke exactly. Weaver (1963) and Weaver and Thomson (1972) produced analytic approximate solution for a non-uniform earth with an overhead line current.

Numerical methods are used for modelling conductors of arbitrary shapes. Three methods have been widely used.

The transmission line analogy method. Madden and Swift (1969) and Wright (1969) produced solution for two-dimensional bodies. Both E- and H- polarization cases were considered. The method rests on analogy between the Maxwell's electromagnetic equations and the transmission line equations. Consider a periodic magnetic field (H_x, H_y, H_z) and electric field (E_x, E_y, E_z). The following field equations hold for H-polarization case

$$\frac{\partial E_y}{\partial x} = i\omega\mu H_z \tag{1.66}$$

$$\frac{\partial E_y}{\partial z} = -i\omega\mu H_x \tag{1.67}$$

$$\frac{\partial H_x}{\partial z} - \frac{\partial H_z}{\partial x} = \sigma E_y \tag{1.68}$$

are analogous to the following two-dimensional transmission line equations.

$$\frac{\partial V}{\partial x} = - Z I_x \tag{1.69}$$

$$\frac{\partial V}{\partial z} = - Z I_z \tag{1.70}$$

$$\frac{\partial I_x}{\partial x} + \frac{\partial I_z}{\partial z} = - YV \tag{1.71}$$

where V, I, Z and Y are the voltage, current impedance and admittance respectively.

The anomalous region to be modelled is divided into cells. The transmission lines equations are written for each corner of the cell. The system of linear equations resulting are solved for the voltage (corresponding to E_y) by matrix inversion.

The finite difference method. Jones and Price (1970) have developed a finite difference method applicable to any two-dimensional conductor. The diffusion equation is decomposed into two parts

$$\nabla^2 f = -\beta^2 f \tag{1.72}$$

$$\nabla^2 g = \beta^2 g \tag{1.73}$$

where either E_x or H_y is given by f + ig. The equations above are expressed in finite difference form at each mesh point. At the boundaries between meshes, the tangential magnetic and electric field components are continuous. By the use of the Gauss-Seidel iterative method, the solutions at the mesh points are iterated until stable convergence is obtained.

The method has been extended to non-uniform source fields over conducting anomalies. Jones and Pascoe (1972) have shown how to use a cubic mesh in modelling three-dimensional bodies. The number of grid points required for this type of problem is always large and hence a rather long computing time is required for convergence to take place. Lines and Jones

(1973) have used the three dimensional modelling techniques to study the induction effects due to island. The cost factor limits the use of three-dimensional modelling.

The finite element method. Coggan (1971) employed the finite element method to model two-dimensional bodies. The method is based on the use of Hamilton's principle to minimize an energy function. The total electromagnetic energy U can be written for example for magnetic field with magnetic sources

$$U = \int_{Vol} \left\{ \frac{1}{2\omega\sigma} \beta^2 H^2 - (\nabla \times \vec{H})^2 + \mu_o \vec{M} \cdot \vec{H} \right\} dv \qquad (1.74)$$

where the integration is over volume, $\beta^2 = \omega\sigma\mu_o$ and $\vec{M}$ is the source magnetic moment.

This equation can be shortly written as

$$U = \int_{vol} f(A)dv \qquad (1.75)$$

The integral is expressed as a known function of G of the N independent variables A_1, ... A_N thus

$$U = G(A_1, A_2, ..., A_N) \qquad (1.76)$$

The minimization of the energy involves

$$\begin{aligned} \frac{\partial G}{\partial A_1} &= 0 \\ &\vdots \\ \frac{\partial G}{\partial A_N} &= 0 \end{aligned} \qquad (1.77)$$

Usually triangular meshes are drawn to cover the region under investigation, with f(A) assumed linear over each mesh. The required values of A_1, A_2, ... A_N of A are obtained at the nodes on solving eq. (1.77) by matrix inversion.

Although the finite element method is more recent than the two other numerical methods just reviewed it has not enjoyed as much popularity as either of them, probably because it is more difficult to apply to problems of interest in geomagnetic depth sounding. All the numerical methods require fine mesh texture for high accuracy. This requirement involves high computing cost, which is not always available.

CHAPTER II

A CONTRIBUTION IN PROCESSING MAGNETOMETER ARRAY DATA

2.1. Introduction

Large arrays of magnetometers produce four time series corresponding to a baseline and three time-varying orthogonal components D (magnetic east), H (magnetic north) and Z (down) at each station of the array. In the array studies by the University of Alberta group magnetometers of the type described by Gough and Reitzel (1967) produce analogue records consisting of dot sequences on 35 mm photographic film. Typical time series 3 hours long for each of five polar magnetic substorms may be required in digitized form at one-minute intervals: substorm data from an array of 40 instruments will thus involve, for the four traces, $40x4x180x5 = 1.44x10^5$ numbers. When the daily variation is studied from records digitized at 15 minute intervals over 5 days, the corresponding data set comprises $40x4x1440x5/15 = 0.768x10^5$ numbers. Some form of automatic analogue-to-digital conversion system is necessary. In addition to the problem of the size of the data set, traces cross over one another on the film and editing is required to sort them.

A short section of a record from a Gough-Reitzel magnetometer is shown in Fig. 2.1. The dots are spaced 10

Fig. 2.1. A section of Gough-Reitzel magnetometer record. Note the five traces. Hour marks are also shown on this diagram.

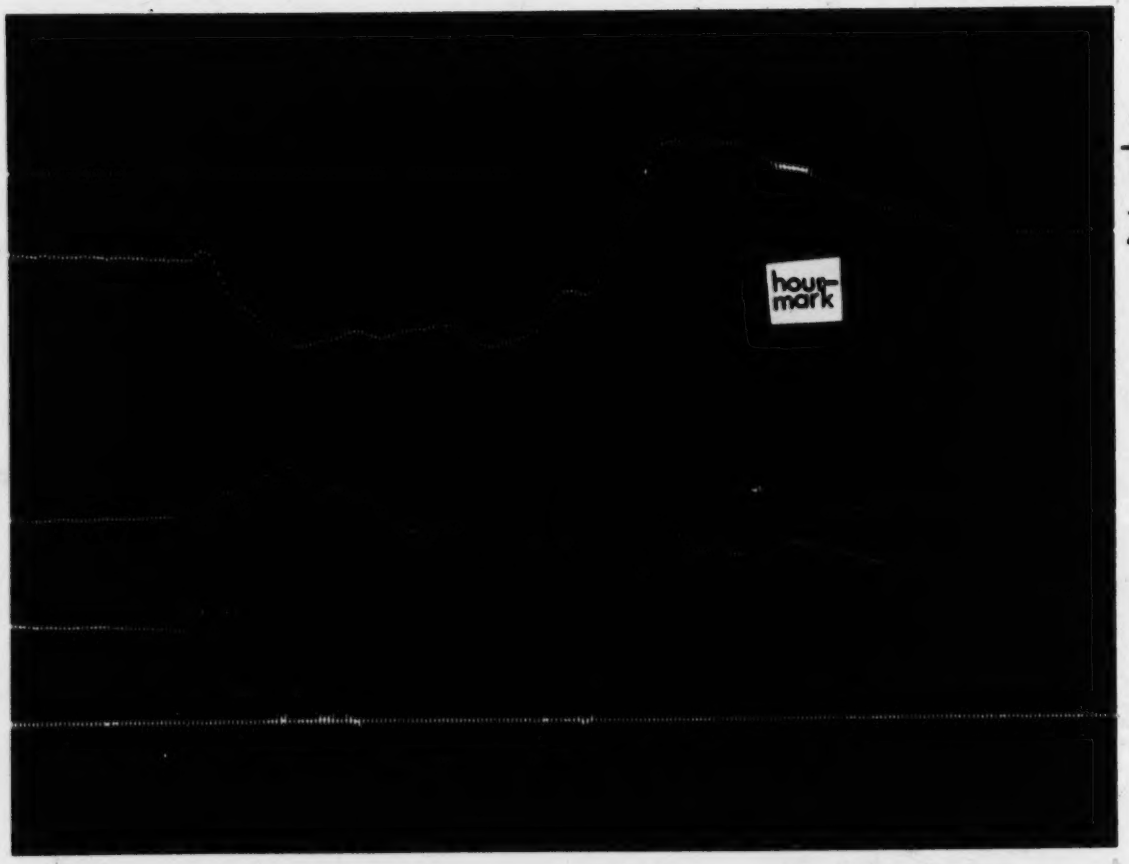

Top base line

Z trace

H trace

D trace

Bottom base line

seconds apart in time and approximately 0.2 mm apart on the film. Two base-lines are recorded from fixed mirrors in the magnetometer, in addition to the three traces reflected from suspended magnets. The three moving traces are displaced for about 40 seconds each hour, thus providing hour marks. The base-line traces are not accurately straight because the film wanders sideways on the sprocket teeth which are narrower than the sprocket holes.

In earlier magnetometer array studies by the Alberta group, prints at 15x magnification on paper were made of selected events and were digitized by a data-processing company by means of a pencil-following table. This process is slow and expensive and the resulting data are subject to errors of order of 1 percent of the film width, or several percent of a moderate variation amplitude. To provide fast and accurate digital data a high-speed optical scanner was designed by Mr. M. D. Burke and built under his direction by Mr. H. J. McCullough and others. This scanner operates under the control of a PDP-11 computer, in which preliminary editing is done to reduce the bulk of the digital data. The control and editing programmes for the PDP-11 were written by Mr. Lawrence Lewis. The data are recorded in I. B. M. compatible format on a 9-track synchronous tape recorder. All further data processing and editing are done in an I. B. M. 360/67 system. The writer's task was to write and test programmes in Fortran for data processing and editing in the 360/67.

2.2. The Film Scanner

The scanner and PDP-11 system will be briefly described for completeness. As has been mentioned above, they are the results of the work of others and the writer made only a minor contribution as a user during the hardware testing and PDP-11 software writing phases.

The optical and mechanical part of the scanner are schematically represented in Fig. 2.2. The high-precision cathode ray tube produces a fine light spot and a lens system forms a real image of the spot in the plane of the film. The spot is displaced so that its image crosses the film in 1024 equal discrete steps. On reaching its 1024th position, it is blanked out and returned to its starting point. The film being scanned is fed between two reels (see Fig. 2.2). It is advanced stepwise after each scan by a stepping motor.

The film used is a print from the original record with clear dots on a dark background. The flying spot scans from above the top baseline trace to below the bottom baseline. The clear dots are usually about 0.3 mm wide along the scan (magnetic component) axis and 0.2 mm long along the time axis. The flying spot is lengthened to a bar about 0.6 mm long along the time axis by means of a high frequency signal so that it always intercepts one or two dots in each trace. Each step in the scan is about 0.025 mm so light will reach the photomultiplier through a typical trace at about 12 spot positions. After each scan the film is stepped 0.43 mm. The

Figure 2.2. The basic hardware components of the optical flying spot scanner.

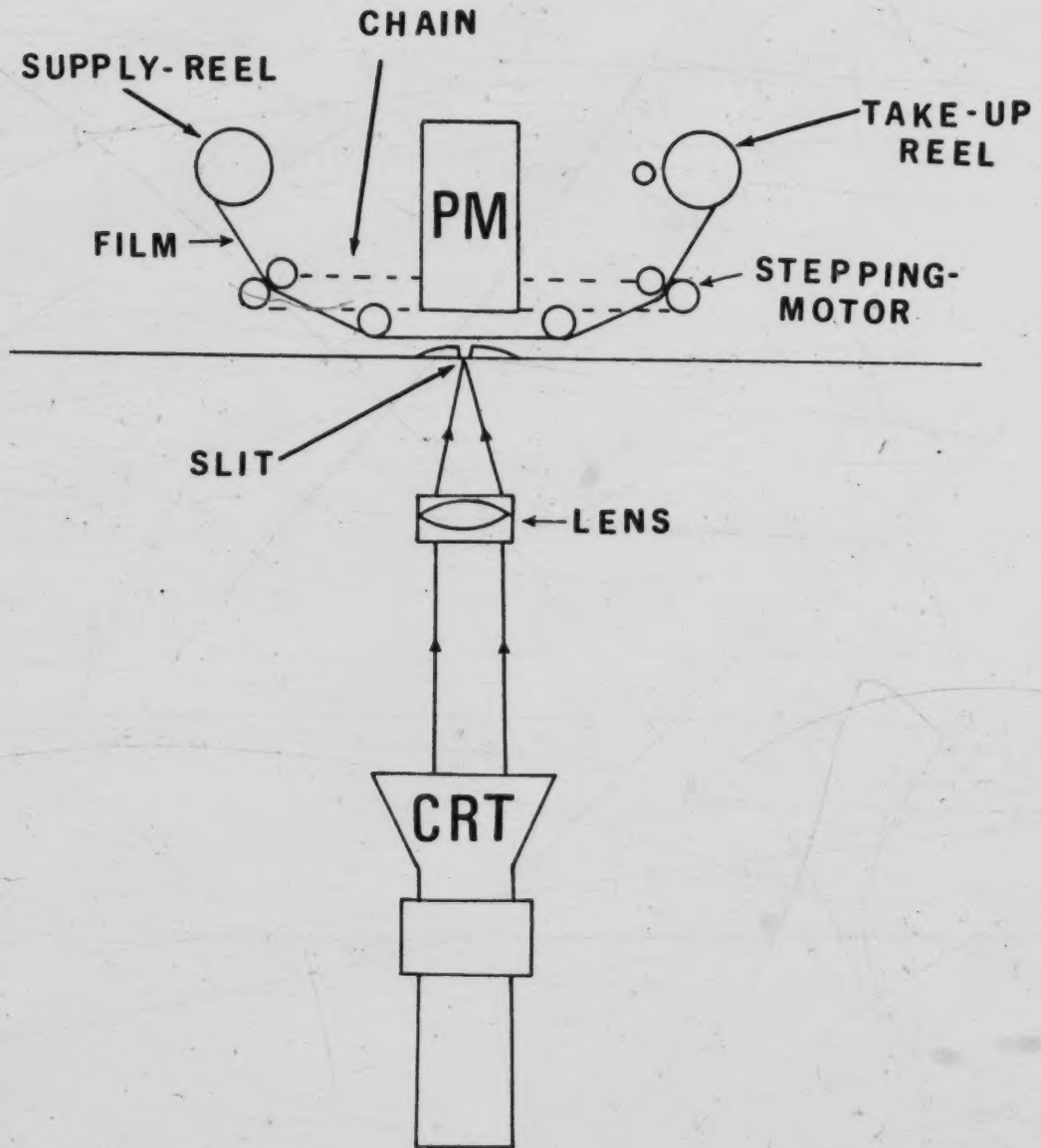
CHAIN
SUPPLY-REEL
TAKE-UP REEL
PM
FILM
STEPPING-MOTOR
SLIT
LENS
CRT

scan rate is one per two seconds, and a one-hour record is scanned in 5 minutes.

The scan of the flying spot is controlled by the PDP-11 in which its position is represented by a position count. At every position of the scanning spot some light passes through the film to the photomultiplier tube and produces an electrical signal. This signal is compared with a preset threshold. If it exceeds the threshold its amplitude is converted into 5 bits of digital information by a 10-bit A-D converter. The position count already exists as 10 bits of digital information. The two digital numbers are merged into a word of 16 bits coded in the following manner:

Bits	0 - 9	position count
Bits	10 - 14	intensity
Bit	15	'End Scan' (when set ON)

At the 1024th clock pulse the End Scan signal is generated and the stepping motor actuated to increment the film position.

2.3. The Film Scanner/PDP-11 System

The film scanner operates under the control of a PDP-11 computer in the Geophysics Data Centre of the University of Alberta. The computer time is shared with data acquisition and editing of data from the University's Geophysical Observatory. The PDP-11 initiates and stops data acceptance

from the film scanner on a lowest priority basis in relation to the real-time observatory data. Programmes in assembler language by Mr. L. Lewis manage the time sharing and acquire data from the film scanner in the manner described in section 2.2. Fig. 2.3 shows block diagram of the system.

As has been explained, the flying spot passes light through each of the five traces at about 12 consecutive positions for each. Thus, even with threshold rejection of all non-trace data (scratches, sprocket holes, etc.) about sixty 16-bit words are generated from each scan. With scans 0.43 mm apart and a film speed of 66 mm/hour in the camera a one-hour record generates about 9,000 16-bit words. To save time in the I.B.M. system a preliminary editing step in the PDP-11 combines the position and intensity data from each trace (i.e. from each set of consecutive positions giving data-words) to find a trace centroid position ordinate. The position of each trace is now represented by one word, but the intensity information is discarded.

All the spot ordinates found in a scan are organized into a unit of tape information called a logical record. Under normal circumstances, at most five spot ordinates can be produced from a scan. Experience acquired in the initial use of the scanner indicated that provision should be made for extra ordinates which might have survived the scanner threshold. Therefore, each logical record includes eight ordinates. When less than eight ordinates are found in a scan, the vacant

Fig. 2.3. Block diagram illustrating the operation of the scanning system.

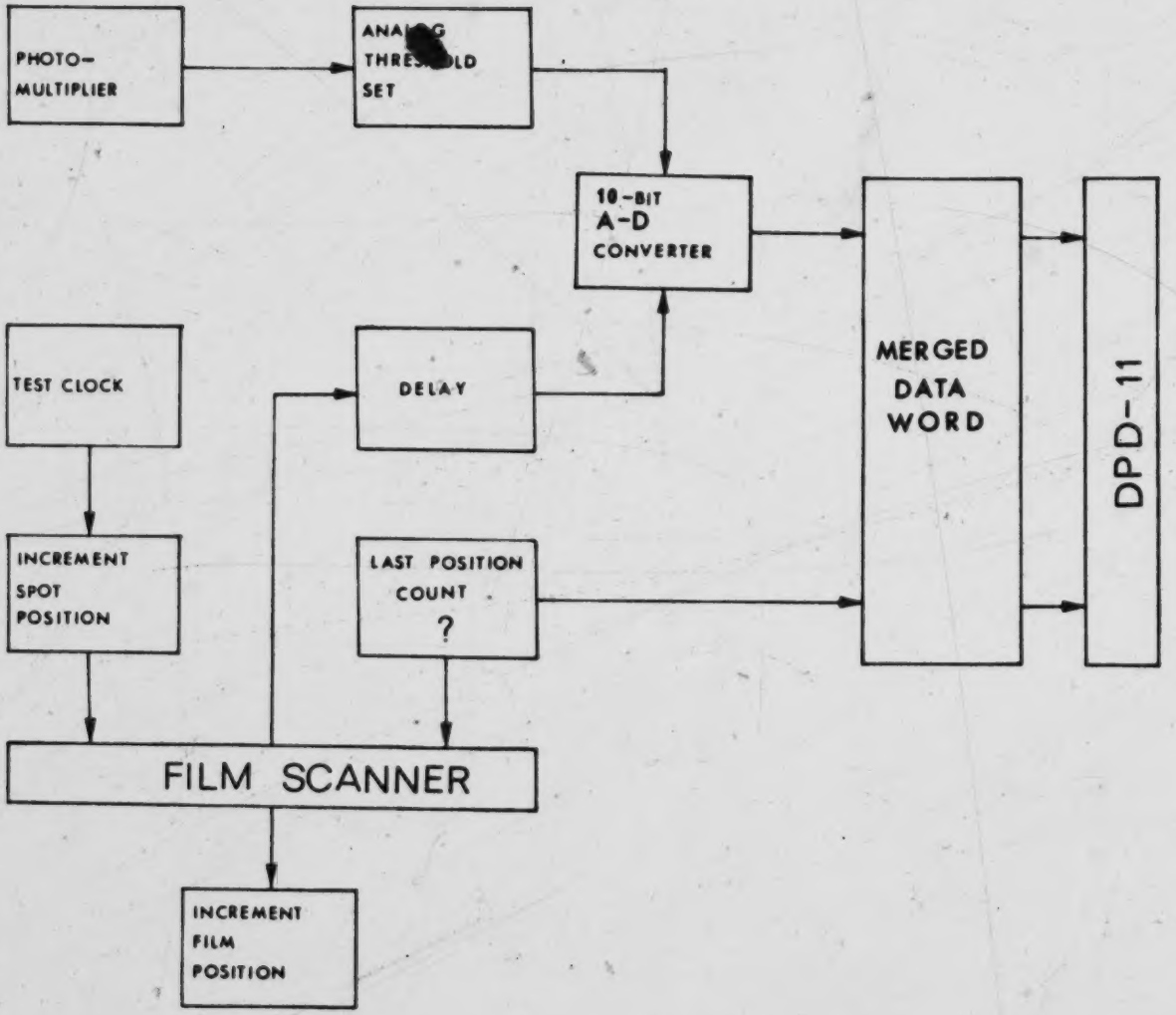
PHOTO-
MULTIPLIER
ANALOG
THRESHOLD
SET
10-BIT
A-D
CONVERTER
MERGED
DATA
WORD
DPD-11
TEST CLOCK
DELAY
INCREMENT
SPOT
POSITION
LAST POSITION
COUNT
?
FILM SCANNER
INCREMENT
FILM
POSITION

positions in the logical records are filled with negative numbers. Sixteen logical records are organized into a block. When a block of ordinates has been assembled, the block of information is written by a synchronous recorder on magnetic tape in I.B.M. compatible format.

Peripherals of the Geophysical Data Centre include a CRT graphic display and hard-copier. Each logical record (i.e., the group of ordinates found in a vertical scan) is displayed as a column of dots on the CRT display. The row of logical records thus resembles the original analogue film record and provides a useful check of the system. When the screen is full, a hard-copy may be obtained if desired. False ordinates due to the sprocket holes, dust or scratches on the film are edited out later in the I.B.M. system.

2.4. An Introduction to the Editing Programmes

For the purpose of editing the digital ordinates tapes, the original analogue records were categorized into two classes depending on the ease with which the analogue form of the record can be retrieved from the converted digital form. Figures 2.4 (a) and (b) are examples of the records that belong to the first class. In this type of records, the traces remain separate from each other without crossing over or merging. The editing of this class of records involves sorting the ordinates into time-series representing the original traces. False ordinates and ordinates that can introduce spikes

Fig. 2.4. Records that can be edited with the programme AUTO-EDIT. Notice in (a) the traces are well separated. In (b) there are false ordinates due to sprocket holes. TF, BF are top and bottom baseline (fiducial) traces.

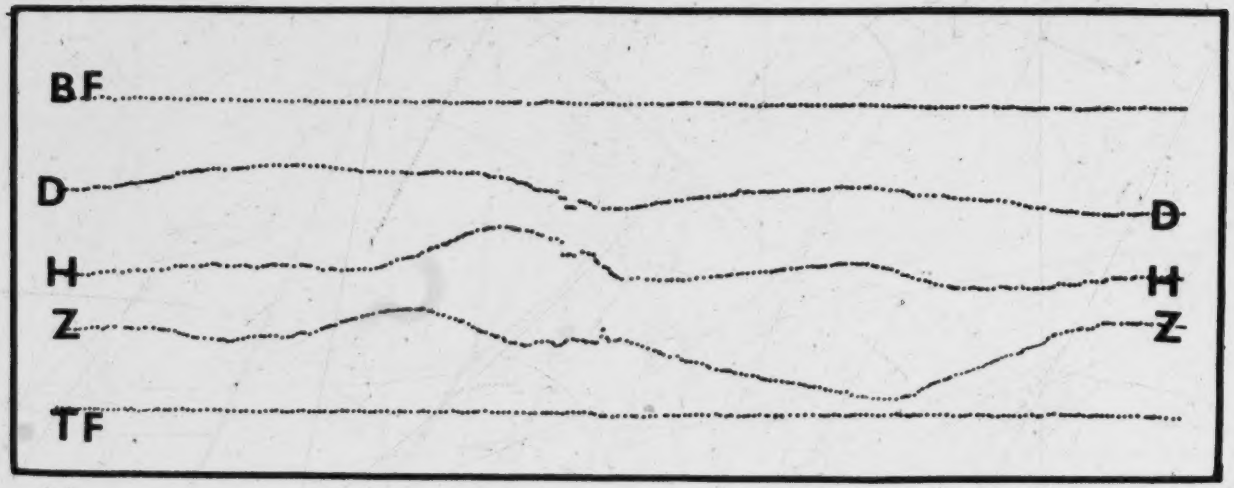

a

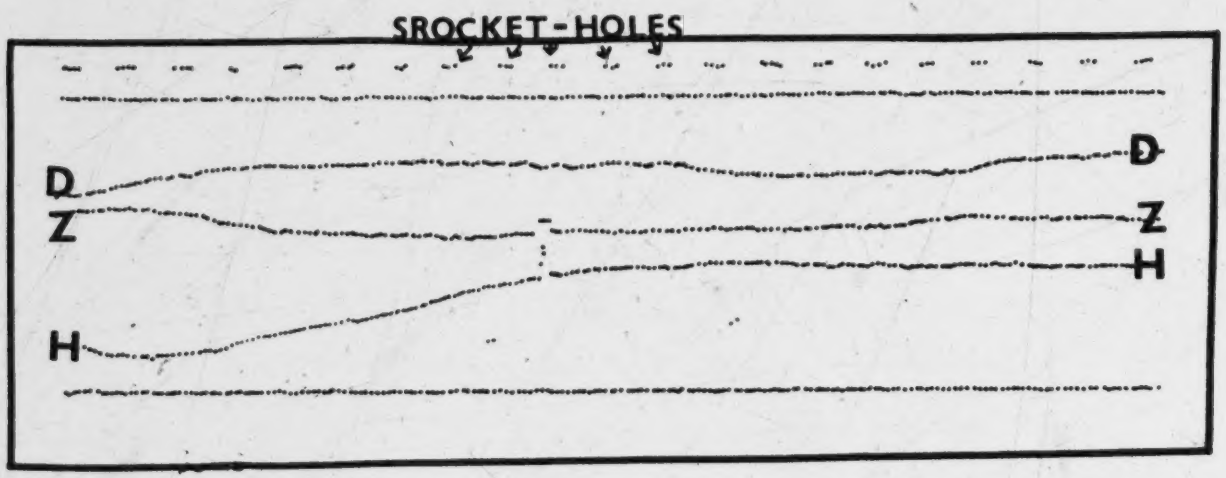

b

into the analogue form of the record are rejected, and missing ordinates (for instance in time marks) are interpolated. A Fortran programme code-named AUTO-EDIT was written for editing such records. In a moderate substorm event, about half of the stations in an array record the event without the traces crossing over or merging and can be edited by means of AUTO-EDIT, which has the capability of editing any number of records in a single run.

In Figures 2.5 (a) and 2.5 (b), the traces both cross over and remain merged for some length of time. These are examples of records in the second class. A computer programme named SEMI-AUTO was written for editing such records. The programme allows a human operator to make use of the iteracting facilities of a graphic display annexed to a computer to disentangle the traces. About half of the records from substorm events require such interactive editing.

In the remaining part of this chapter, the algorithms of both programmes will be described.

2.5. The Programme Package: AUTO-EDIT

The flow diagram given in Fig. 2.6 should be consulted in reading this section.

An event selected for analysis in an array observation is usually scanned and stored as a set of files of ordinates on 9-track tape as described in section 2.3. Each file of scanned data is acquired at a station in the array. The editing

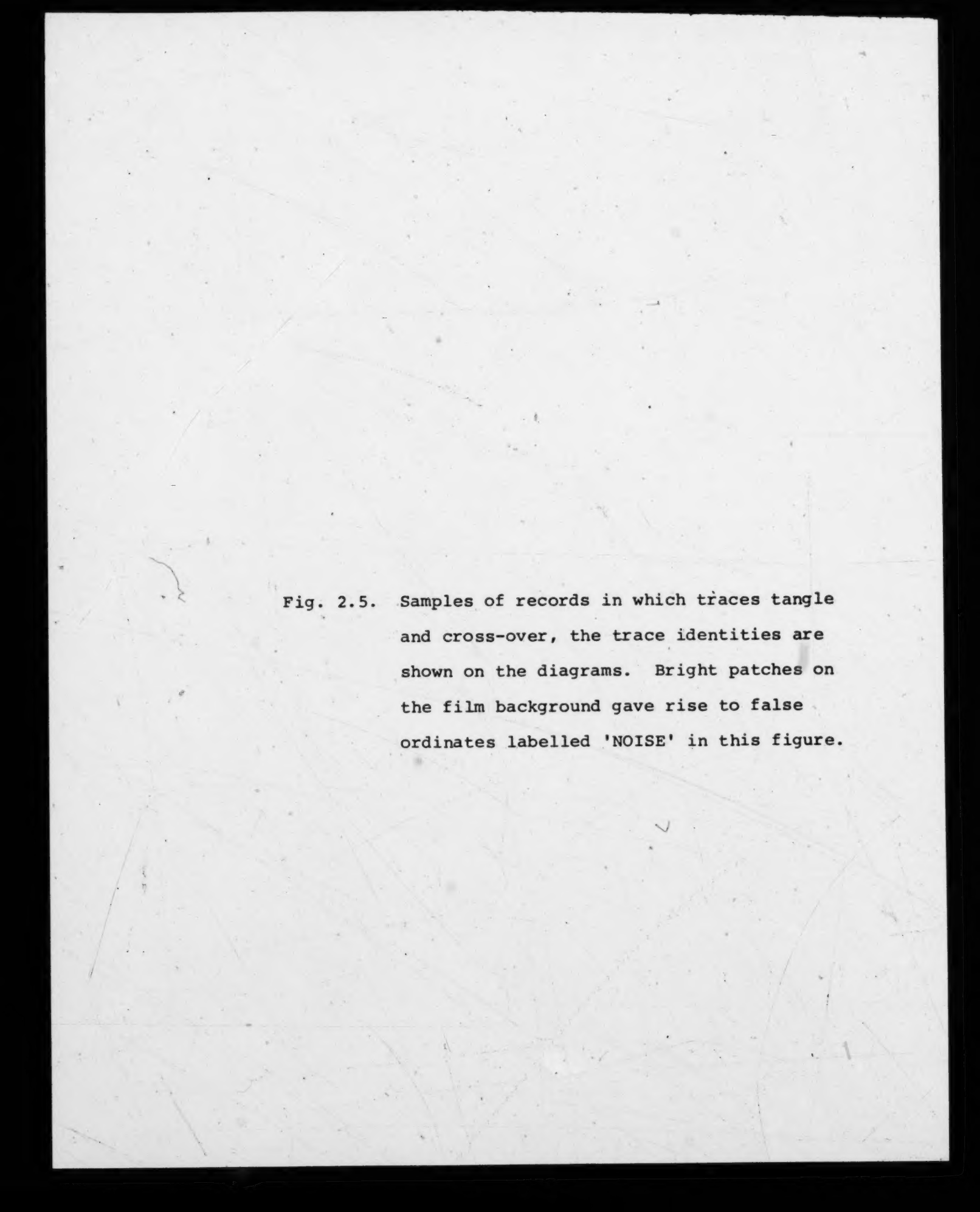

Fig. 2.5. Samples of records in which traces tangle and cross-over, the trace identities are shown on the diagrams. Bright patches on the film background gave rise to false ordinates labelled 'NOISE' in this figure.

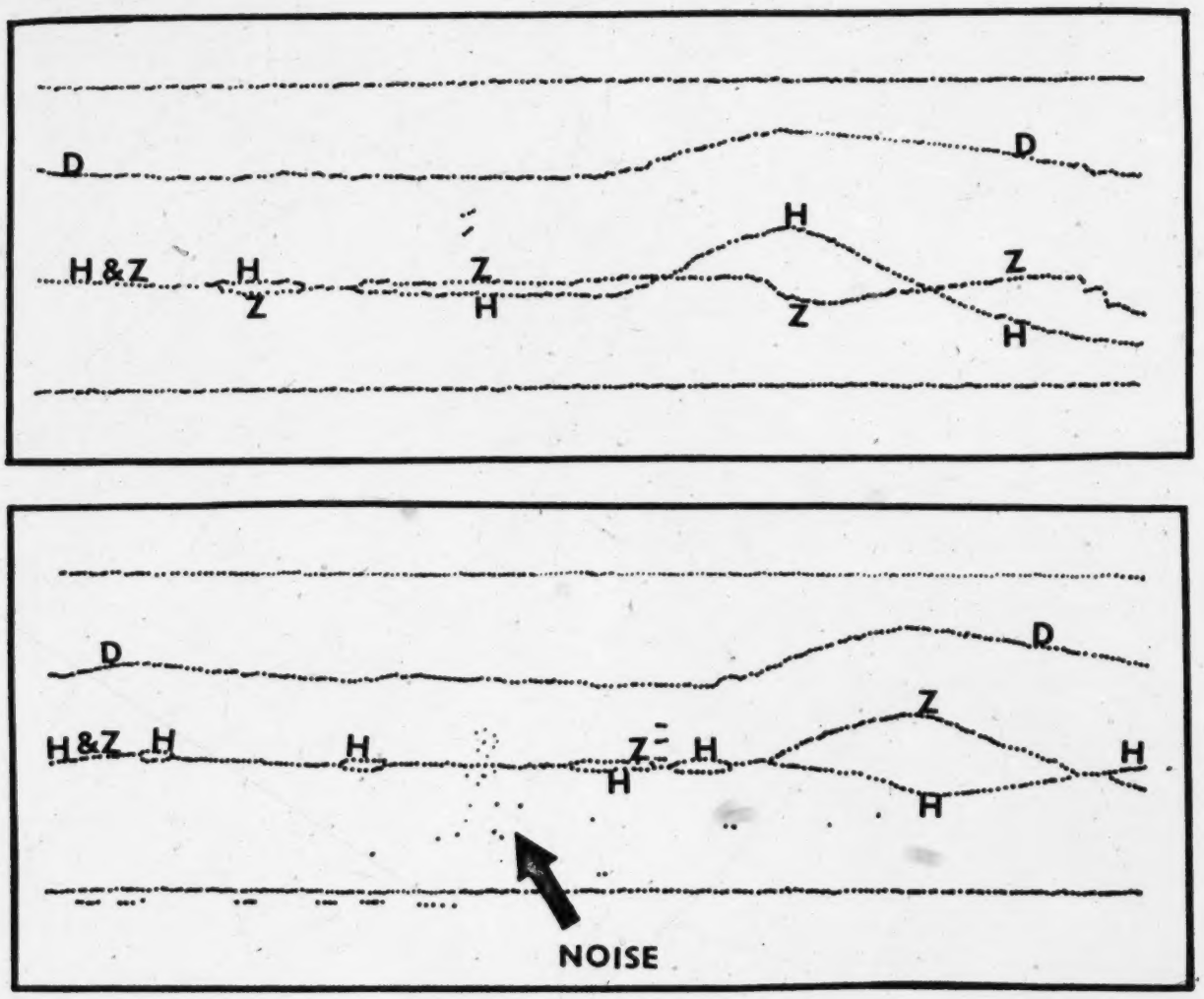
D
D
H&Z
H
Z
Z
H
H
Z
Z
H
a
D
D
H&Z
H
H
Z
H
Z
H
H
H
b
NOISE

Fig. 2.6. A flow diagram showing the processing steps involved in programme AUTO-EDIT described in section 2.5.

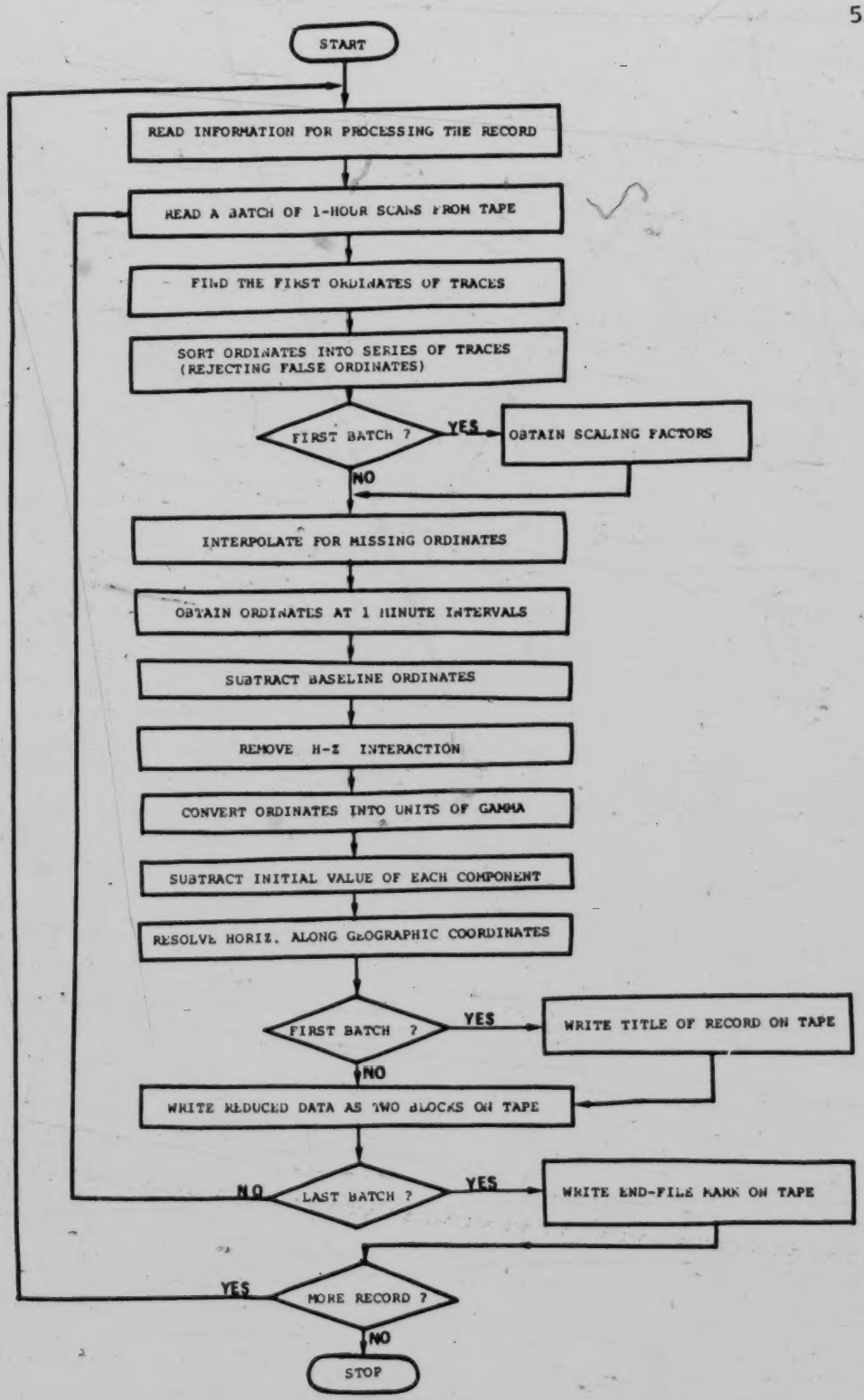
START
READ INFORMATION FOR PROCESSING THE RECORD
READ A BATCH OF 1-HOUR SCANS FROM TAPE
FIND THE FIRST ORDINATES OF TRACES
SORT ORDINATES INTO SERIES OF TRACES (REJECTING FALSE ORDINATES)
FIRST BATCH ?
YES
OBTAIN SCALING FACTORS
NO
INTERPOLATE FOR MISSING ORDINATES
OBTAIN ORDINATES AT 1 MINUTE INTERVALS
SUBTRACT BASELINE ORDINATES
REMOVE H-Z INTERACTION
CONVERT ORDINATES INTO UNITS OF GAMMA
SUBTRACT INITIAL VALUE OF EACH COMPONENT
RESOLVE HORIZ. ALONG GEOGRAPHIC COORDINATES
FIRST BATCH ?
YES
WRITE TITLE OF RECORD ON TAPE
NO
WRITE REDUCED DATA AS TWO BLOCKS ON TAPE
NO
LAST BATCH ?
YES
WRITE END-FILE MARK ON TAPE
YES
MORE RECORD ?
NO
STOP

of all files of records in which the traces do not cross-over or merge is done in a single batch-mode The programme AUTO-EDIT handles this situation. Magnetometers have slightly different film speeds (in their cameras), thus the number of scans in an hour film record varies. The expression of the time series in the usual geomagnetic units of nanoteslas or gammas requires that the field calibration constants of the instruments be known. For each file to be edited, these data and others that vary from record to record or from event to event, such as the date and duration of the event, are specified on cards.

A tape file specified for auto-editing is read in batches of scans of one hour length in the time domain. The reading starts from the scan at which the event starts. The ordinates are organized into an array suitable for manipulation by the computer. When the editing of a file is just begun, a subroutine makes use of a sorting procedure to find the first ordinate on each component trace. A dynamic selection rule is employed to sort all the ordinates into sequences representing the original component traces. The essential of the selection rule is that any pair of consecutive ordinates belonging to the same component trace may only differ from each other by less than a preset value. This preset value is optimized according to the magnetic activity in the record.

When the programme finds it impossible to allocate ordinates to a component at three consecutive positions, a

subroutine LOOK is called to check the remaining array of ordinates and determine the length of the gap just begun in the sequence. If the length is found to be longer than 10 minutes in the time domain, the editing of the file is terminated. Otherwise, the sorting subroutine AUTRAK proceeds with the search with this gap in mind. Assignment of the ordinates to this component is resumed only for positions after the gap. In the time sequence for a component, positions at which ordinates are not allocated are assigned the number -99.

An hour of film record is scanned in a number of steps which is not in general an integral multiple of 60. Thus, a subroutine linearly interpolates between scans to obtain the trace sequence positions at exactly 1 minute intervals. Scaling factors computed from the supplied field calibration factors are used to convert the ordinates into nanoteslas. The first number in each sequence is subtracted from all the other members. A small H-Z interaction in the instrument is removed. The lower baseline ordinate is subtracted from those of Z, H and D. The time-sequences of the H and D components are transformed into geographic co-ordinates X (north positive) and Y (east positive) according to the formulae:

$$X = H\cos\delta - D\sin\delta$$
$$Y = D\cos\delta + H\sin\delta \qquad (2.1)$$

where δ is the magnetic declination of the station specified

for the file. The record has now been reduced.

The reduced data sequences are written on 9-track tape in blocks of 90 bytes of information. The first block is an identification for the file. The code-name of the station at which the record was acquired is the most significant part of the identification. The other blocks are composed of 30 triplets of the magnetic values (X, Y, Z) corresponding to half-hour data in time domain. When a particular component has not been recorded at a station, the data file for the station has -9990 written for the member of the triplet corresponding to this component. The magnetic values are written in 2-byte integers. Hence, each triplet gives rise to 6 byte data and 30 triplets therefore to the 90 bytes making up a block. A complete data file contains the reduced data of an event at a station.

2.6. The Programme Package: SEMI-AUTO

SEMI-AUTO differs considerably from AUTO-EDIT described in the last section. The programme to be described allows a human operator to disentangle the traces which are displayed on a graphic terminal by using interactive devices such as the light-pen. The graphic terminal of the University of Alberta consists of a CRT unit and a display controller (computer) interfaced to the I.B.M. 360/67 system. The CRT has a screen area of 12 inches by 12 inches which consists of 1024 by 1024 addressable positions. A programmed light-pen,

alphanumeric and functional keys are used to interact with items displayed on the CRT.

Fig. 2.7 is a flow diagram which may be used in conjunction with this section. Data to be displayed are transformed from magnetic tape to disc files. After editing, the reduced data are stored on some disc file, to be transferred to magnetic tape at a later stage.

The editing subprogramme initiates a 'question and answer' dialogue between the user and the computer. The aim is to secure information for processing the record. The name of the input and the output disc files are supplied. Once the station's name is given by the user, the instrument calibration factors and magnetic declination of this station are read from the disc file on which they are stored. The user must divide the record into sections called frames using the hardcopy of the record as a guide. If the records were obtained with a magnetometer sampling the field at 10 seconds interval, a frame is composed of scans 30 minutes long in the time domain. Twenty seconds sampling interval allows the frame to be an hour long. The user by visual inspection of hardcopy classifies each frame into two classes, those whose traces do or do not cross over. The frame in which the traces are well separated are specified for automatic editing during the user-computer dialogue. A subprogramme then transfers the data from the 9-track tape onto input disc files. Each frame forms the main part of a line in an input file. A

Fig. 2.7. The flow diagram of the programme SEMI-AUTO.

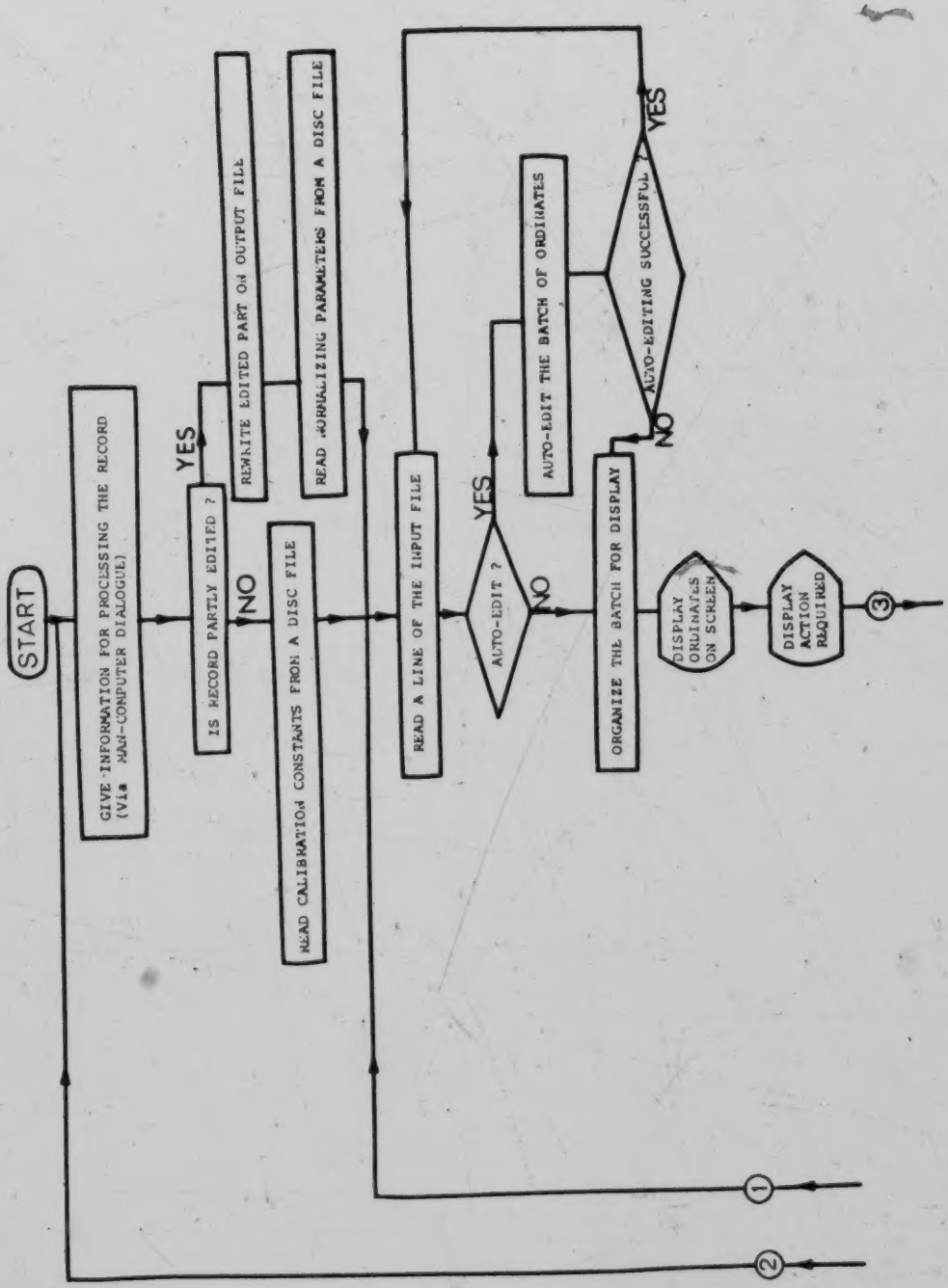
START
GIVE INFORMATION FOR PROCESSING THE RECORD (Via MAN-COMPUTER DIALOGUE)
IS RECORD PARTLY EDITED ?
YES
NO
REWRITE EDITED PART ON OUTPUT FILE
READ CALIBRATION CONSTANTS FROM A DISC FILE
READ NORMALIZING PARAMETERS FROM A DISC FILE
READ A LINE OF THE INPUT FILE
AUTO-EDIT ?
YES
NO
AUTO-EDIT THE BATCH OF ORDINATES
AUTO-EDITING SUCCESSFUL ?
YES
NO
ORGANIZE THE BATCH FOR DISPLAY
DISPLAY ORDINATES ON SCREEN
DISPLAY ACTION REQUIRED
1
2
3

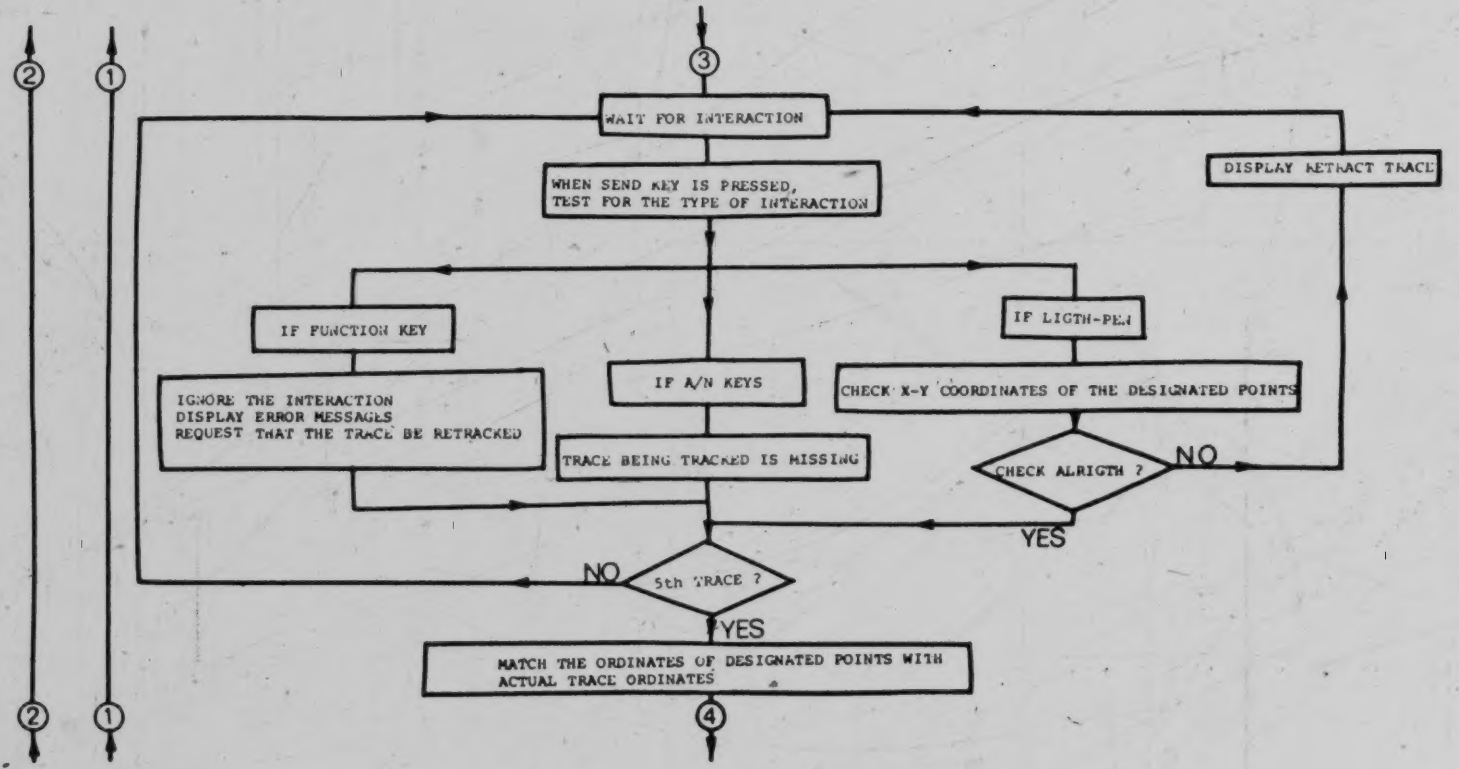
3
WAIT FOR INTERACTION
WHEN SEND KEY IS PRESSED,
TEST FOR THE TYPE OF INTERACTION
DISPLAY RETRACT TRACE
IF FUNCTION KEY
IF LIGTH-PEN
IF A/N KEYS
IGNORE THE INTERACTION
DISPLAY ERROR MESSAGES
REQUEST THAT THE TRACE BE RETRACKED
CHECK X-Y COORDINATES OF THE DESIGNATED POINTS
TRACE BEING TRACKED IS MISSING
CHECK ALRIGTH ?
NO
YES
NO
5th TRACE ?
YES
MATCH THE ORDINATES OF DESIGNATED POINTS WITH
ACTUAL TRACE ORDINATES
4
2
1
2
1

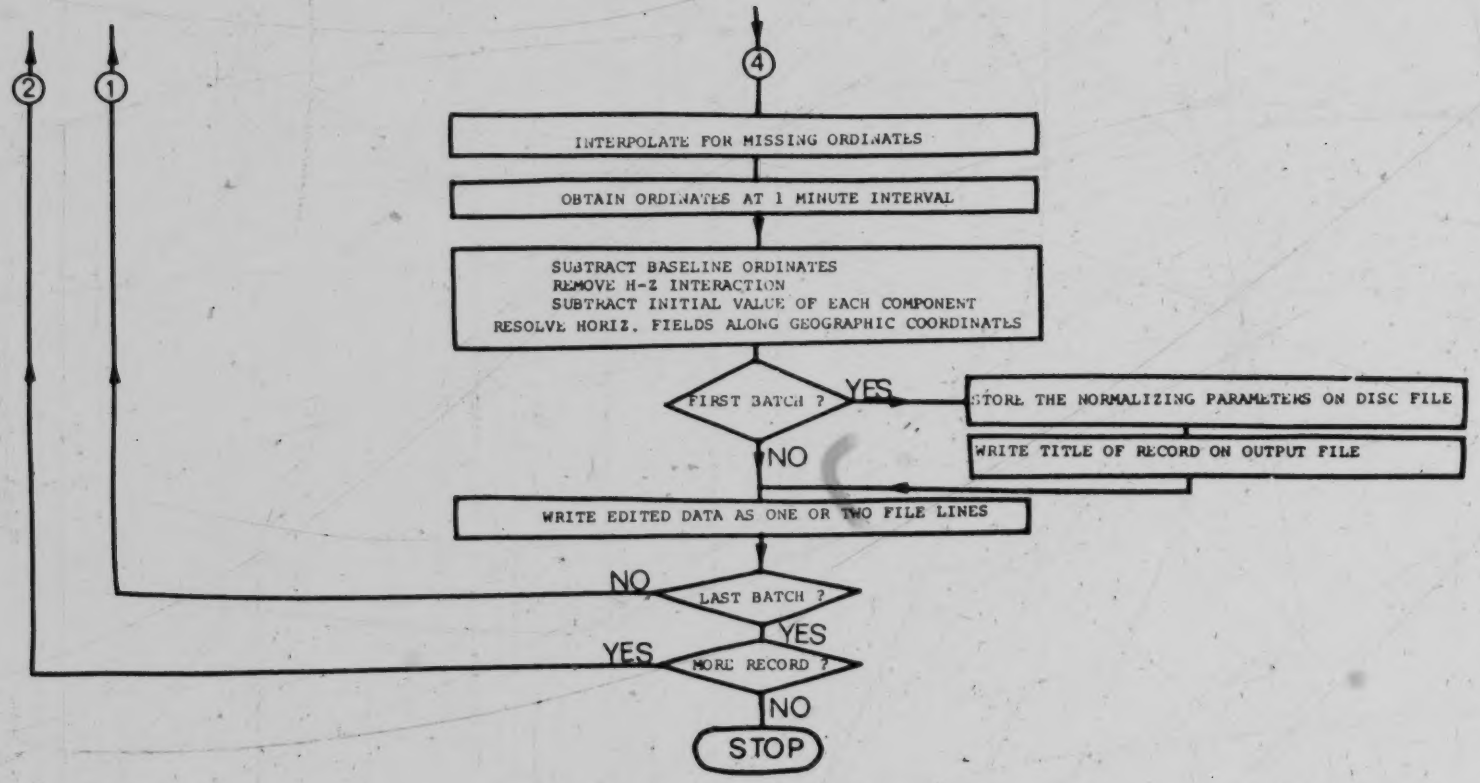
2
1
4
INTERPOLATE FOR MISSING ORDINATES
OBTAIN ORDINATES AT 1 MINUTE INTERVAL
SUBTRACT BASELINE ORDINATES
REMOVE H-Z INTERACTION
SUBTRACT INITIAL VALUE OF EACH COMPONENT
RESOLVE HORIZ. FIELDS ALONG GEOGRAPHIC COORDINATES
FIRST BATCH ?
YES
STORE THE NORMALIZING PARAMETERS ON DISC FILE
WRITE TITLE OF RECORD ON OUTPUT FILE
NO
WRITE EDITED DATA AS ONE OR TWO FILE LINES
NO
LAST BATCH ?
YES
YES
MORE RECORD ?
NO
STOP

subroutine now reads the record from the disc file one line at a time and organizes it into an array. If a frame has been specified for automatic editing the sorting of the array of ordinates into sequences is carried out by modified versions of subroutines AUTRAK and LOOK of AUTO-EDIT.

Automatic sorting of a frame may result in failure. The programme then demands that the frame be edited by the interacting procedures to be described. A frame not specified for automatic editing is organized into a form, supported by the graphic terminal software, for display. The data are displayed on the screen of the CRT, which is divided into four zones as indicated on Fig. 2.8 (a). In zone A, the last thirty scans in a previous frame are displayed, in B, the portion of the record being edited and in C, the first thirty scans in the next frame are displayed. Zone D displays instructions to guide the user's response to the computer's request. The display of the data of the frame being edited, together with portions of the data of adjacent frames, facilitates visual correlation of data. This was found useful for recognizing features in tangled traces near the extremes of the frame. All the ordinates found in a scan are displayed with the same abscissa.

The displays in zones A and C are such that consecutive scans are separated by 4-screen co-ordinates while in the main frame (displayed in Zone B) the separation is 6 screen coordinates. This provides easy visual recognition of the

Fig. 2.8. The division of the graphic terminal screen into zones is illustrated in Fig. 2.8 (a). A sample of designated points on a tracer (shown as dots on the trace) is given in Fig. 2.8 (b).

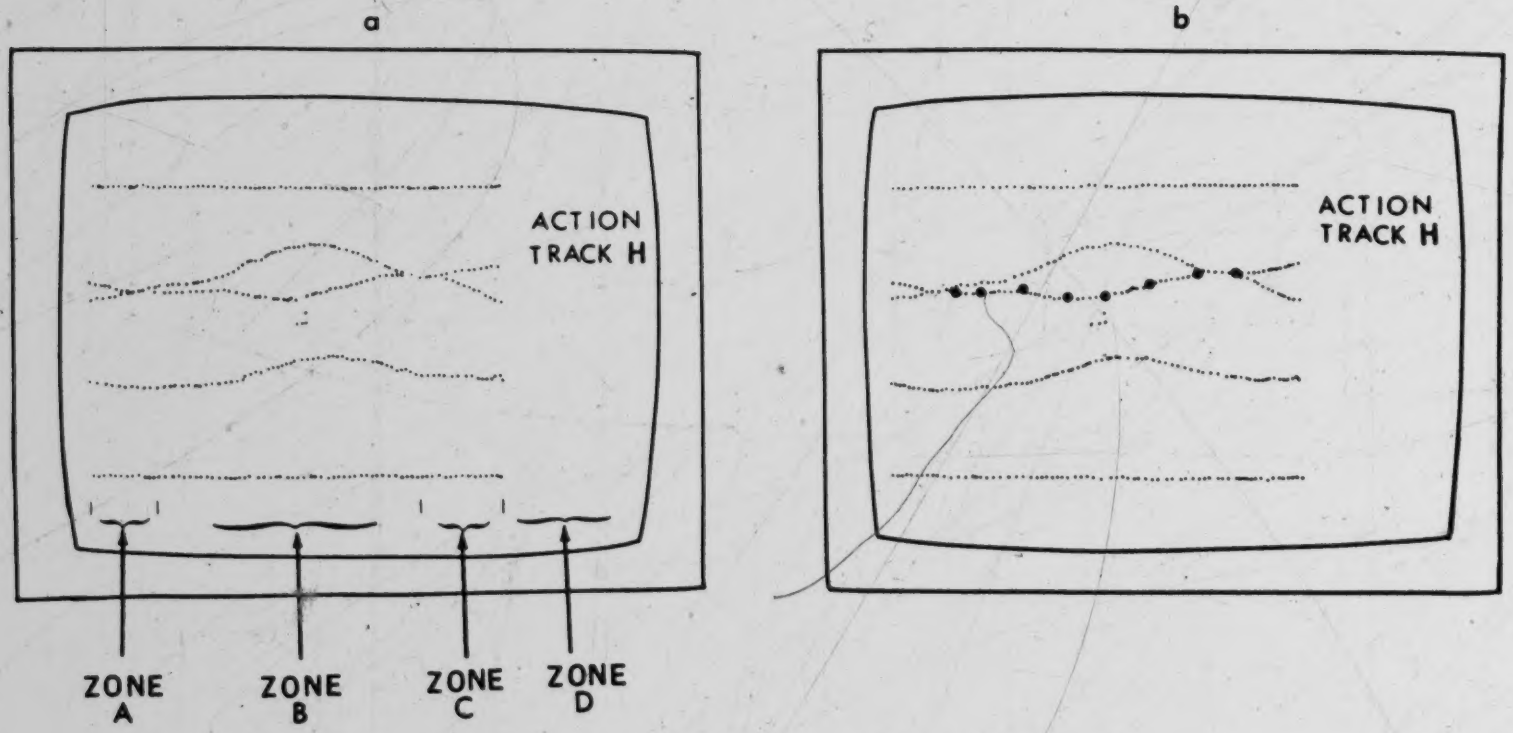
a
ACTION
TRACK H
ZONE
A
ZONE
B
ZONE
C
ZONE
D
b
ACTION
TRACK H

different zones.

Once the traces have been displayed, the programme goes into waiting mode. A subroutine which schedules the interaction required by the computers, displays the appropriate instruction in zone D of the screen. In Figure 2.8 (b), an example of such instruction is shown. The request 'TRACK H' means that the user is expected to designate points with light pen on trace H of the display. If this trace is missing the user types in 'NO' with the alphanumeric keys. Otherwise, light-pen is used to put points on the H trace as demonstrated in the Figure 2.8 (b). At least two points are required to define a trace and not more than 50 points were found necessary. The first point put on a trace must be close to the first column of dots in zone B and the last point must be close to the last column of dots in zone B. When up to 10 points have been designated on a trace, the programme sends the points to the computer. The designated points now available in the 360 system are examined to see if enough points have been put on the trace. If the designated points are insufficient, a message 'MORE TRACK' is displayed and the user must put more points on the trace in order of ascending screen x-coordinate. When sufficient points have been defined on a trace, a sub-routine checks the x- and y- coordinates of the points to see that none of them is negative or outside the allowed range of 0 to 1023. Hardware problems resulting in transmission of negative or large coordinate values were found to be uncommon.

Such unwanted situations result in the programme displaying the message 'REPEAT' together with the name of the trace to be retracked. Transmission of a message which is neither from the light-pen nor from alphanumeric keys is not allowed and error messages are displayed. The programme is not capable of recognizing some users' errors such as tracking the H trace when the computer requires that Z-trace be tracked. The pre-editing of the traces on hard-copies of the records must be available for editing the graphic terminal system.

A subroutine interpolates linearly between the light-pen assigned points to obtain sequences of y-coordinates corresponding to each x-coordinate at which a column of dots has been displayed on the screen. These sequences are close approximations to the sequences of the component traces. A subroutine uses these approximate sequences to sort the data. When the traces cross-over, the sorting is done in a more rigorous manner. For example, the light-pen points in each of the columns involved in the cross-over or merging section are scanned through to determine if more than one trace must share the same ordinates or not.

Missing members in the sequence are interpolated for. The time series are obtained at 1 minute interval. The base-line ordinates are deducted, the first value of each sequence is deducted from the others and the Z-H interaction is removed. Station calibration data are used to convert these sequences to gammas. Horizontal components are transformed into geographic

coordinates. All these operations are done as described for AUTO-EDIT. The reduced data are written on disc file. A small subprogramme is used later to transfer the data from the disc file onto 9-track magnetic tape in blocks of half-hour data.

In a terminal session of an hour up to four records can be edited. A file can be edited in parts. This provision allows a user to resume the editing of a record that had been terminated by hardware problems, an essential feature with a busy computer.

2.7. Comments on the Present System

The scanner and the editing programmes were used in processing the array data reported in this thesis. The hardware/software problems of the graphic terminal which cause poor results when editing fast-varying events are the only difficulties experienced. The computing centre of the University of Alberta is improving the hardware and software of the system. For substorm events only a few records require re-editing. Although each programme involves more than 2,000 Fortran statements, they are user-oriented in the sense that a user need not know most of the concepts of the algorithms. The user-computer dialogue and the error messages are self explanatory and the interaction sequence is easily followed.

CHAPTER III

THE NORTH AMERICAN CENTRAL PLAINS ANOMALY

In 1967 and 1969 two large two-dimensional magnetometer arrays were operated in the western United States and south western Canada. Fig. 3.1 shows the stations of the two array studies. The North American Central Plains anomaly was first noticed in the north-east corner of the 1967 array. The 1969 array was designed so that magnetic variation records were obtained at a number of closely spaced stations across the anomaly, which passes through the Black Hills uplift in the Central Plains. This thesis reports a more complete study of the North American Central Plains anomaly. In this chapter the findings of the 1967 and 1969 array studied on the North American Central plains are reviewed.

3.1. The 1967 Magnetometer Array Study

In the summer of 1967, the geomagnetic induction groups of the University of Alberta and of the University of Texas at Dallas operated 42 Gough-Reitzel magnetometers (Gough and Reitzel, 1967) on four east-west lines between latitudes 36° and 42° N. and longitudes 102° and 116°W. in the western United States. This two-dimensional array was designed to map an anomaly previously discovered by a linear magnetometer array in Colorado (Gough and Reitzel, 1969) and to look for a possible anomaly under the Wasatch Front in Utah.

Fig. 3.1. The stations of 1967 and 1969 studies. The open circles show the 1967 array stations and the dots the 1969 stations. The 1972 array covered the region enclosed in the rectangle. Four of the 1967 array stations, CRW, CAS, STE and LYO are labelled. (The figure is adapted from Camfield, 1973).

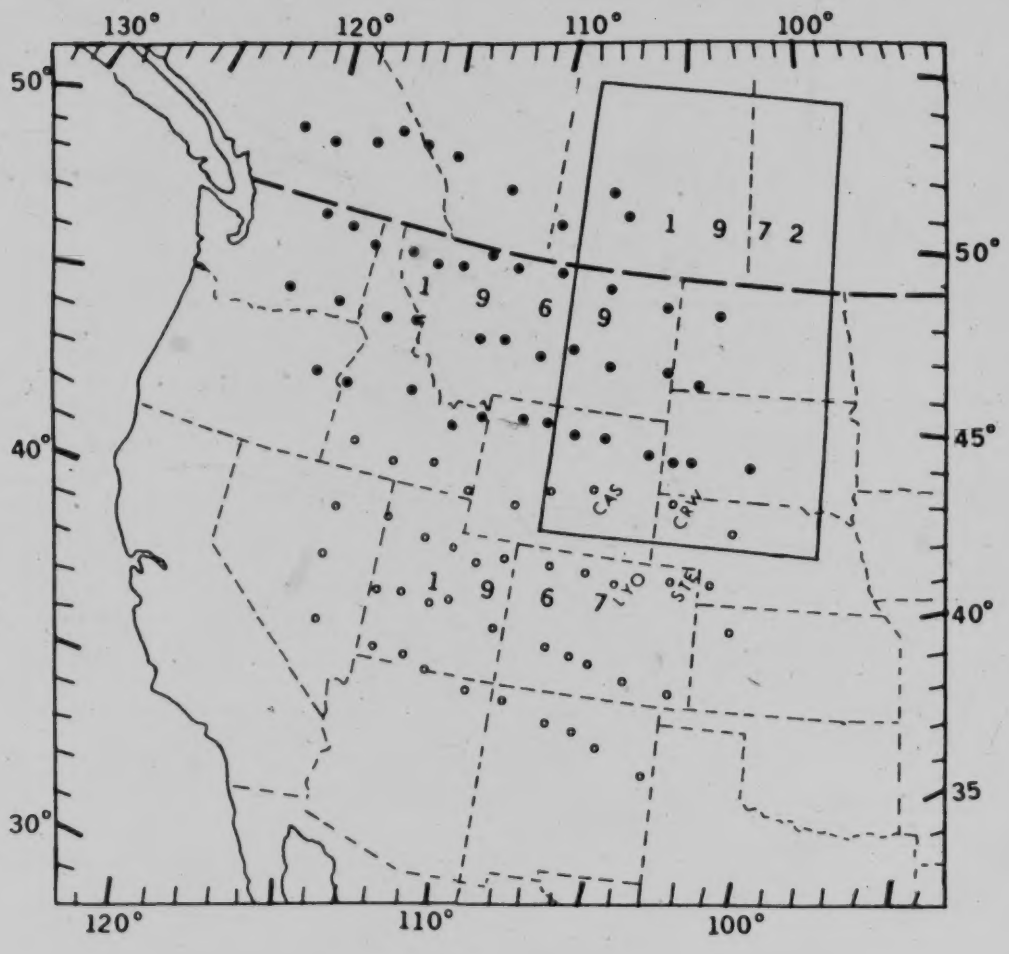
130°
120°
110°
100°
50°
40°
30°
45°
35
1 9 7 2
1 9 6 9
1 9 6 7
CAS
CRV
LYO
STE

A substorm event of September 1, 1967 was analyzed and the variation field anomalies were interpreted in terms of conductivity anomalies. Contour maps of the separated fields in the time domain revealed two north-south striking conductive bodies, one under the Southern Rockies and the other under the Wasatch Front. Only the Southern Rockies anomaly overlaps the region of the 1972 array.

Reitzel, Gough, Porath and Anderson (1970), discussed the anomaly in detail. The Southern Rockies anomaly appears in magnetograms of the vertical and the eastward horizontal components of the variation field. The vertical and the east-west horizontal components are very strongly enhanced at CRW on line 1 and less prominently on line 2 at STE. These stations are marked in Fig. 3.1.

Maps of Fourier transform parameters were introduced as a new type of geophysical anomaly map by Reitzel et al. (1970) and drawn at several periods for unseparated variation field components. In Fig. 3.2 a reproduction of a set of amplitude and phase maps at period 30 minutes reveals the Southern Rockies anomaly as a narrow ridge of high contour values in the vertical and the east-west horizontal components.

In a second paper on the 1967 array, Porath, Oldenburg and Gough (1970) separated the fields of the substorm of September 1, 1967 into parts due to external and internal currents, by the surface integral method described in Chapter I. Such separation in both the time and period domains showed

Fig. 3.2. The amplitude and phase maps of the unseparated field of a substorm at 30 minutes period. The two ridges of the high contour values in the east-west horizontal (Y) component and in the vertical (Z) component are surface expressions of the Wasatch Front anomaly (West) and the Southern Rockies anomaly (East) (Anderson, 1970).

SUBSTORM SEPT 1, 1967

CONTOUR INTERVAL : 0.5 GAMMA

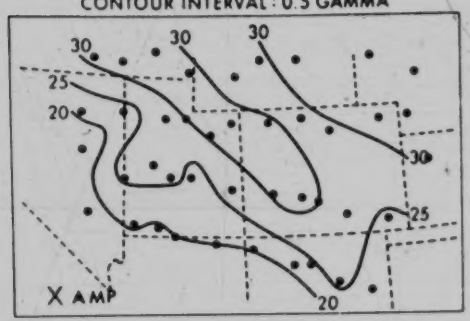

CONTOUR INTERVAL : 2 MINUTES

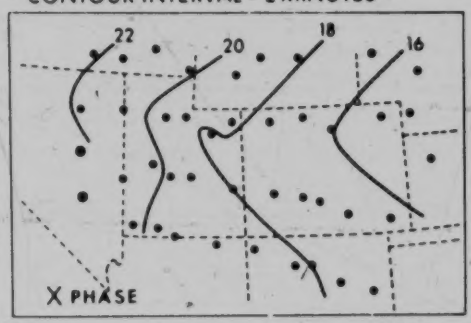

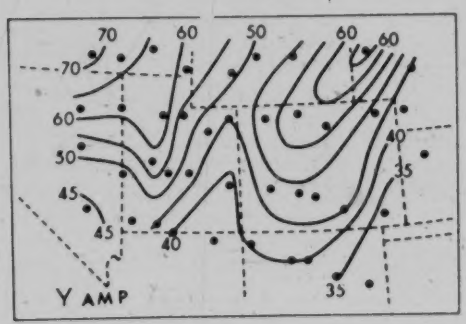

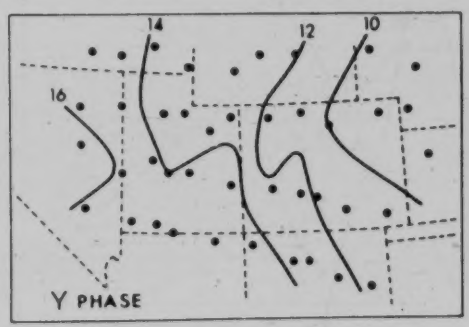

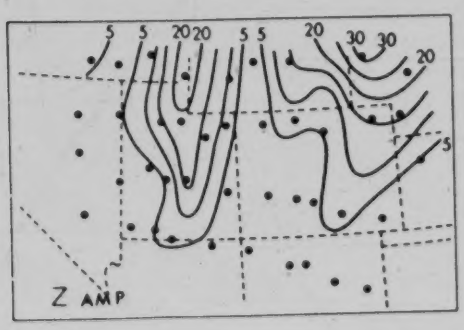

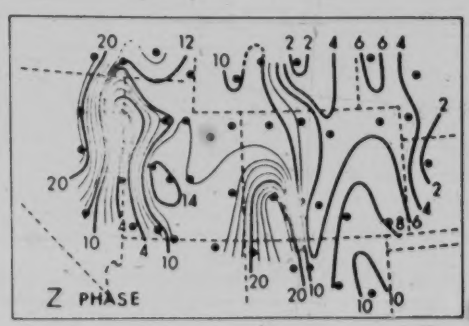

the local anomalies to be due to internal currents. Porath, Oldenburg and Gough estimated normalized anomalous fields at three periods and for two components. They were able to fit these by induction by a horizontal field in two-dimensional conductive structures. A model fitting the anomalies is shown in Fig. 3.3, from Porath and Gough (1971). It consists of ridges and a step on the highly conducting half-space, and would be appropriate if vertical motions displaced isotherms in the upper mantle in the depth range to about 600 km.

The phase difference of about 30° between the normal and anomalous fields and the high heat flow reported for this region (Roy et al. (1972)) support the location of the conductivity anomaly in the upper mantle. Gough and Porath (1970) suggested that the conductive ridge if it is at a depth of about 200 km., must have been hot for a long time (order of 10^8 years). Gough (1974) proposed that the Southern Rockies anomaly could result from subduction of a lithospheric plate moving eastward.

In an alternative conductive model fitting the Southern Rockies anomaly Porath (1971) placed the structures in the depth range 27-80 km, in the region of the seismic low velocity layer (Fig. 3.3.) The underlying hypothesis here is that the conductivity rises in association with partial melting (Presnall et al., 1972; Chan et al., 1973). The very different depths of two models, both of which fit the data, illustrate the poor depth resolution of magnetometer arrays. However, a vital

Fig. 3.3. Conductive models which fit normalized anomalous fields recorded by the 1967 array. The upper is from Porath and Gough (1971), the lower from Porath (1971).

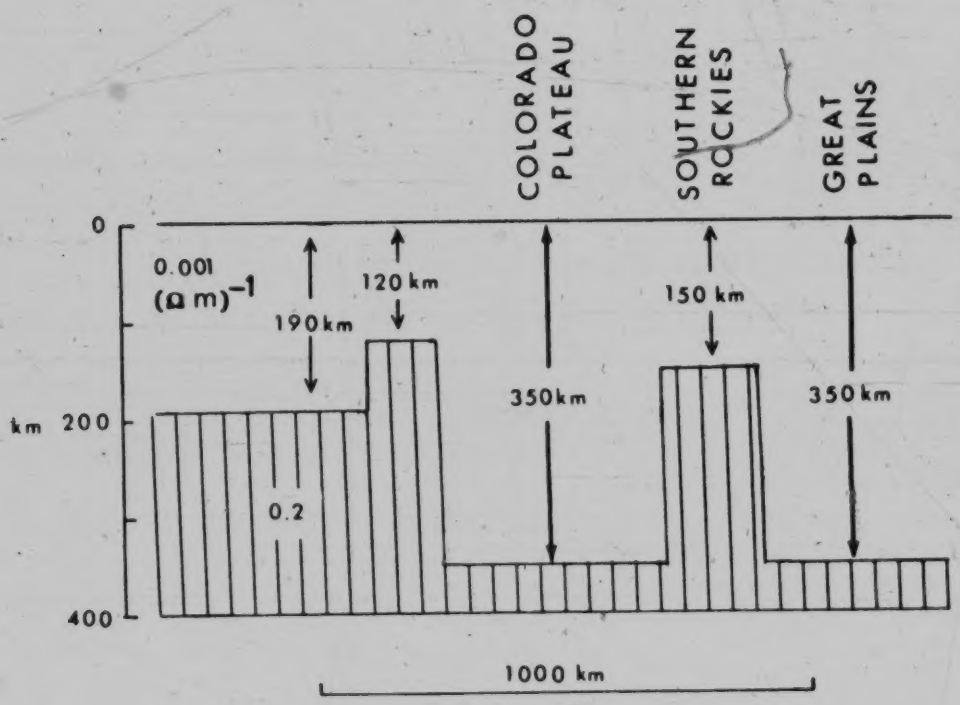
COLORADO PLATEAU
SOUTHERN ROCKIES
GREAT PLAINS
0
0.001 (Ω m)⁻¹
190 km
120 km
150 km
350 km
350 km
km 200
0.2
400
1000 km

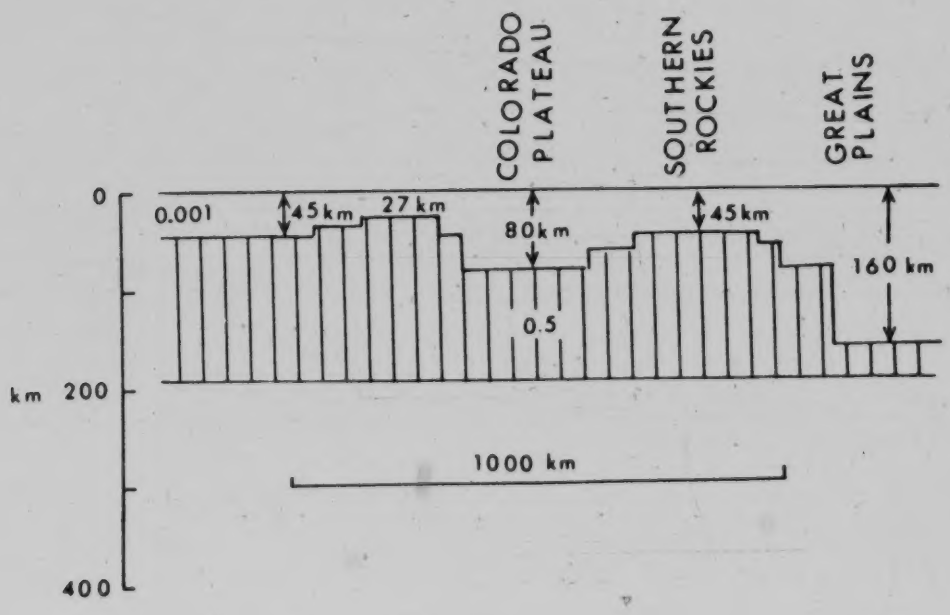
COLORADO PLATEAU
SOUTHERN ROCKIES
GREAT PLAINS
0
0.001
45 km
27 km
80 km
45 km
160 km
0.5
km 200
400
1000 km

point is that in either model the conductor under the Southern Rockies must be at least 100 km thick (with $\sigma = 0.2$ (ohm-m)$^{-1}$) to give the observed phase relationships. Hence the structure is thicker than the crust and must be, wholly or in part, in the upper mantle (Gough, 1973).

In several sets of Fourier spectral maps from the 1967 array, notably at period 89 minutes, an enhancement of the east-west horizontal and the vertical components was observed at the north-east corner of the array especially at Crawford, Nebraska. This was " . . . associated with a strong local increase in conductivity related to the Black Hills thermal area of South Dakota." (Reitzel et al., 1970).

3.2. The 1969 Magnetometer Array Study

A two-dimensional magnetometer array was operated in 1969 by the Universities of Alberta and Texas at Dallas. The array covered north western United States and south western Canada between latitudes 44° and 51° N. and between longitudes 100° and 121°W. A total of 46 stations on four east-west lines were used. The aim of the study was to map the northward continuation of the Southern Rockies and Wasatch Front anomalies. Magnetometers were arranged at close spacing over the Black Hills uplift to extend knowledge of the anomaly found there in 1967. Fig. 3.4 shows the array on a simplified tectonic map.

Numerous geomagnetic events were recorded. Camfield et al., (1971) chose three of them for detailed study. These

Fig. 3.4 The location of the stations operated in the 1969 array plotted on simplified tectonic map (Camfield, Gough and Porath, 1971; Camfield 1973). The trapezium in the figure indicates the area covered in the 1972 array.

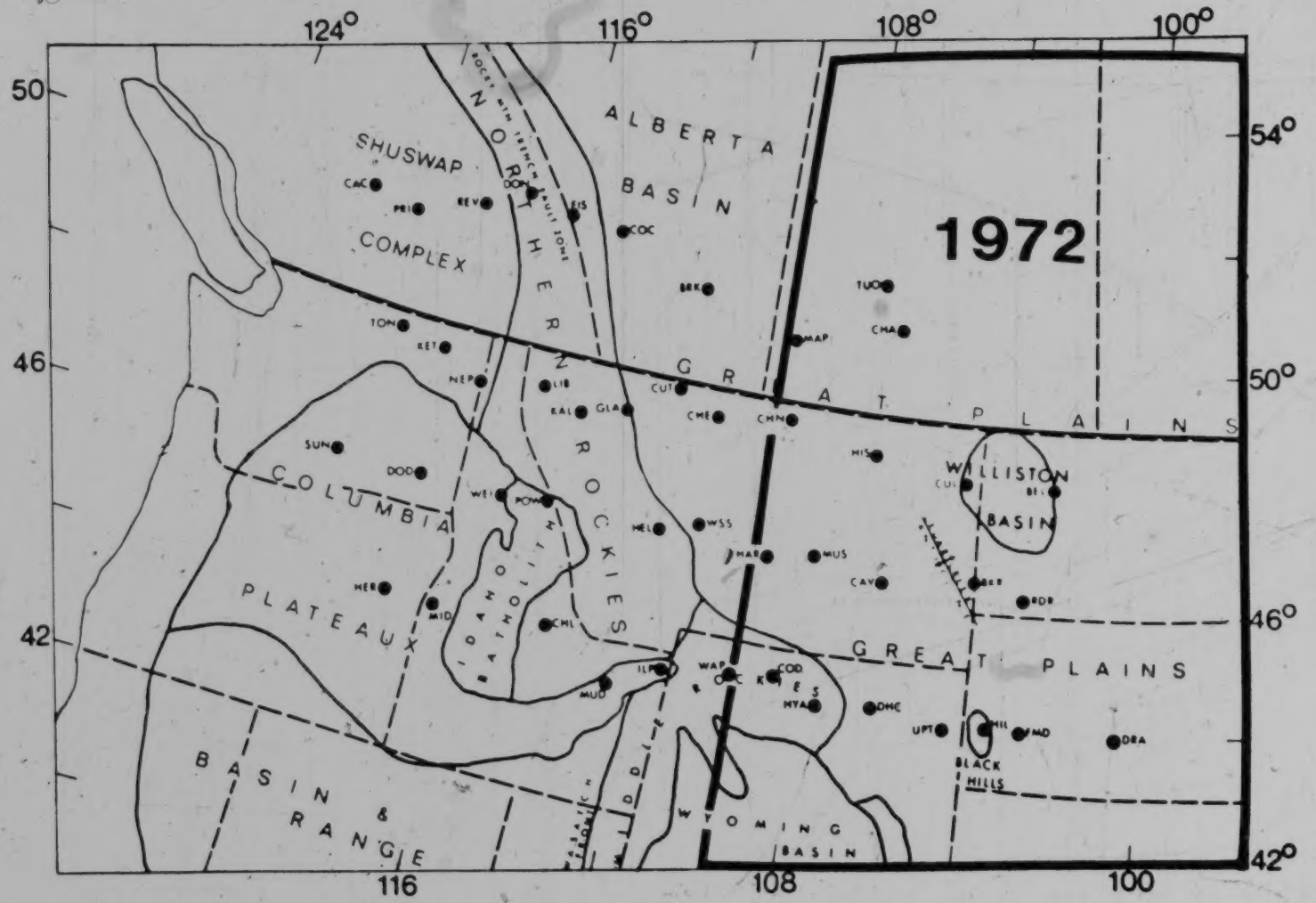
124°
116°
108°
100°
50
46
42
54°
50°
46°
42°
116
108
100
1972
SHUSWAP
COMPLEX
ALBERTA
BASIN
NORTHERN
ROCKIES
COLUMBIA
PLATEAUX
BASIN &
RANGE
GREAT PLAINS
WILLISTON
BASIN
WYOMING
BASIN
BLACK
HILLS
CAC
REV
EIS
COC
BRK
TUO
CHA
MAP
TON
KET
NEP
LIB
RAL
GLA
CUT
CHE
CHN
SUN
DOD
WES
POW
HEL
WSS
HAR
MUS
HIS
CAV
BEB
RDP
HER
MID
CHL
ILP
MUD
WAP
COD
MYA
OHC
UPT
HIL
MD
DRA

were a substorm of August 10, 1969, a portion of storm activity of August 12, and a disturbance event of August 20. Magnetograms of these events showed amplitude anomalies in Y and Z and phase anomalies in Z, consistent with long a line current whose axis passes close to HIL (Line 4), BKR (Line 3), CUL (Line 2), and flows under the Black Hills (Fig. 3.4). Line 1 did not extend eastward far enough to yield any information as to whether the current continues further north or not.

Camfield, Gough and Porath (1971) (see also Camfield, 1973) took Fourier transforms of the variation events and drew maps of Fourier amplitudes and phases at the following periods; 47.6 minutes (for the event of August 10), 40.2 minutes (for the event of August 12), 25.3, 47.6, 85.3 and 102.4 minutes (for the event of August 20). In all the amplitude and phase maps for the Y and Z components the North American Central Plains anomaly associated with the Black Hills was the dominant feature. Fig. 3.5 shows Fourier amplitude and phase maps at period 47.6 minutes from the August 10 substorm. The anomaly as observed from the Fourier maps has large amplitude and small width. To first order, it could be modelled by a line current under the maximum in the geographic eastward (Y) field. Camfield et al., (1971) used their anomaly maps to conclude that the conductor strikes northward from the eastern edge of the Black Hills along the boundary between Montana and the Dakotas. They conjectured that it might continue into Saskatchewan. The half-width of the anomaly was estimated to be 75 km on

Fig. 3.5. Fourier spectral maps at period 47.6 minutes. The amplitudes are in arbitrary units while the phases are in minutes (Camfield et al., 1971).

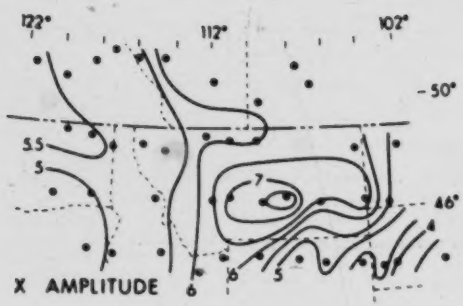
122°
112°
102°
50°
46°
X AMPLITUDE

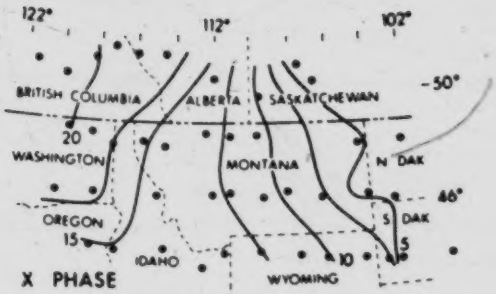
122°
112°
102°
50°
46°
BRITISH COLUMBIA
ALBERTA
SASKATCHEWAN
WASHINGTON
MONTANA
N DAK
S DAK
OREGON
IDAHO
WYOMING
X PHASE

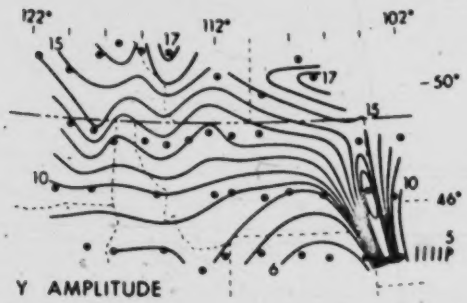
122°
112°
102°
50°
46°
Y AMPLITUDE

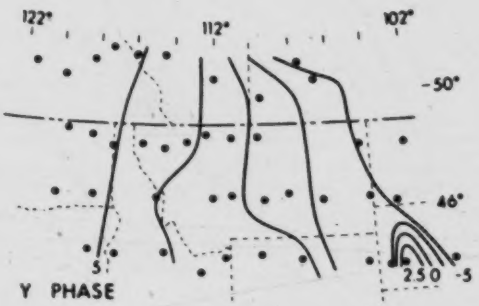
122°
112°
102°
50°
46°
Y PHASE

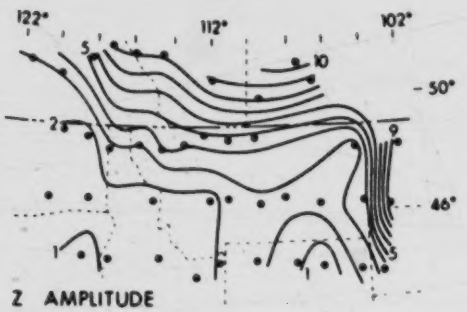
122°
112°
102°
50°
46°
Z AMPLITUDE

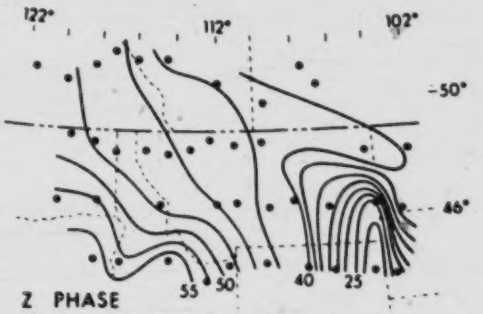
122°
112°
102°
50°
46°
Z PHASE

line 4, so that the depth of a line current was 38 km and the depth to a distributed conductor no greater than this. On lines 2 and 3 the anomaly half-width was less well-defined because of the large spacing between stations. The present study gives better definition of the anomaly.

Camfield, Gough and Porath (1971) suggested a tentative physical explanation of the local conductor. They proposed the presence of an elongated belt of metamorphic rocks containing graphite schist in the crust under the Black Hills as a possible cause of the anomalously high conductivity in this region. Mathisrud and Sumner (1967) using the induced polarization exploration technique had observed high conductivity values in the Lead district in western South Dakota. Lidiak (1971), using gravity and (static) magnetic observations combined with bore-hole data, proposed independently a metamorphic belt in exact coincidence with the North American Central Plains conductivity anomaly in South Dakota, lending strong support to the hypothesis of Camfield et al., (1971) of a compositional conductor in the crust (Gough & Camfield, 1972).

Porath, Gough and Camfield (1971) attempted to model the conductive body as a two-dimensional body using the transmission line analogy method of Madden and Swift (1969) (Chapter I). On line 4 of the 1969 array, the Z_a and D_a anomalous fields were normalized with respect to the normal D_n field regarding the fields observed at HYA and DRA as normal fields. Fig. 3.6 shows the normalized anomalous field amplitudes

Fig. 3.6 Profiles of the normalized anomalous fields across the Black Hills uplift (Porath et al., 1971)

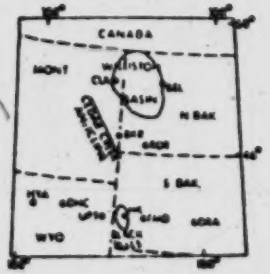

Normalized anomalous fields

$o - D_e / D_N$

$x - Z / D_N$

100 km

1969 August 10

T = 24·4 min

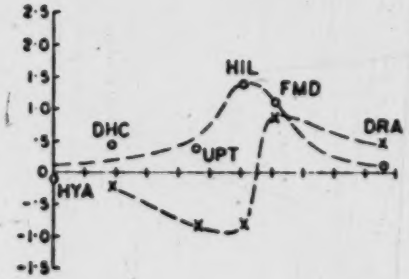

T = 50 min

T = 120·5 min

1969 August 20

T = 25·3 min

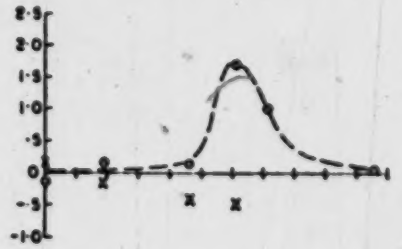

T = 47·6 min

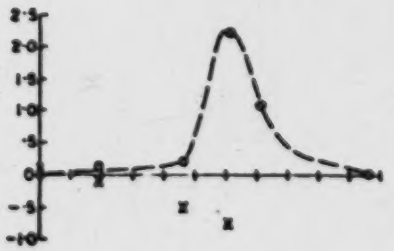

T = 85·3 min

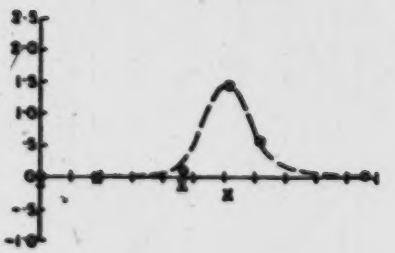

(Z_a/D_n and D_a/D_n) at periods 24.4, 25.3, 47.6, 50.0, 85.3 and 120 minutes. As observed from this figure, the amplitudes of the normalized anomalous fields depend strongly on period. The maximum amplitude occurred near period 50 minutes. The profile of normalized Z_a was displaced to the east with respect to the D_a amplitude. This was interpreted as due to either insufficiently close station spacing or to the presence of a significant normal Z field. At the period of 50 minutes a conductor 30 km wide and 3 km thick buried at a depth of 2 km from the surface and having a conductivity of 10 (ohm m)$^{-1}$ gave a response that fits the observed small phase difference. The amplitude response of the model changed very little with period. This is in conflict with observation. The agreement in phase became worse when the conductivity of the model was varied. No model was found which fitted both the phase difference and the period dependence observed.

The failure of the attempt to model the conductor in two dimensions was explained by Porath et al., (1971) as indicating the structure is in fact three-dimensional. A long narrow conductor in the crust under the North American central plains and the Black Hills of South Dakota channels currents induced in large undefined regions of the Earth. Modelling of such a three-dimensional body by numerical methods is only now being developed (Lines and Jones, 1973) and is still strongly limited by computing costs.

The study reported in this thesis was aimed at mapping the northward continuation of the anomaly, at securing improved coverage of the central part of the structure in South Dakota and at studying the relation between the southern end of the Black Hills conductor and that under the Southern Rockies.

CHAPTER IV

THE ARRAY STUDY OF 1972

4.1. The Observations

Forty-two magnetometers were operated in the North American Central Plains jointly by the University of Alberta and the Earth Physics Branch (EPB) of the department of Energy, Mines and Resources, (EMR), Government of Canada. Twenty-four of the instruments of the type described by Gough and Reitzel (1967), were operated by the writer under the guidance of Professor D. I. Gough. Fifteen fluxgate magnetometers were operated by Dr. P. A. Camfield of EPB. Magnetograms were obtained from the standard magnetic observatory of Meanook (MEA). At Norway House (NGV) and Winnipeg (WPG), the magnetograms were those acquired from the Space Physics Division EMR. The array occupied a region between latitudes 41.7° and 58°N and between longitudes 95° and 119° W (see Fig. 4.1).

The forty-two instruments were arranged on eight approximately east-west lines. On lines 1 through 4, from north to south counting, fluxgate magnetometers recorded the fields and on lines 5 through 8 and at SMI (Fig. 4.1) on line 4 Gough-Reitzel magnetometers were operated. The spacing between east-west lines ranged from 120 to 240 km. On the three northernmost lines, the spacing between stations averaged

Fig. 1.1 The location of the stations in the 1972 array drawn on a simplified tectonic map.

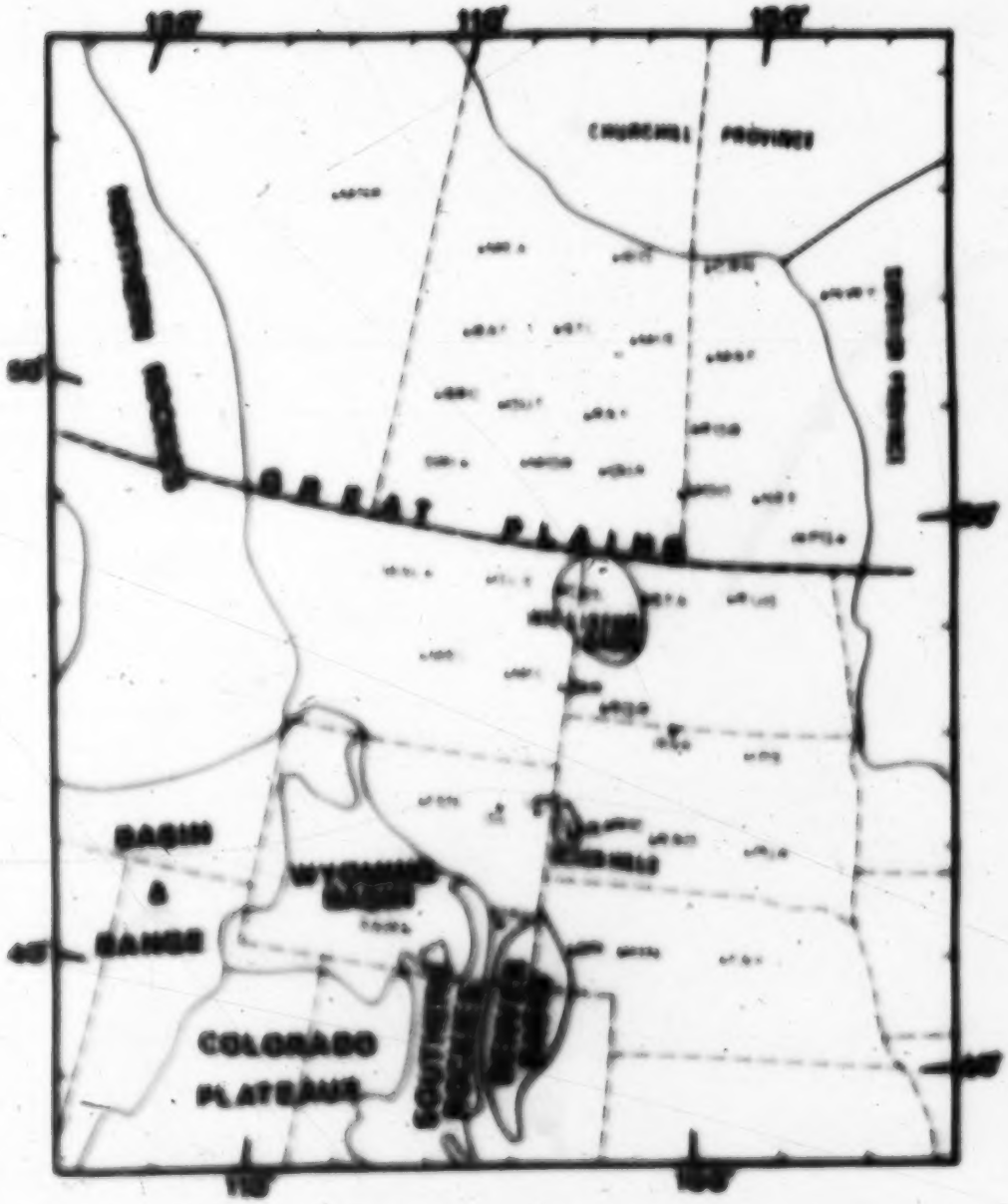
110°
110°
110°
CHURCHILL PROVINCE
GREAT PLAINS
BASIN
&
RANGE
WYOMING
BASIN
COLORADO
PLATEAUS
COLORADO
PLATEAUS
110°
110°

200 km, but considerably less (order of 130 km) on the other lines. Close to the axis of the anomaly the spacing was less than 100 km. Stations code names are given in Fig. 4.1. The geographic co-ordinates and magnetic declinations at the stations are given in Appendix A.

The observation period of nine weeks began in early August and the first instrument was retrieved by the end of September. The instruments were serviced at 21 day intervals. The whole field season, including installation lasted three months and involved driving about 10,000 miles by each of the two research groups.

The usual field procedure has been described excellently by Canfield (1971) and will not be repeated here. For the 1972 field season the tuning-fork controlled electric keyboard timers, used on the magnetometers in previous arrays, were replaced with solid-state electronic clocks powered by four 1.35 batteries. The use of these clocks designed by W. H. G. Burke enhanced the efficiency of the array very considerably.

4.1 Magnetograms

Several disturbance events were recorded by the array. All the magnetograms were visually inspected and six events were selected with different polarizations and which were recorded by not less than 10 of the 12 magnetometers. They were digitized and reduced for analysis. Table 4.1 shows the

TABLE 4.1.

The dates, times of occurrence and types of disturbance events. The K_p indices refer to eight 3-hour periods through the day

Date	Time (UT)	Type of Event	K_p Indices
August 28/73	0910-1210	Substorm	1o1o1o1-1-1o1-1+
August 10/73	1010-1310	Substorm	1o1-0+2o2o1o1+2o2-
August 11/73	1400-1800	Substorm	1-2+1-1-1o1+1o1o
September 8/73	0300-0400	Pulsation	2+2+2o2+2+2o2o1-
September 12/73	0110-0910	Substorm	1+1-2o2-1o1-1-0+
September 15/73	1400-1800	Part of Storm	1o2-1-1+1-0-1+0-

dates, the time intervals and K_p indices for the six events. The events were classified into types on the basis of visual examination of magnetograms in the high-, middle- and low-latitudes. The help of Mr. R. Wiens in this examination is acknowledged. Four of the events were isolated polar magnetic substorms. A brief review of the nature of substorms is given in Appendix B. A full discussion is given by Rostoker (1972).

For a preliminary inspection of the variation anomaly, the sets of normalised time series representing the three orthogonal components in the geographic (X northward, Y eastward, Z downward positive) coordinate system were plotted by means of a calcomp plotter in stacks. Each stack of magnetograms shows data acquired from an east-west line of stations, the easternmost station is at the top. The lines are numbered from 1 to 8, line 1 being the northernmost while line 8 is the southernmost line. Time marks are in Universal Time (UT) and the local midnight in the centre of the array is around 0700 UT. Scale bars relate the amplitudes to gamma ($1\gamma = 10^{-9}$ tesla = 10^{-5} oersted). For each event all the magnetograms are plotted with the same scale unless otherwise indicated.

As earlier stated the variation anomaly can be considered to be made up of a normal part with a superimposed local anomalous part. The magnetograms from the 1969 array revealed the north American (normal plains) anomaly as a reversal

in Z accompanied by an enhancement in Y on lines of magnetograms which crossed the anomaly (Chapter III). On a line of magnetograms across a region where there is linear conductivity anomaly in the upper mantle, the features of the fields of a dipping line-current would be expected. The dipping current can be pictured as consisting of two components, horizontal and vertical. The horizontal component would produce an enhancement of the eastward horizontal field over the axis and vertical fields of opposite signs on either sides of the axis. The vertical current component gives rise to northward horizontal fields of opposite signs on either sides of the axis such that if the normal northward horizontal field is enhanced on one side it is reduced on the other. These features and others are to be found in the sets of magnetograms displayed in this chapter.

4.2.1 Event of August 28, 1972

Figs. 4.2a through 4.2d show the set of magnetograms for the moderate substorm of August 28. The visual examination of magnetograms at high-, middle- and low- latitudes described in the Appendix B shows that the westward electrojet associated with this event flows well north of line 1 of the 1972 array (north of COLLEGE, see Fig. B-2 in Appendix B). On lines 1, 2, and 3 however, the source effect is still observed as large amplitudes in all the three magnetic components and strong resemblance between the waveform of Z and of X.

Fig. 4.2a. Magnetograms for the substorm of August 28 1972, lines 1 and 2.

AUGUST 28 1972

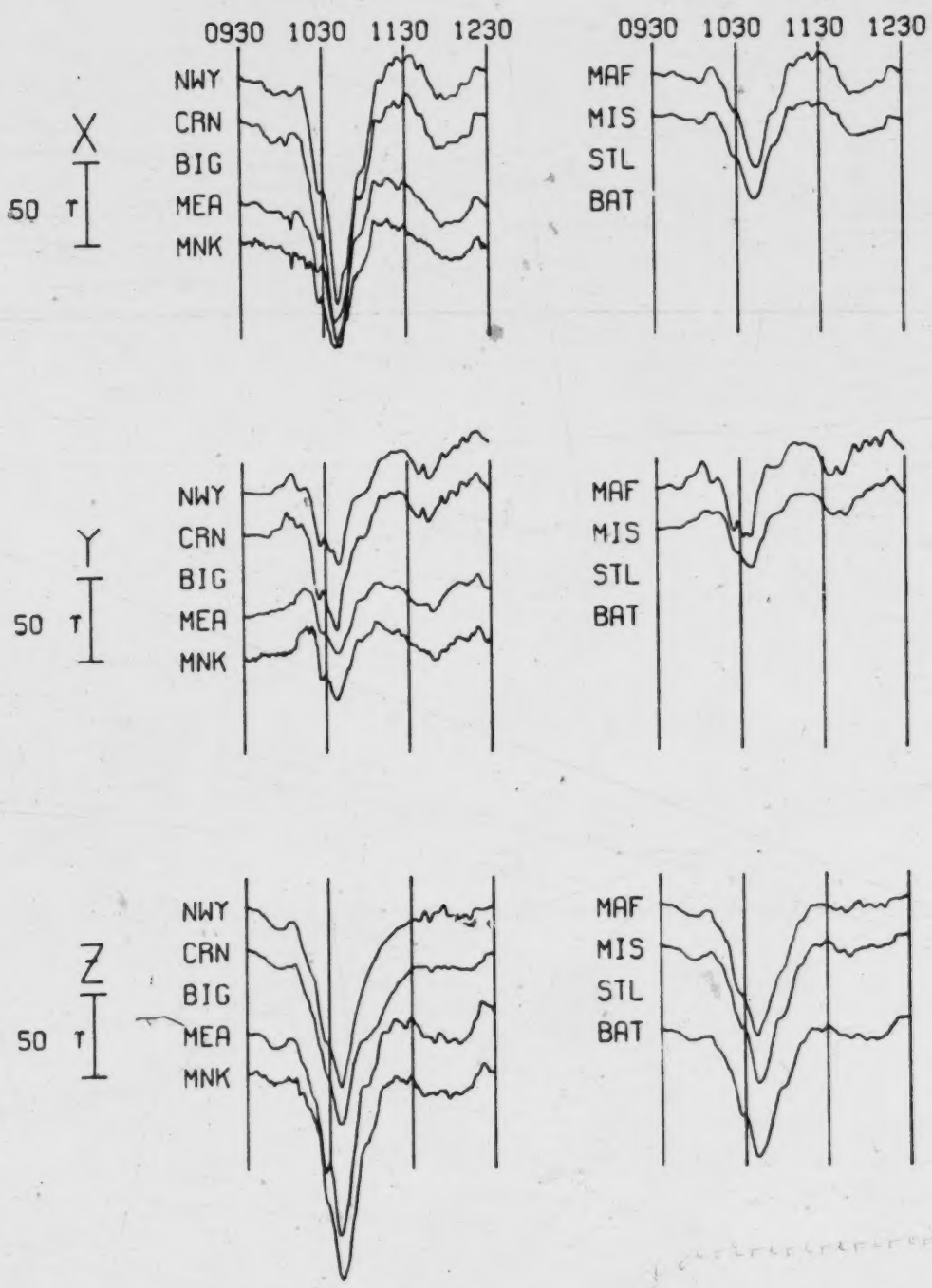

Fig. 4.2b. Magnetograms for the substorm of August 28 1972, lines 3 and 4.

AUGUST 28 1972

LINE 3

LINE 4

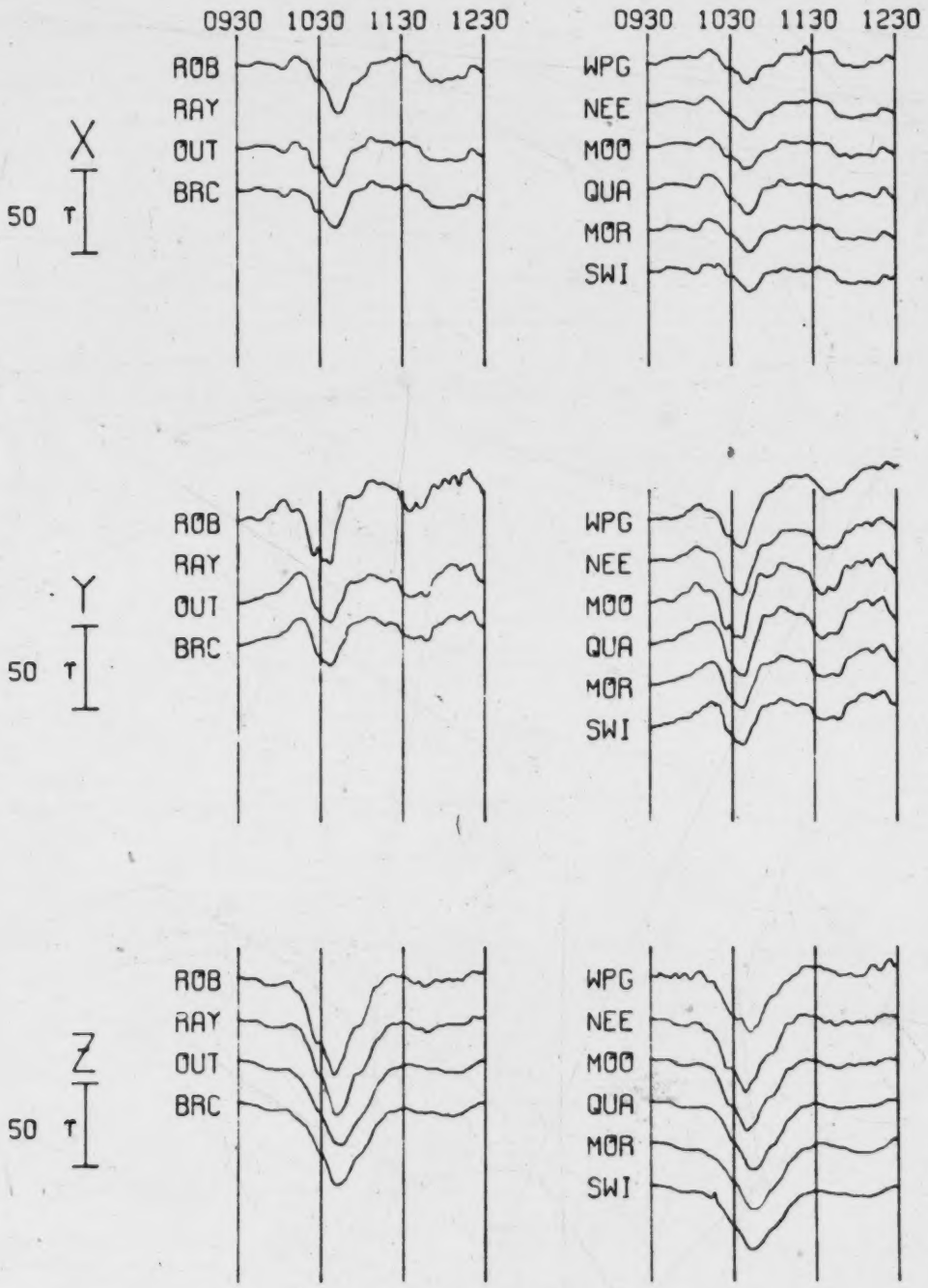

Fig. 4.2c. Magnetograms for the substorm of August 28 1972, lines 5 and 6.

AUGUST 28 1972

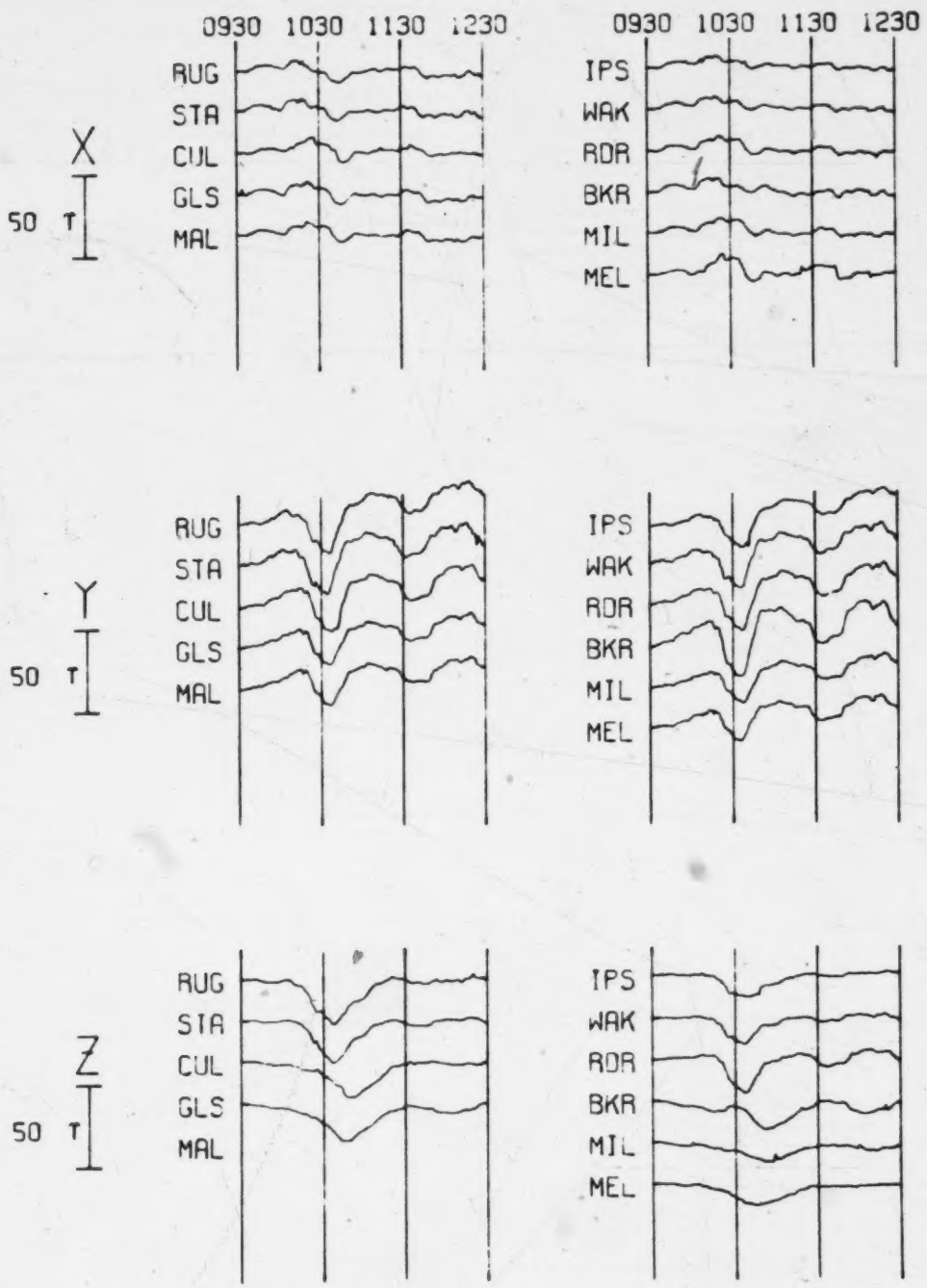

Fig. 4.2d. Magnetograms for the substorm of August 28 1972, lines 7 and 8.

AUGUST 28 1972

LINE 7

LINE 8

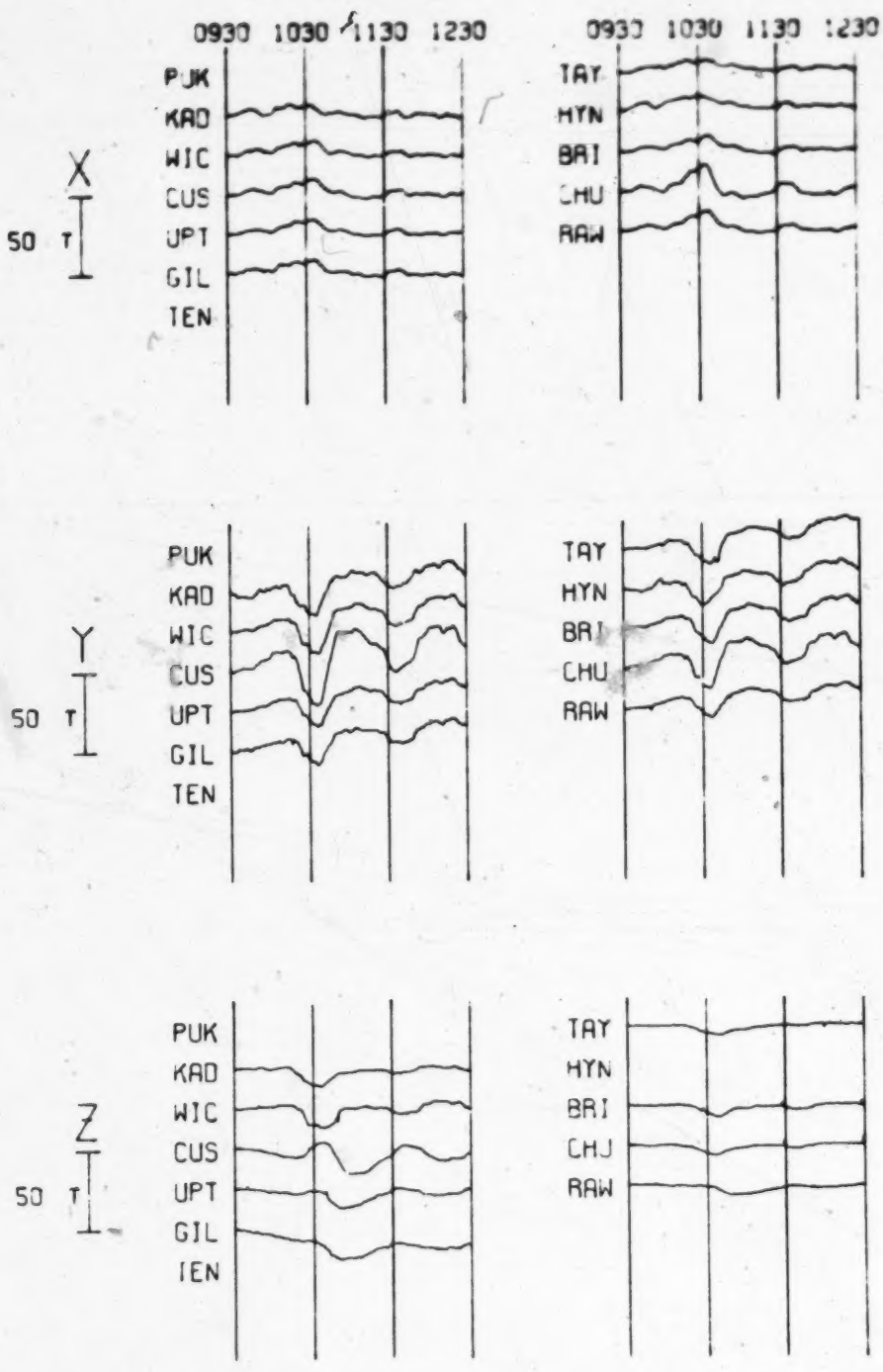

On line 4, the resemblance between X and Z is reduced considerably. The eastern group of stations (WPG, NEE, MOO) leads the western group (QUA, MOR, SWI) in the phase of the Z variation field (see Fig. 4.2b). This phenomenon is consistent with the presence of a linear conductor passing somewhere between MOO and QUA. Line 4 of the 1972 array corresponds with and extends eastward line 1 of the 1969 array which did not detect the anomaly. It is now clear that the 1969 stations on this line all lay to the west of the anomaly. In line 5 the eastern stations (RUG, STA) lead the western stations (CUL, GLS) in the phase of Z (Fig. 4.2c). Unfortunately Z was not recorded at MAL for any of the six events analyzed. The phase anomalies in Z on lines 4 and 5 are not accompanied by appreciable amplitude changes in the horizontal fields, presumably because the source field dominates the latter.

On line 6 BKR (Fig. 4.2c) and stations west of it exhibit reversed phase in Z relative to stations east of BKR. The amplitude of Y is appreciably enhanced at BKR in a manner consistent with a current passing just east of BKR. In Fig. 4.2d at line 7, Y has a strongly increased amplitude at CUS and Z is reversed in phase between WIC and CUS (a distance of 70 km). The current axis clearly passes just east of CUS.

On line 8 between RAW and CHU Z although small in amplitude is reversed in phase and Y has increased amplitude at CHU (Fig. 4.2d). X amplitude at CHU is larger than at RAW. These features in X, Y and Z between RAW and CHU are consistent with those of a crustal linear conductor dipping to merge with a deeper upper mantle conductor. Hence, it is suggested here that the narrow crustal conductive body in the North American Central Plains swings southwest of the Black Hills to make an almost vertical link with the Southern Rockies upper mantle conductor reported by Reitzel et al., (1970). As will be seen later, magnetograms across line 8 for other events exhibit the same features.

At TAY, Z is significantly damped. This is perhaps due to thicker sedimentary layer around TAY.

4.2.2 The Event of August 30, 1972

A moderate substorm occurred after local midnight on August 30, 1972. Figs. 4.3a through 4.3d are the magnetograms for the event. In Fig. 4.3a, the event has the appearance of two superimposed bay-type events especially for X and Y. The first and larger substorm occurred between 0900 and 1100 UT. The westward electrojet causing the substorm had its axis between COLLEGE and BARROW and passed between BAKERLAKE and CHURCHILL to the north of the array (see Fig. B-2 in Appendix B for the locations of these stations). On lines

Fig. 4.3a Magnetograms for the substorm of August 30 1972, lines 1 and 2.

AUGUST 30 1972

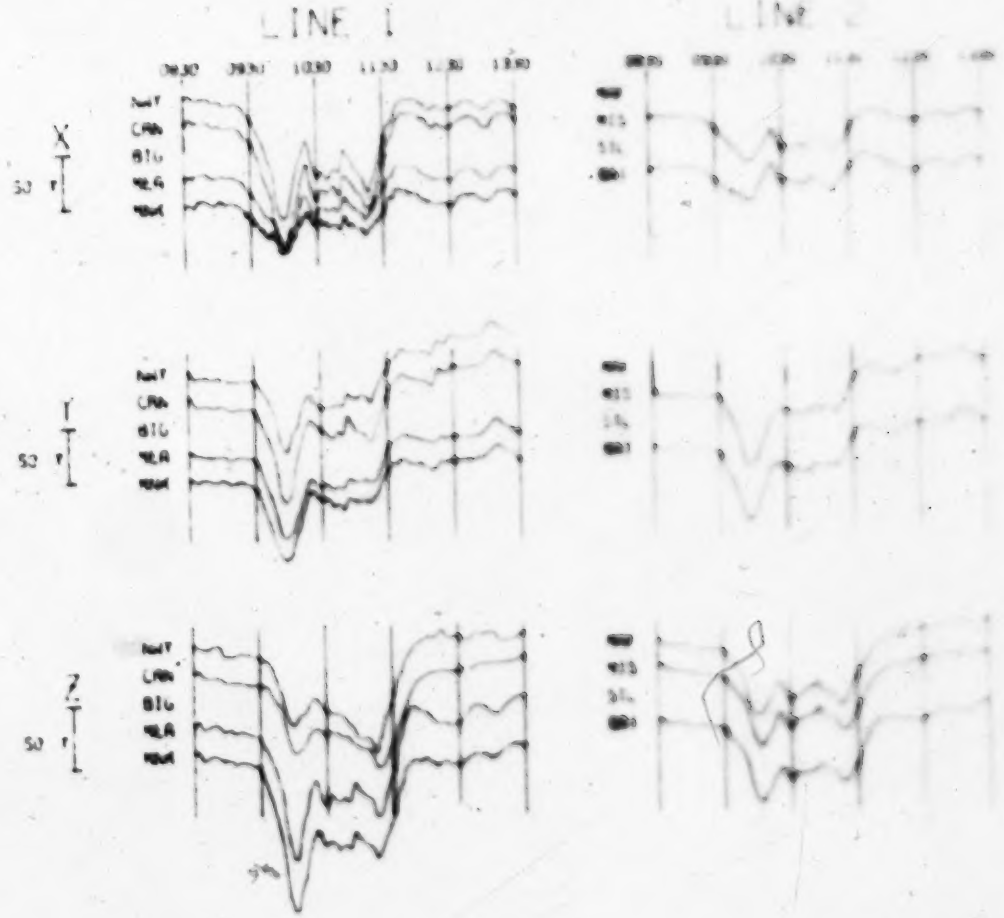

Fig. 4.3b Magnetograms for the substorm of August 30 1972, lines 3 and 4.

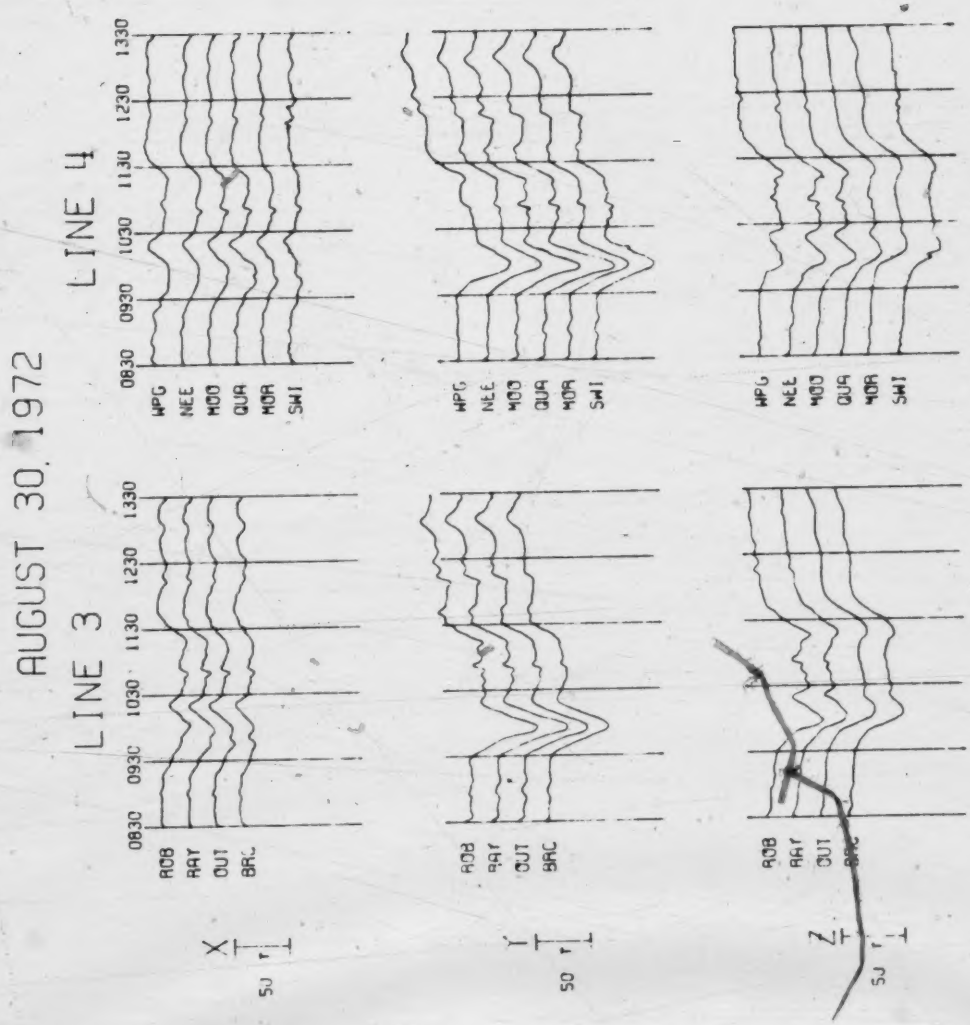
AUGUST 30, 1972
LINE 3
LINE 4
0830
0930
1030
1130
1230
1330
ROB
RAY
OUT
BRC
WPG
NEE
MOO
QUA
MOR
SWI
X
Y
Z
50

Fig. 4.3c Magnetograms for the substorm of August 30 1972, lines 5 and 6.

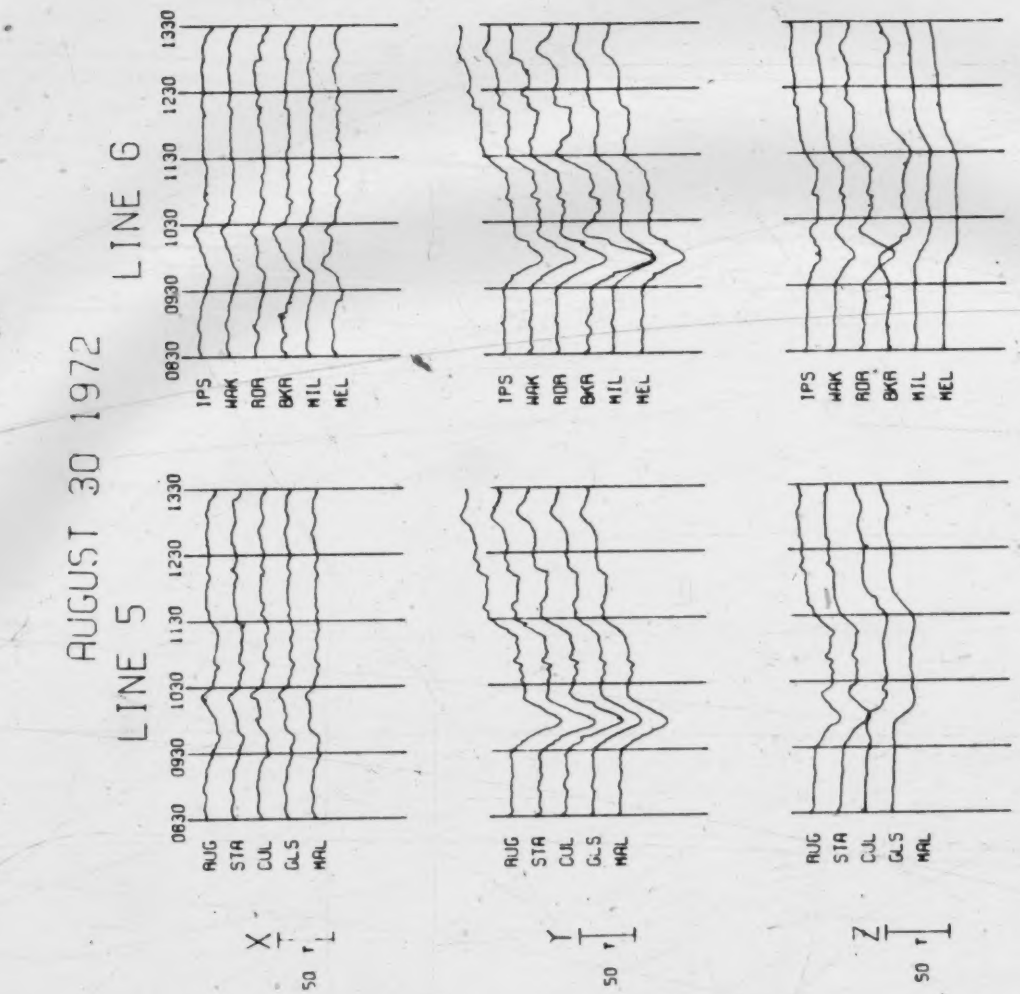
AUGUST 30 1972
LINE 5
LINE 6
0830
0930
1030
1130
1230
1330
AUG
STA
CUL
GLS
MAL
IPS
WAK
ADA
BKA
MIL
MEL
X
Y
Z
50

Fig. 4.3d Magnetograms for the substorm of August 30 1972, lines 7 and 8.

AUGUST 30 1972

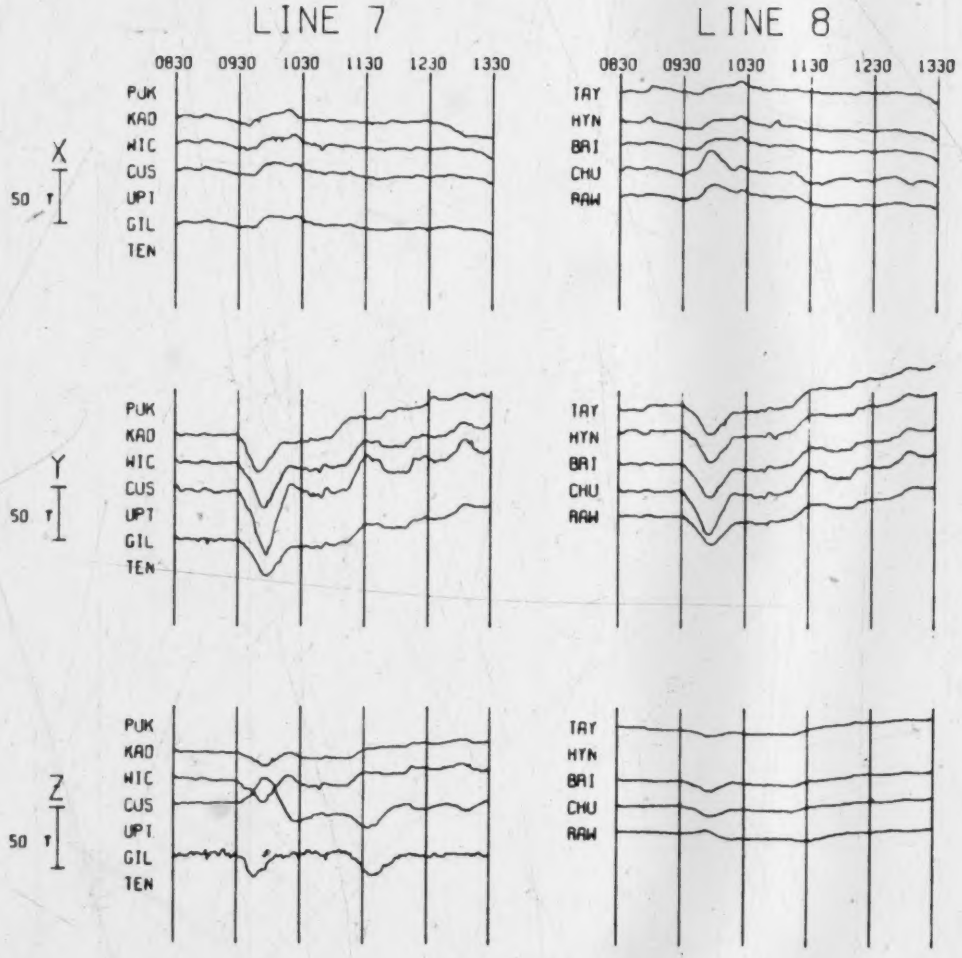

1 and 2 the fields are largely those of the source currents to the north. On line 3 however (Fig. 4.3b), the source effect has diminished. The Z phase shift phenomenon is noticed between RAY and the group of stations west of it. This effect is similarly noticed on line 4 between MOO and QUA. If this indicates a strong linear current, then it appears that the conductor passing through the Black Hills extends northward to latitude 52° N or even beyond.

On the lines in the United States, Z phase reversals occurred between STA and CUL (line 5) between RDR and BKR (line 6) between WIC and CUS (line 7) and between CHU and RAW (line 8) (Figs. 4.3c,d). Enhancements of Y are noticed at CUL (line 5), at BKR (line 6), at CUS (line 7) and X and Y are both enhanced at CHU (line 8). The location of the current under maximum Y for this event yields exactly the same result for the four southern lines as was obtained for the event of August 28.

X amplitude suffers gradual damping from north to south. The normal Y suffers small amplitude attenuation from north to south. This is consistent with the 3-dimensional current source for the event.

On line 7, Z at GIL was digitized manually as the traces were too faint to be recognized by the flying-spot scanner. Most of it was near the edge of the film. The higher noise level on this trace is evident. A reversal of Z at GIL relative to CUS (see Fig. 4.3c) may be present for

the start of the event but is not consistent throughout the magnetogram, in contrast to the reversal between WIC and CUS.

4.2.3. The Event of August 31, 1972

The disturbance of August 31 between 0400 and 1000 UT whose magnetograms are shown in Figs. 4.4a through 4.4d consists of two consecutive substorms. The first substorm occurred between 0430 and 0630 and the second between 0630 and 0830 UT. The first one exhibits a positive D (and Y) variation field while the second has a negative D field (see Fig. 4.4a). Thus, it may be concluded that the array was west of the central meridian of a westward electrojet between 0430 and 0630 and east of it between 0630 and 0830 (Rostoker et al., 1970). For both substorms, the electrojets were north of the array. This difference in the position of the array relative to the central meridian of the electrojet gives rise to the same Z phase shifts as will be shown below.

On lines 1 and 2 (Fig. 4.4a), all the field components have large amplitudes, presumably mainly source fields. From line 3 southward X exhibits gradual reduction in amplitude. On line 3 (Fig. 4.4b) for this substorm occurring between 0430 and 0630 UT, the eastern stations ROB and RAY show a phase lead of about 6 minutes in Z relative to the western stations OUT, BRC. For the second substorm (0530-0830 UT), this phase difference is again a phase lead of the eastern group of stations relative to the western group. A shift in phase is noticed between MOO and QUA on line 4 in similar fashion

Fig. 4.4a Magnetograms for the substorms of August 31 1972, lines 1 and 2.

AUGUST 31 1972

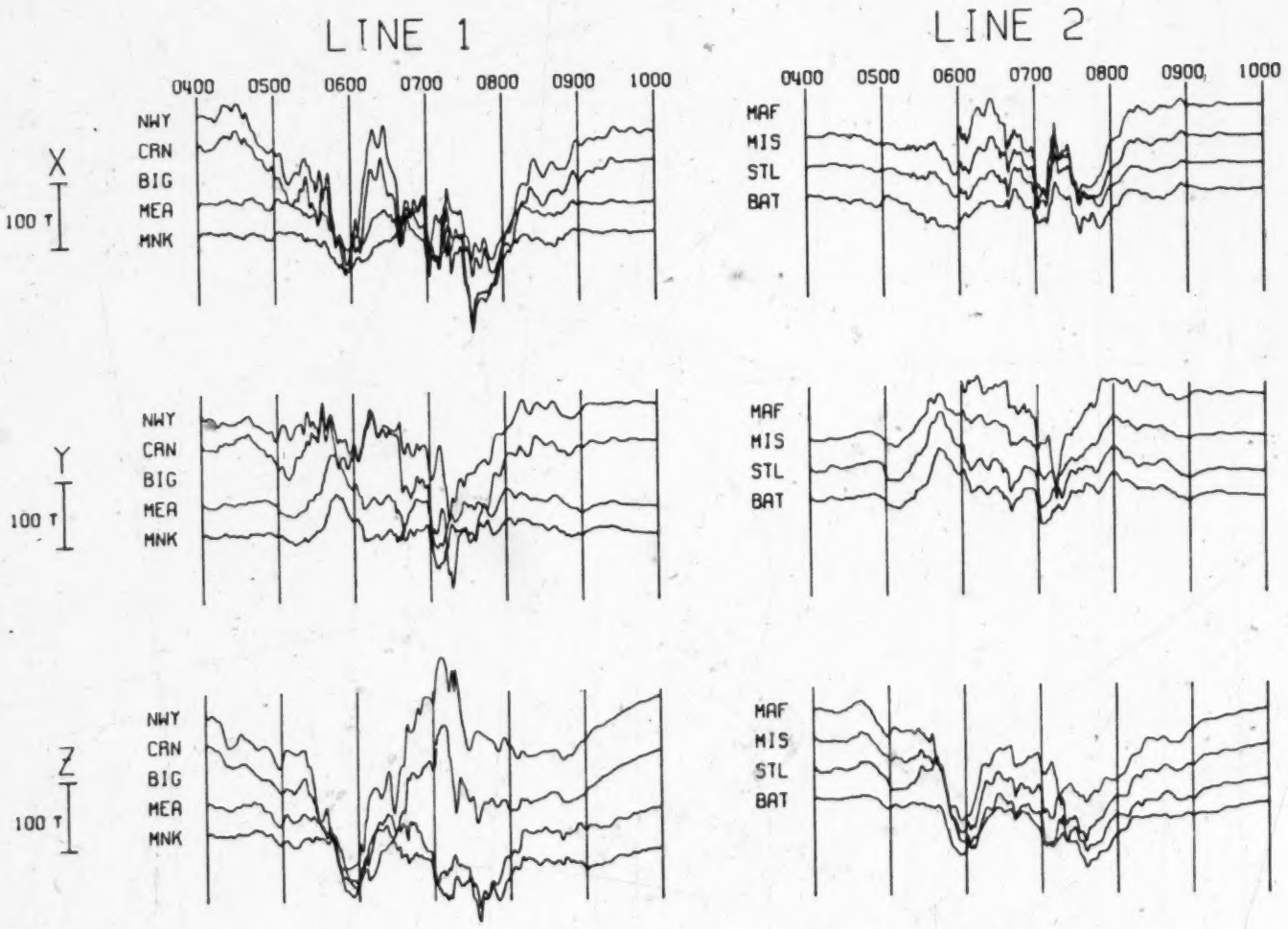

Fig. 4.4b Magnetograms for the substorms of August 31 1972, lines 3 and 4.

AUGUST 31 1972

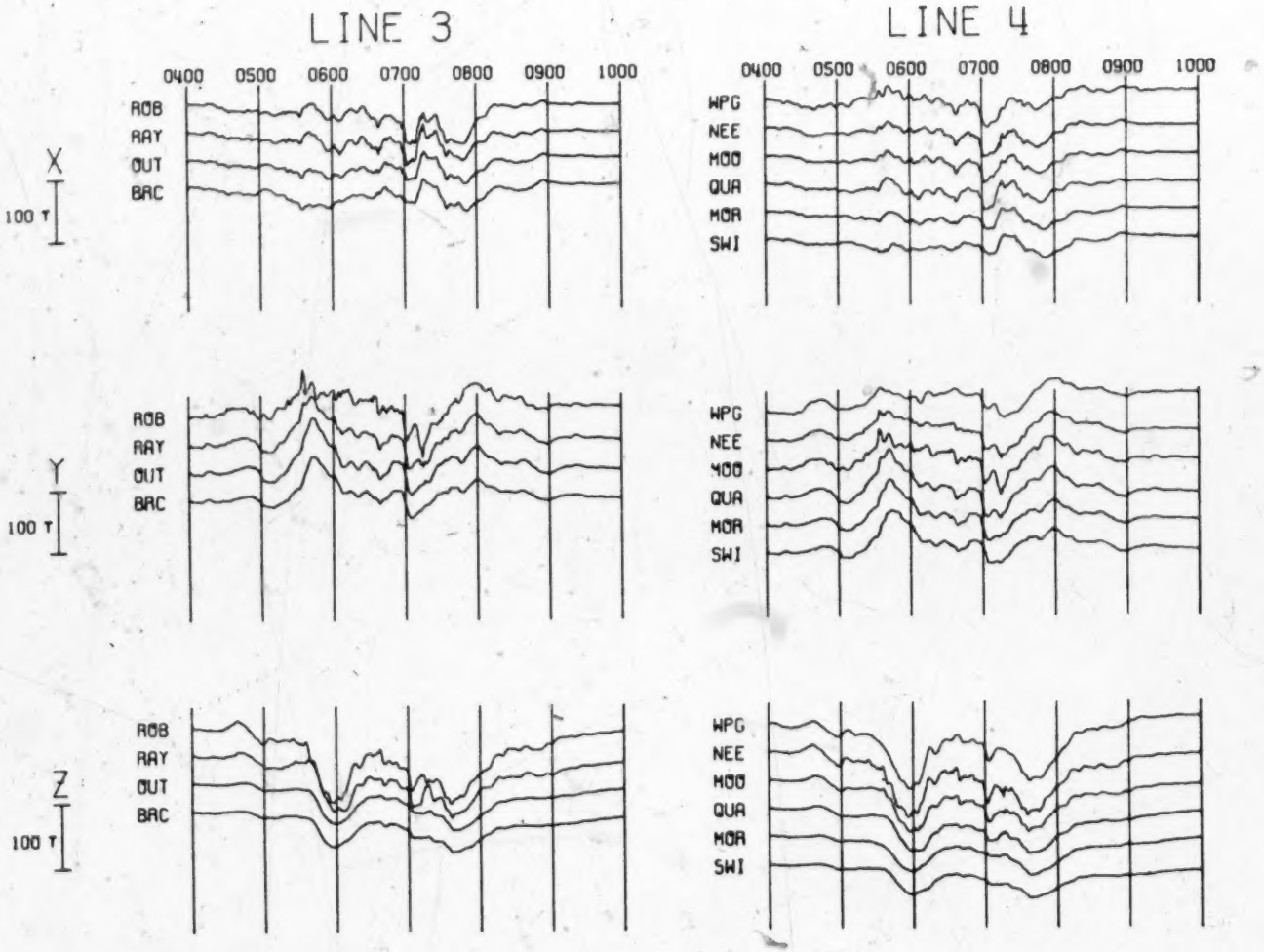

Fig. 4.4c Magnetograms for the substorms of August 31 1972, lines 5 and 6.

AUGUST 31 1972

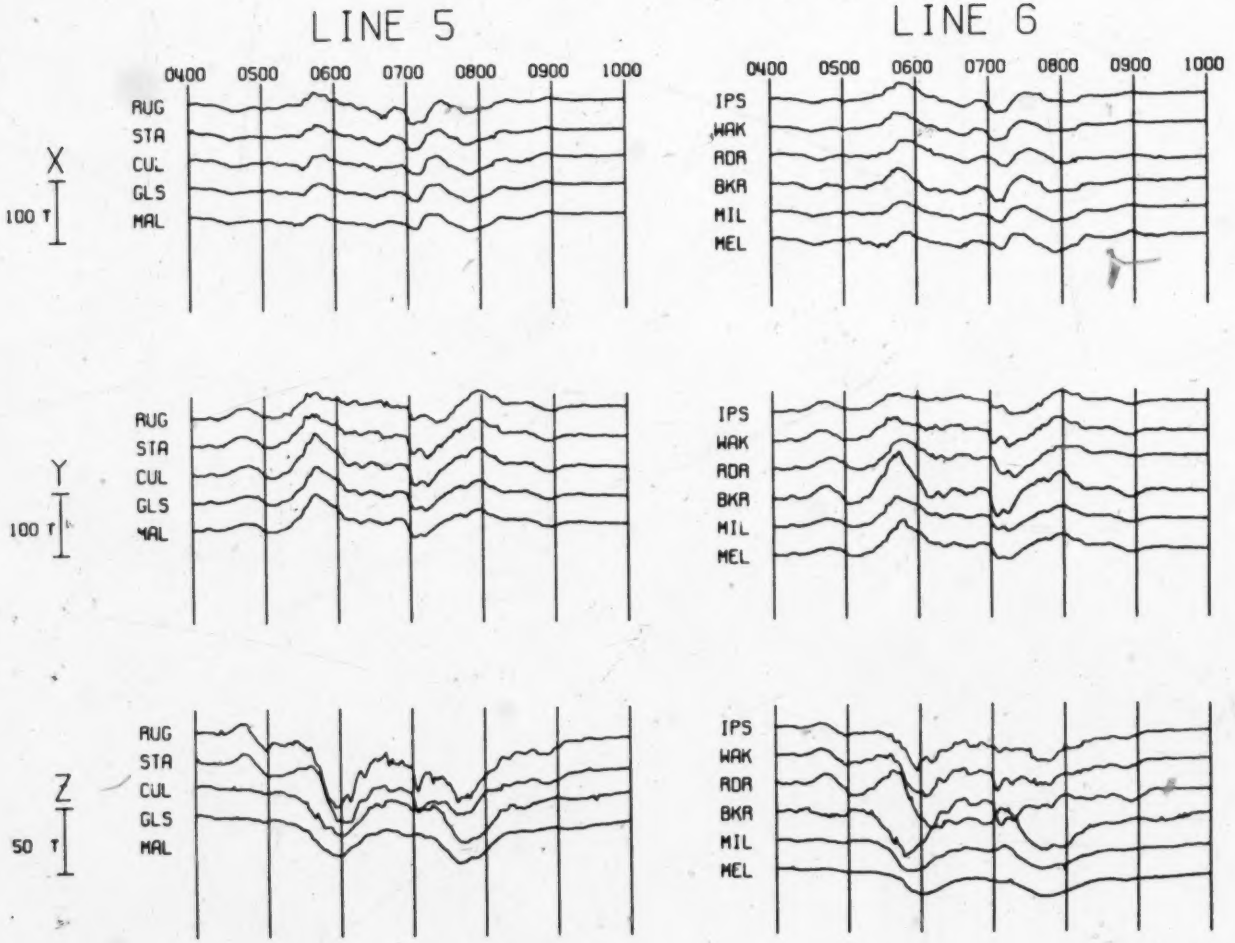

Fig. 4.4d Magnetograms for the substorms of August 31 1972, lines 7 and 8.

AUGUST 31 1972

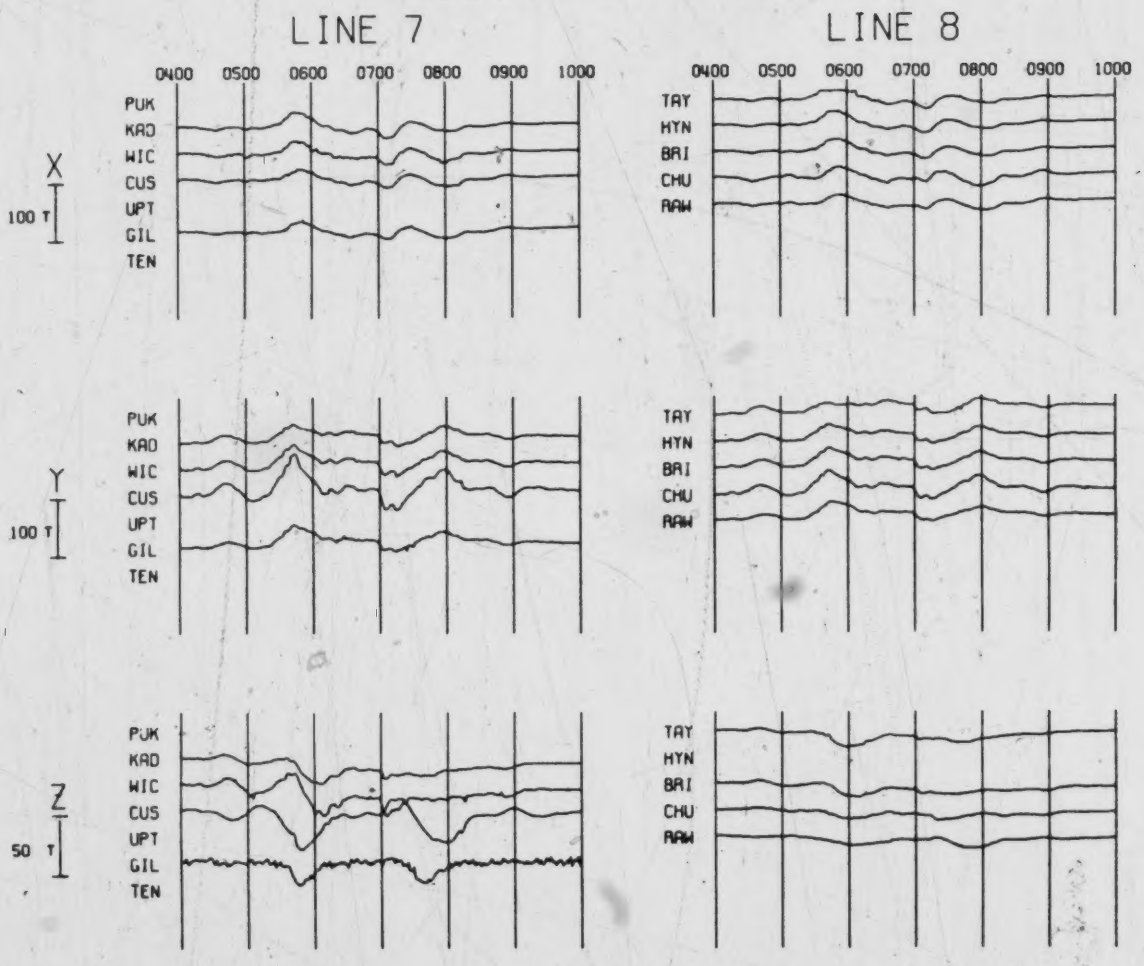

(Fig. 4.4b). The phase shift of about 6 minutes noticed between stations separated by less than 150 km is suggestive of the presence of a conductivity anomaly.

From line 5 downward, the Z magnetograms have been plotted at increased scale to bring out the features contained in the record very clearly. A phase shift of about 6 minutes is observed between STA and CUL on line 5 (Fig. 4.4c) and an enhanced Y at CUL. Z is reversed between BKR and RDR (line 6 Fig. 4.4c) and is enhanced at BKR for both substorms. On line 7, there is a clear reversal in Z phase between WIC and CUS and at CUS (line 7, Fig. 4.4d) the Y normal field is reinforced by anomalous Y field.

On line 8 as before RAW shows a Z trace that is reversed relative to that at CHU. X and Y are both of enhanced amplitude at CHU. These features at CHU and RAW have been observed in all the three variation fields events so far considered. That this is a signature of the disappearance of the crustal anomaly in the North American Central Plains into the upper mantle anomaly under the Southern Rockies is becoming increasingly probable.

4.2.4. The Event of September 8, 1972

Figs. 4.5a through 4.5d show the magnetograms for a pulsation (possibly Pc 5; see Jacobs, 1970) occur on September 8 between 0200 and 0400 U.T. The K_p figures of 2+, 2+ for the period of occurrence (Table 4.1) show that the period was magnetically quiet. This event is worldwide with

Fig. 4.5a The magnetograms for the pulsation of September 08 1972, lines 1 and 2.

SEPTEMBER 08 1972

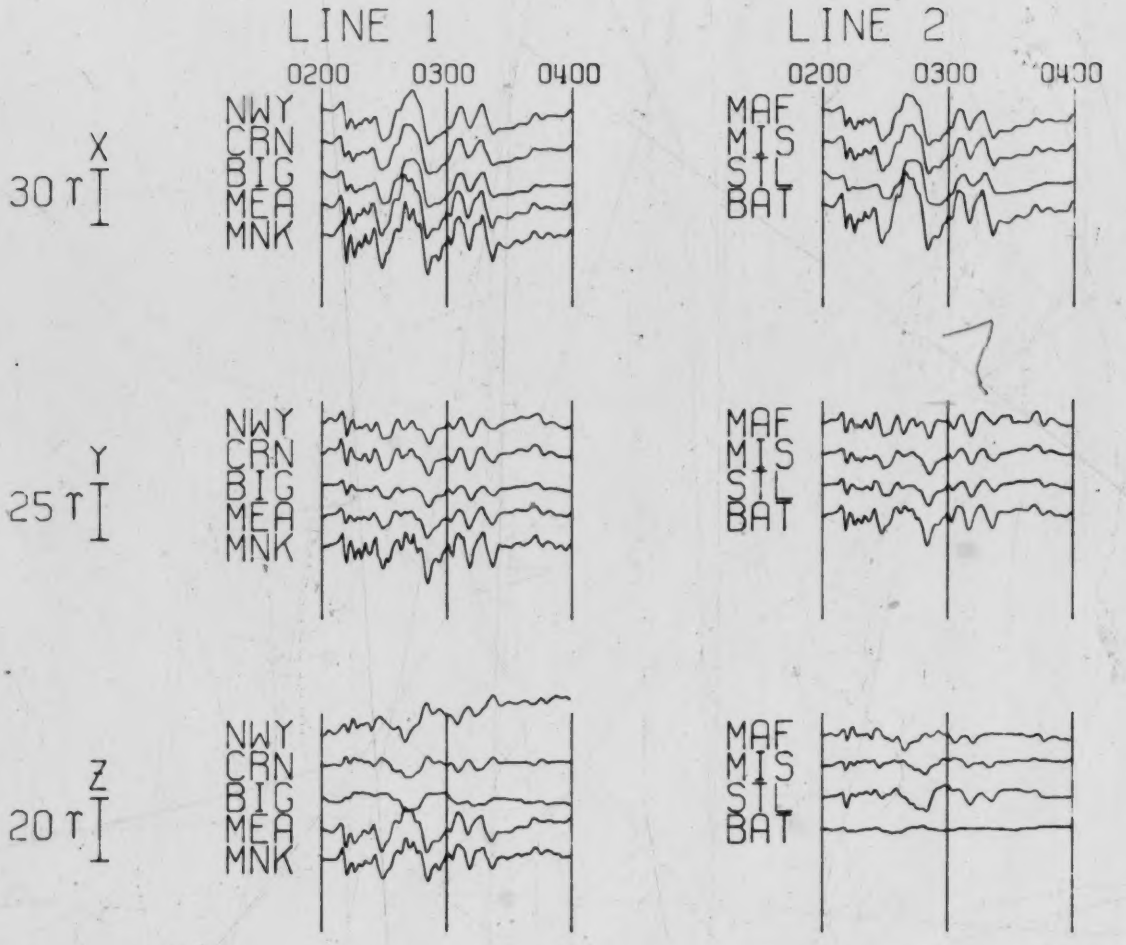

Fig. 4.5b The magnetograms for the pulsation of September 08 1972, lines 3 and 4.

SEPTEMBER 08 1972

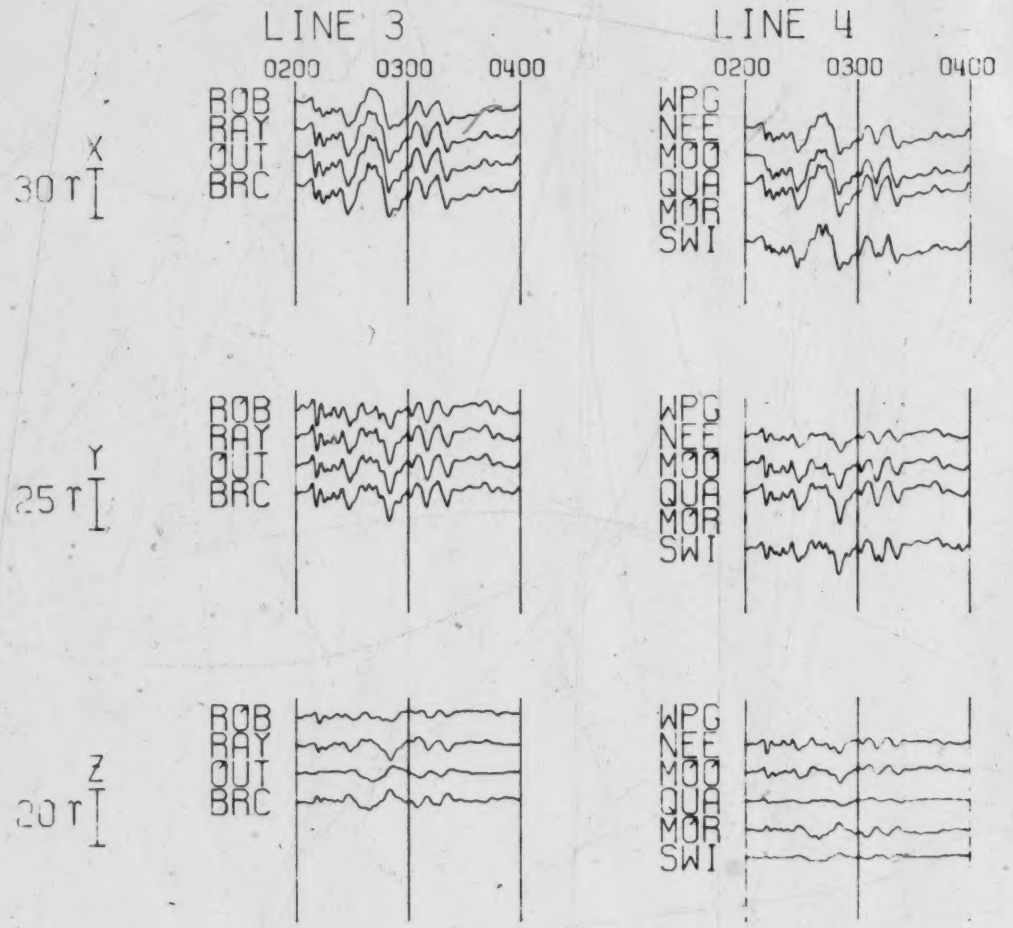

Fig. 4.5c The magnetograms for the pulsation of September 08 1972, lines 5 and 6.

SEPTEMBER 08 1972

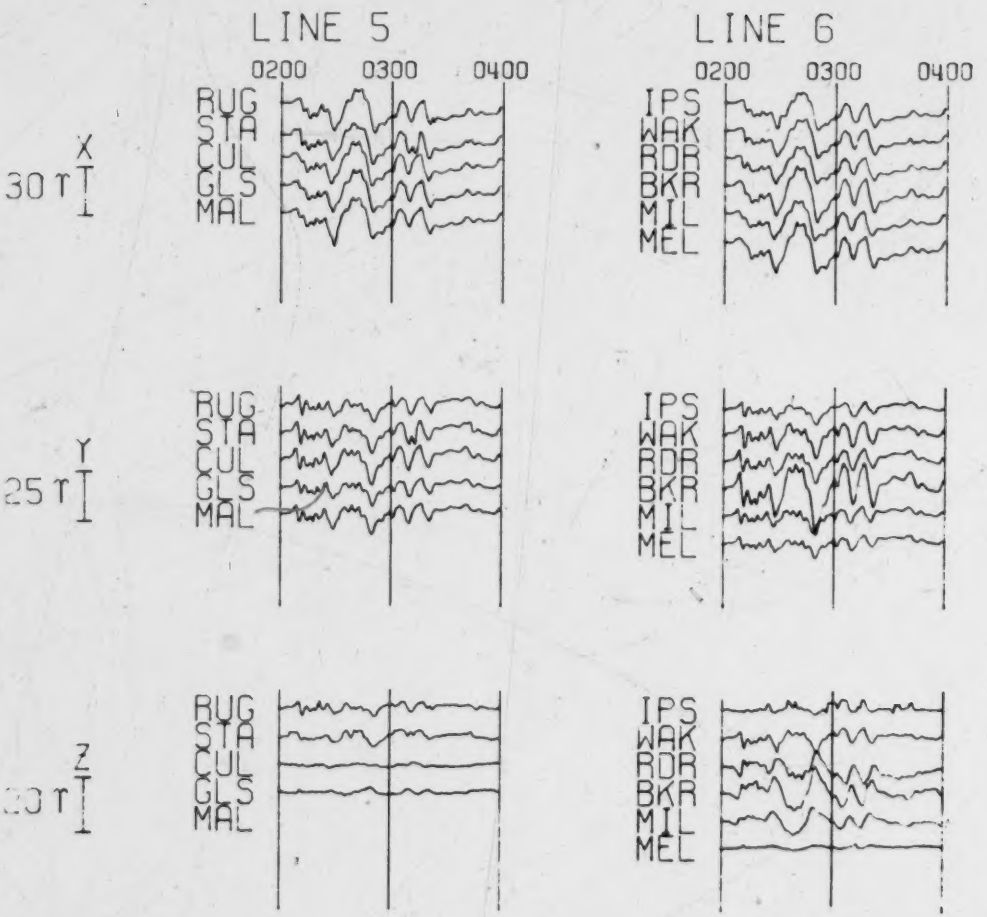

Fig. 4.5d The magnetograms for the pulsation of September 08 1972, lines 7 and 8.

SEPTEMBER 08 1972

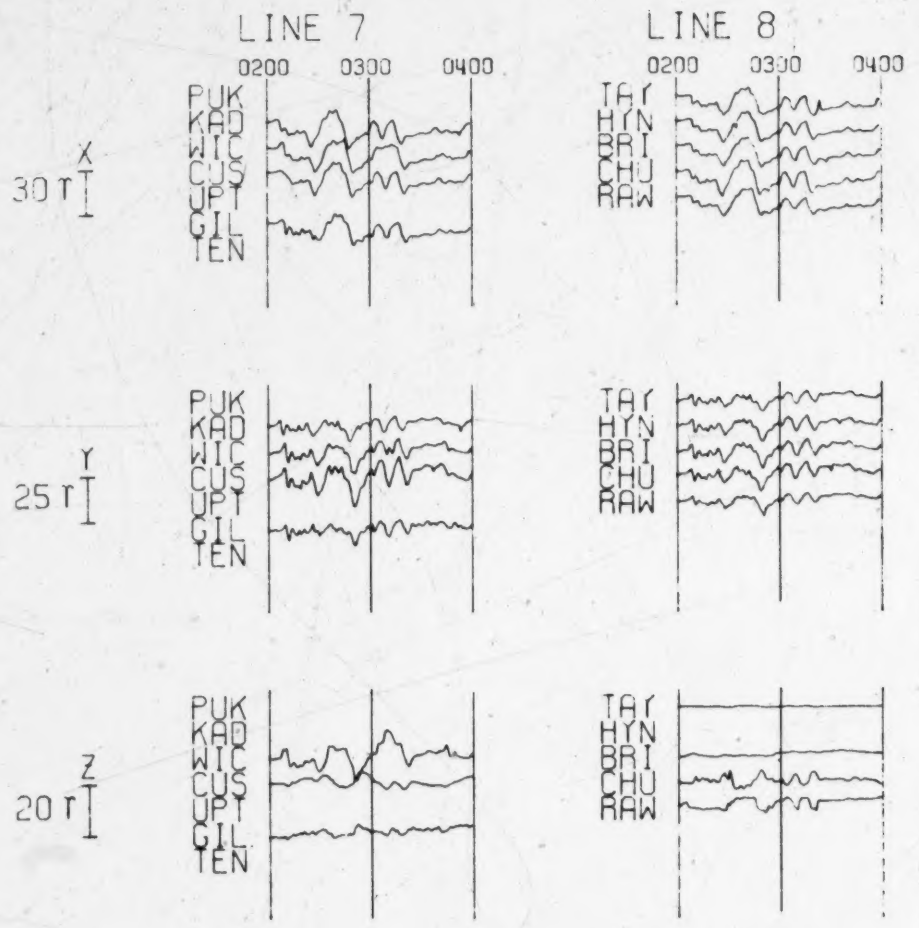

much more nearly uniform distribution over the array for all the normal components of the field than is given by the substorms. The event is particularly rich in short period components. The Z reversal is observed on all the eight lines in the array. The stations between which Z is reversed and the separation between the stations are given below.

Line 1, BIG & MEA (270 km)
Line 2, STL & BAT (85 km)
Line 3, RAY & OUT (180 km)
Line 4, QUA & MOR (170 km)
Line 5, STA & CUL (150 km)
Line 6, WAK & RDR (128 km)
Line 7, WIC & CUS (70 km)
Line 8, CHU & RAW (190 km)

On line 1 the obvious feature in the Y field is an enhancement of amplitude at MNK, which is probably a latitude-related effect in the source field. On line 2 X and Y are enhanced at BAT, where Z is very small; this strongly suggests that the centre of an induced current is close to BAT, and the Z reversal between BAT and STL places the current just east of BAT. Similarly large Y at QUA with small Z at this station places the current centre just west of QUA on line 4, and large Y with small Z places the current close to CUL on line 5. On line 6 Y has a strong maximum at BKR but Z is reversed between WAK and RDR, effects probably indicating a distributed

current poorly approximated at short periods by a line current. The Y and Z magnetograms of line 7 are consistent with a current centred between CUS and WIC but nearer CUS, that is, just east of the Black Hills. On line 8 Y is uninformative but X has a maximum near CHU.

4.2.5. The Event of September 12, 1972

The magnetograms shown in Figs. 4.6a through 4.6d are for a large amplitude substorm occurring between 0330 and 0530 UT on September 12 1972. The westward electrojet responsible for this event was located just north of the array but south of GREAT WHALE RIVER, CHURCHILL and COLLEGE (Fig. B-2). The amplitude of X decreases rapidly southward while Y decreases southward more slowly. Few if any induction effects can be identified with confidence on lines 1 and 2 which were close to the current axis of the source field.

On the next two lines stations east of a phase change lead those west of the change in Z. The phase change is observed between ROB and RAY (line 3) and between MOO and QUA (line 4). On the three lines that follow, Z reversals occur between STA and CUL (line 5), between RDR and BKR (line 6) and between WIC and CUS (line 7). Enhancement of Y occurred at CUL (line 5), BKR (line 6) and CUS (line 7). At CHU on line 8 Y is enhanced with Z reversed between CHU and RAW as before. Z at TAY is attenuated as observed in the events discussed in the subsections 4.2.1, 4.2.2 and 4.2.3.

Fig. 4.6a The magnetograms for a substorm of September 12 1972, lines 1 and 2.

SEPTEMBER 12 1972

LINE 1 LINE 2

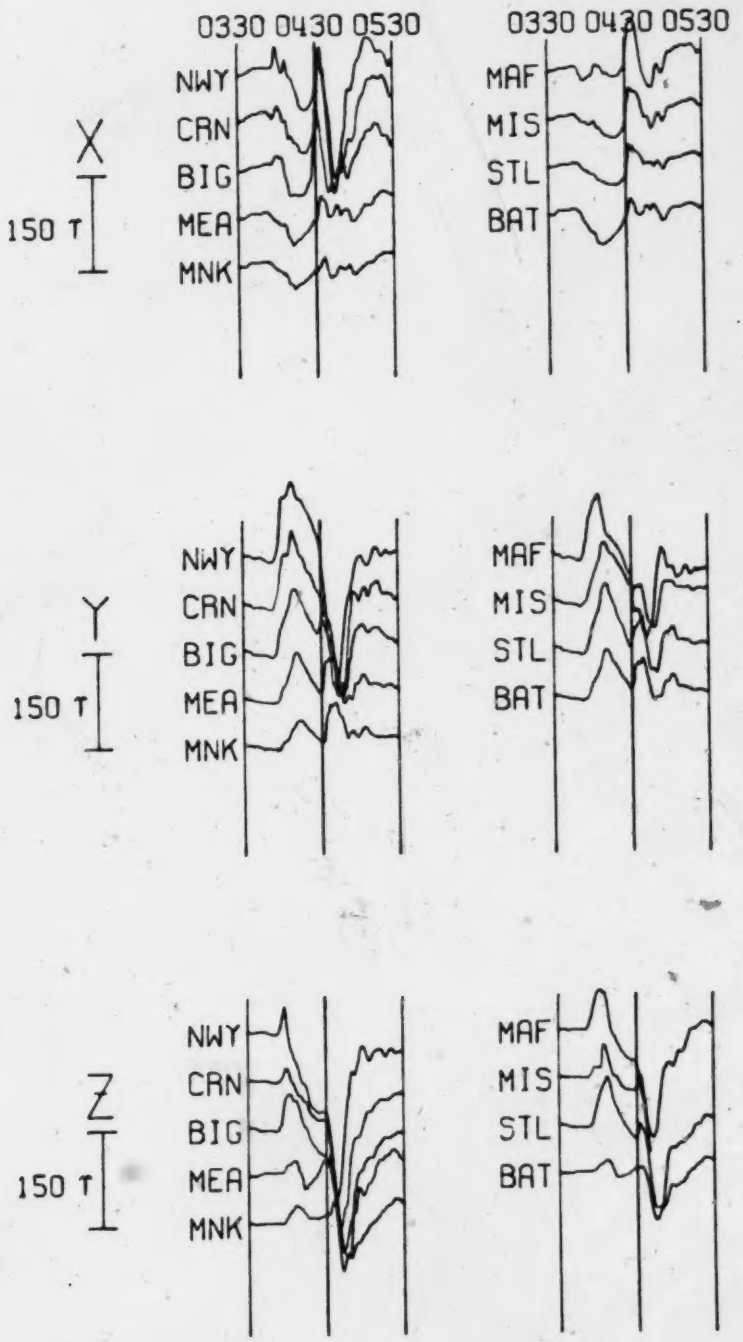

Fig. 4.6b The magnetograms for a substorm of September 12 1972, lines 3 and 4.

SEPTEMBER 12 1972

LINE 3 LINE 4

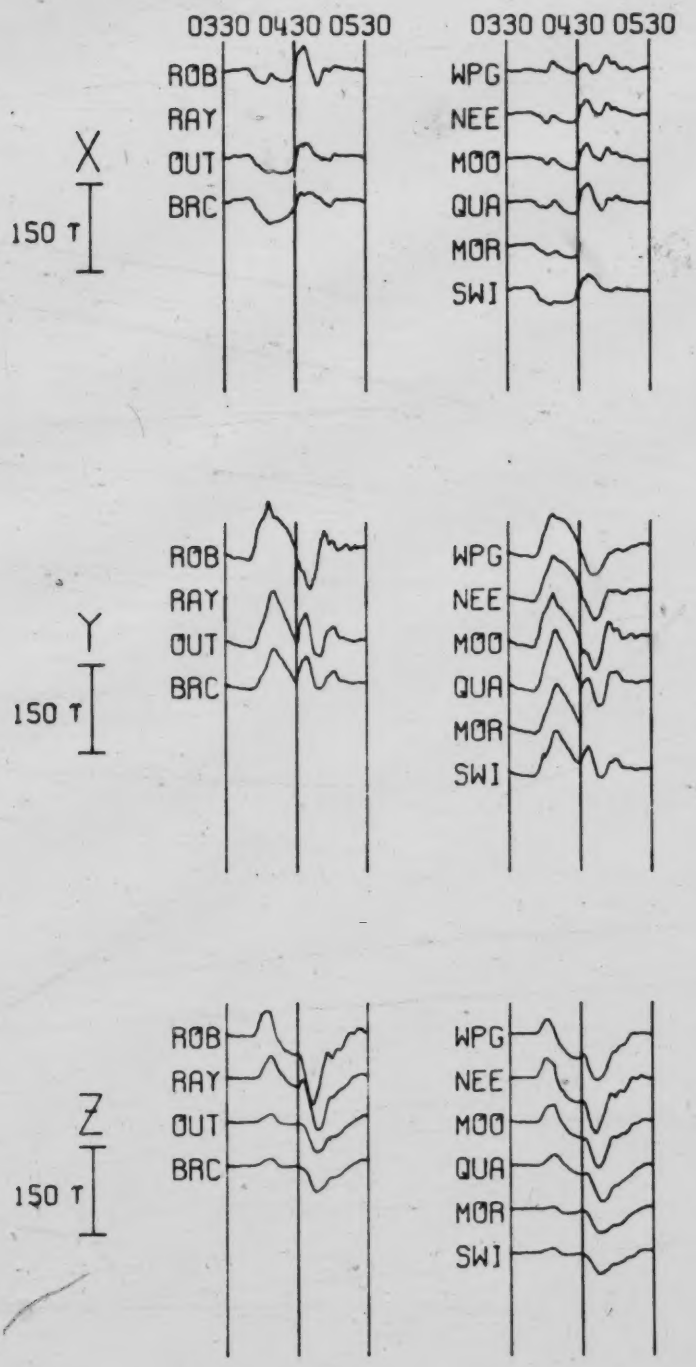

Fig. 4.6c The magnetograms for a substorm of September 12 1972, lines 5 and 6.

SEPTEMBER 12 1972

LINE 5 LINE 6

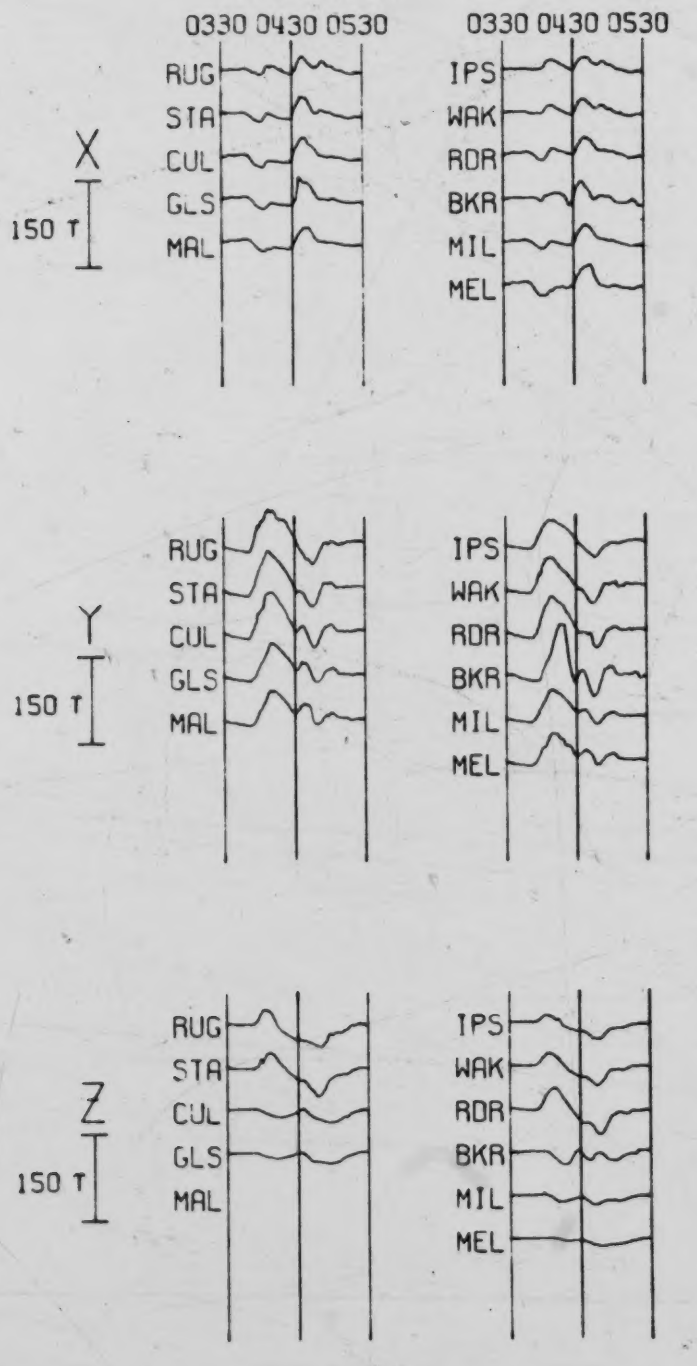

Fig. 4.6d The magnetograms for the substorm of September 12 1972, lines 7 and 8.

SEPTEMBER 12 1972

LINE 7 LINE 8

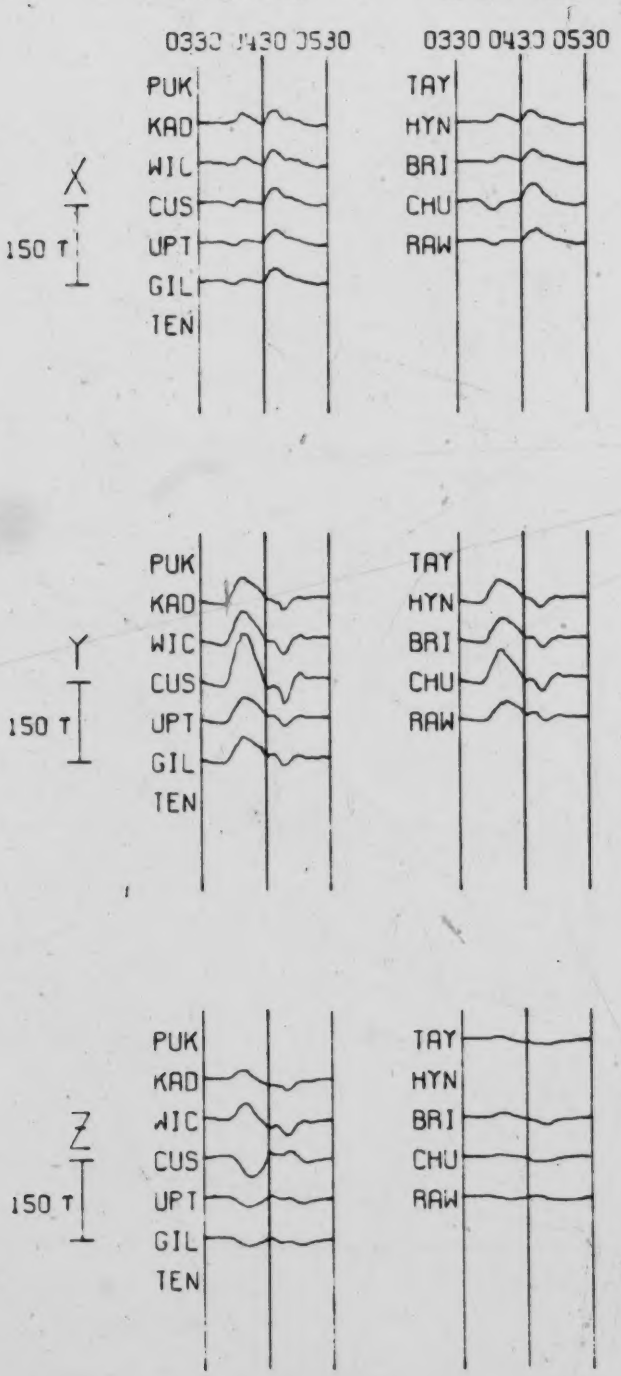

In the pulsation of September 8 1972 on line 3 Z is reversed between RAY and OUT. In the other events a phase shift in Z occurs between these stations. In the event of September 12 however, the phase shift is now between ROB and RAY. The current axis must be under RAY or very close to RAY.

4.2.6. The Event of September 13, 1973

The event whose magnetograms are shown in Figs. 4.7a through 4.7d is a disturbance isolated from a worldwide storm event which began with a sudden commencement on September 13 at 1240 UT. The normal field of this event is fairly uniformly distributed over the array.

The Z variation field shows phase-reversals on all the 8 lines as observed for the event of September 8 1972. The phase reversals in Z and enhancement of Y occur at the same stations as for the pulsation event of September 8.

It may be concluded that the conductor extends across the whole length of the array. Worldwide events such as pulsation and storm events are particularly useful in tracing the conductor close to the latitude of the substorm electrojet currents.

Direct inspection of magnetograms from six magnetic variation events indicates the presence of an anomaly corresponding to a conductor in the approximate position shown in Fig. 4.8. The anomalous fields are strongest between latitudes 43°N and

Fig. 4.7a The magnetograms for a disturbance event of September 13 1972, lines 1 and 2.

SEPTEMBER 13 1972

LINE 1 LINE 2

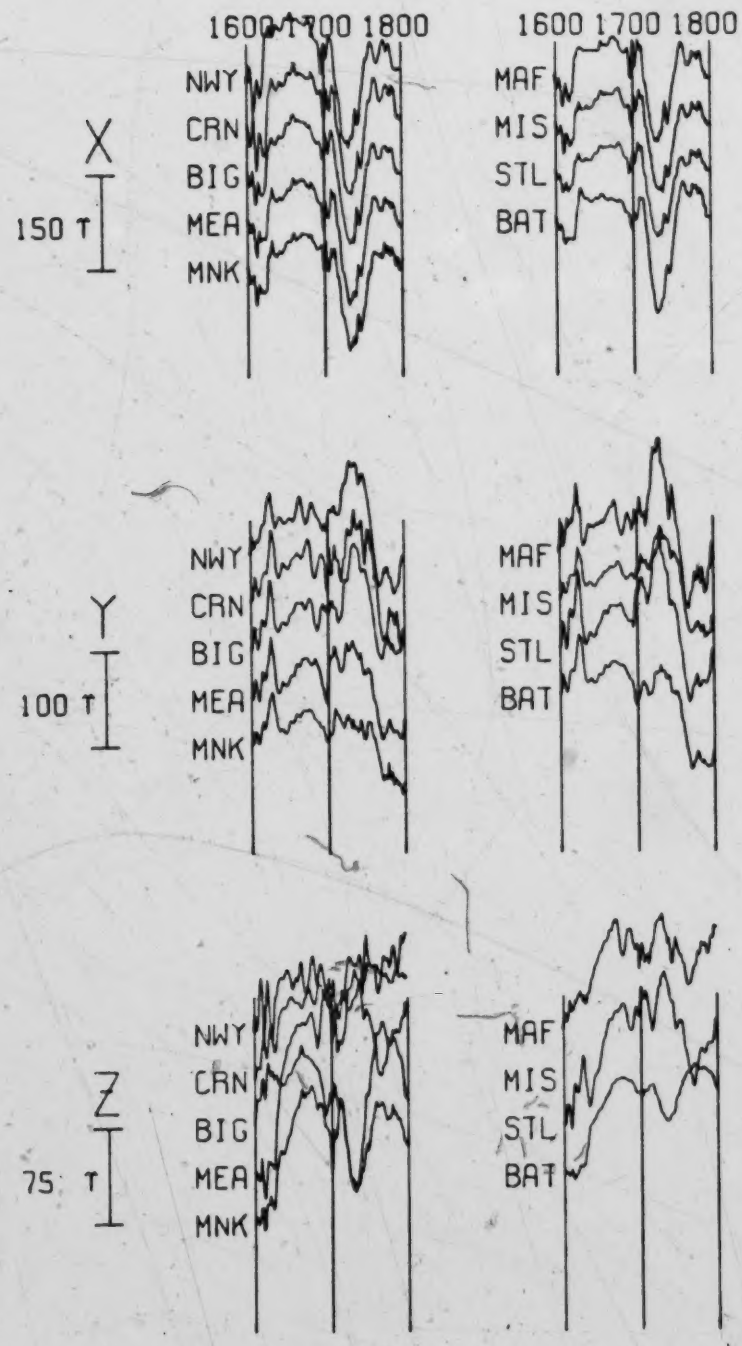

Fig. 4.7b The magnetograms for a disturbance event of September 13 1972, lines 3 and 4.

SEPTEMBER 13 1972

LINE 3 LINE 4

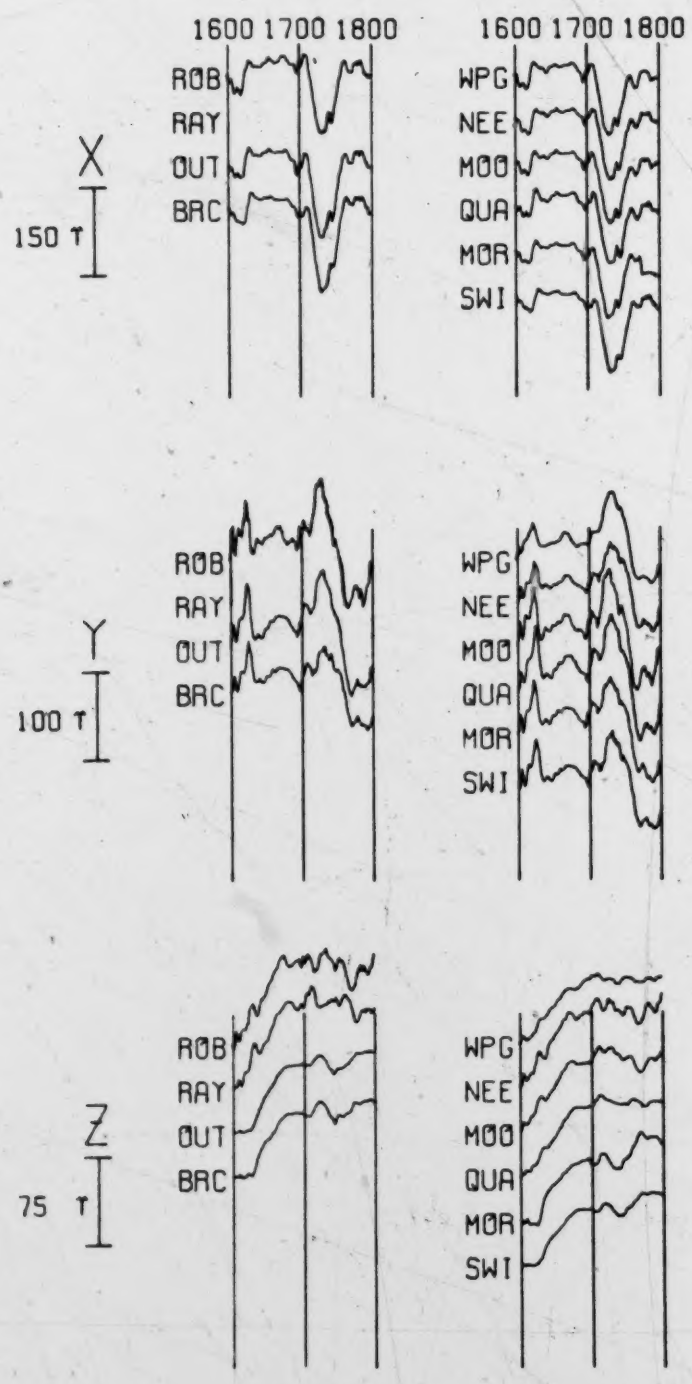

Fig. 4.7c The magnetograms for a disturbance event of September 13 1972, lines 5 and 6.

SEPTEMBER 13 1972

LINE 5 LINE 6

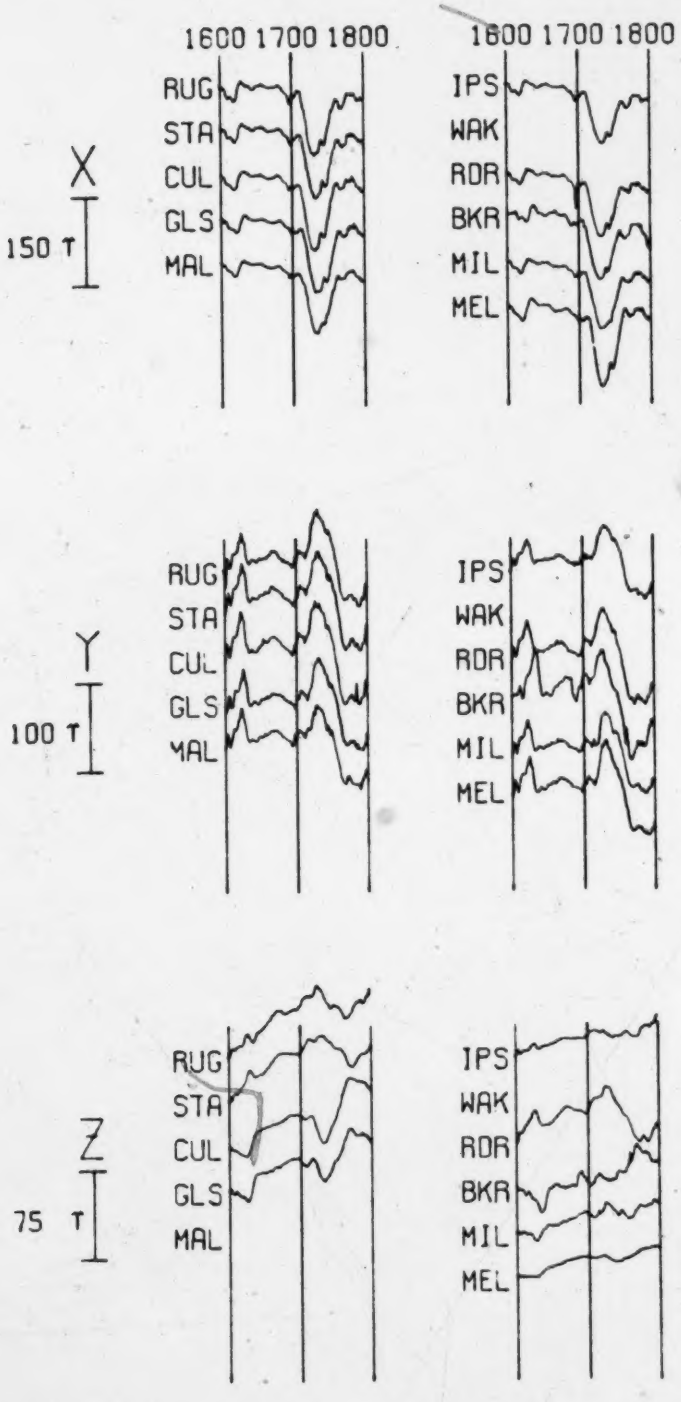

Fig. 4.7d. The magnetograms for a disturance event of September 13 1972, lines 7 and 8.

SEPTEMBER 13 1972

LINE 7 LINE 8

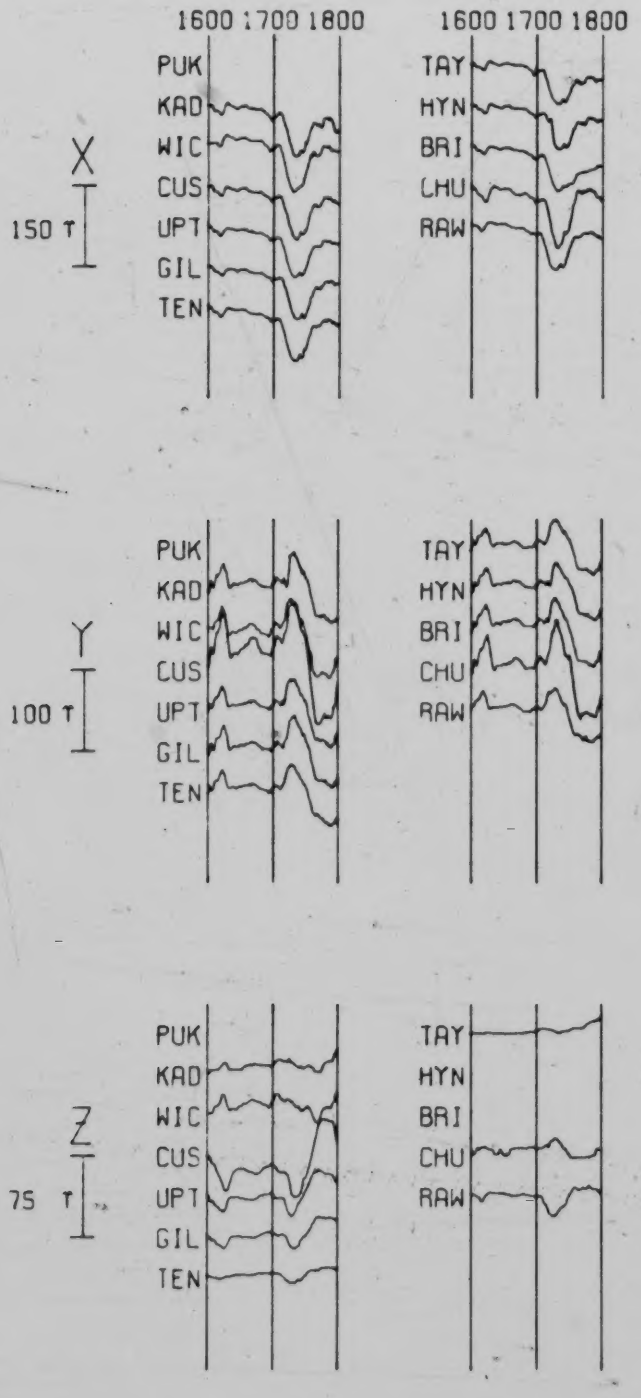

Fig. 4.8. The approximate location of the North American Central Plains conductor deduced from direct inspection of magnetograms of the six variation events.

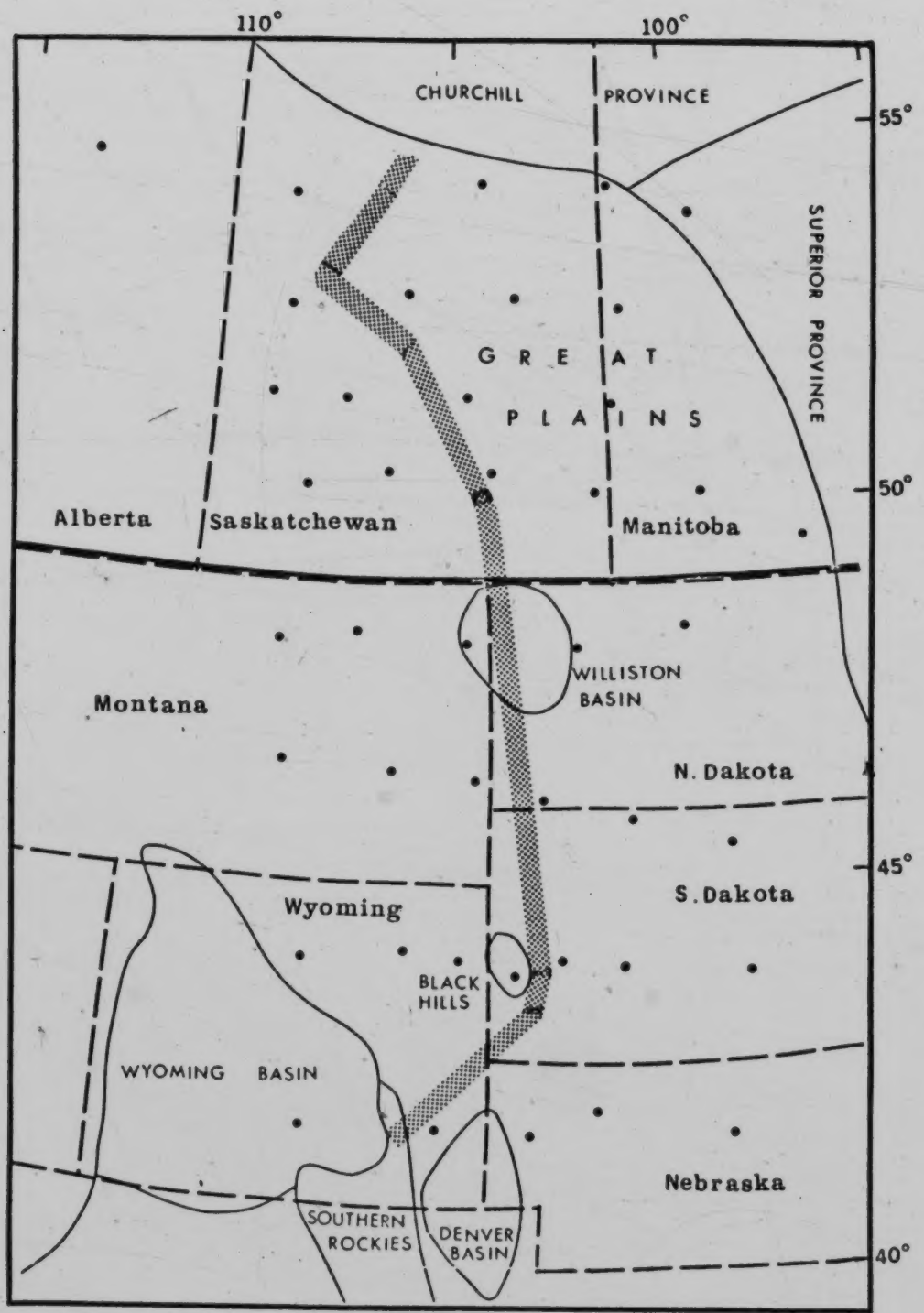
110°
100°
55°
50°
45°
40°
CHURCHILL
PROVINCE
SUPERIOR PROVINCE
GREAT
PLAINS
Alberta
Saskatchewan
Manitoba
WILLISTON
BASIN
Montana
N. Dakota
S. Dakota
Wyoming
BLACK
HILLS
WYOMING BASIN
Nebraska
SOUTHERN
ROCKIES
DENVER
BASIN

48°N, but can be traced throughout the length of the array with the help of events with different source-fields. The merging of the crustal conductor with the deeper conductor in the upper mantle under the Southern Rockies produce features which are perceived in all the six magnetic variation events.

4.3.1. The Fourier Spectra

The time series of the six variation events whose magnetograms are displayed in the preceding section were Fourier transformed. These short-period events can be regarded as transient signals superimposed on longer-period variations such as the S_q daily variation or the stormtime D_{st} variation fields. The trends on which the events were superimposed were removed by fitting straight lines between the ends of event, and the time-series were brought smoothly to zero level at the ends by tapering the first and the last ten data points with a $\sin^2$-window. Each time-series was made into 2^{10} data points by addition of zeros after the real data. This procedure gives additional estimates of transform parameters and is valid on the transient event assumption (Blackman and Tukey, 1959). The subroutine RHARM in the IBM 'Scientific and Statistical Programs', which uses the Cooley-Tukey Fast Fourier Transform algorithm, was used to compute the Fourier spectra. Only time-series without any missing data points were transformed.

Amplitude spectra are illustrated in Figs. 4.9 through 4.11 for the events of August 28, August 30 and September 13

Fig. 4.9 Fourier amplitude spectra in the period range 20-180 minutes for the substorm of August 28 1972, for four normal stations in the array. The period 68.3 min. at which the fields exhibit large amplitude is indicated by an arrow on each spectrum.

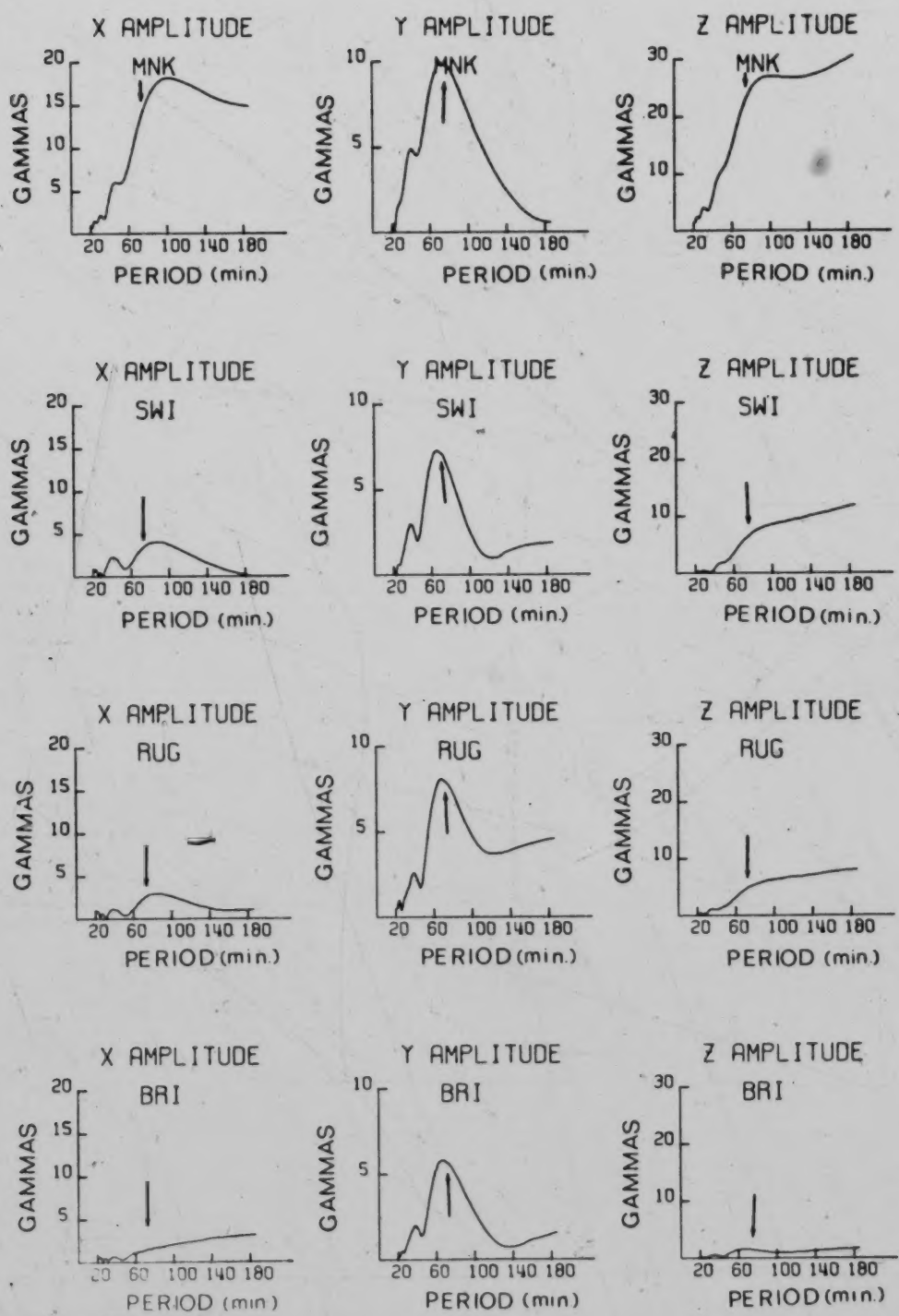
X AMPLITUDE
MNK
Y AMPLITUDE
MNK
Z AMPLITUDE
MNK
X AMPLITUDE
SWI
Y AMPLITUDE
SWI
Z AMPLITUDE
SWI
X AMPLITUDE
RUG
Y AMPLITUDE
RUG
Z AMPLITUDE
RUG
X AMPLITUDE
BRI
Y AMPLITUDE
BRI
Z AMPLITUDE
BRI
GAMMAS
PERIOD (min.)
20 60 100 140 180

Fig. 4.10 Fourier amplitude spectra in the period range 20-180 minutes for the substorm of August 30 1972, for four normal stations in the array. The period 78-8 min. at which the fields exhibit large amplitude is indicated by an arrow on each spectra.

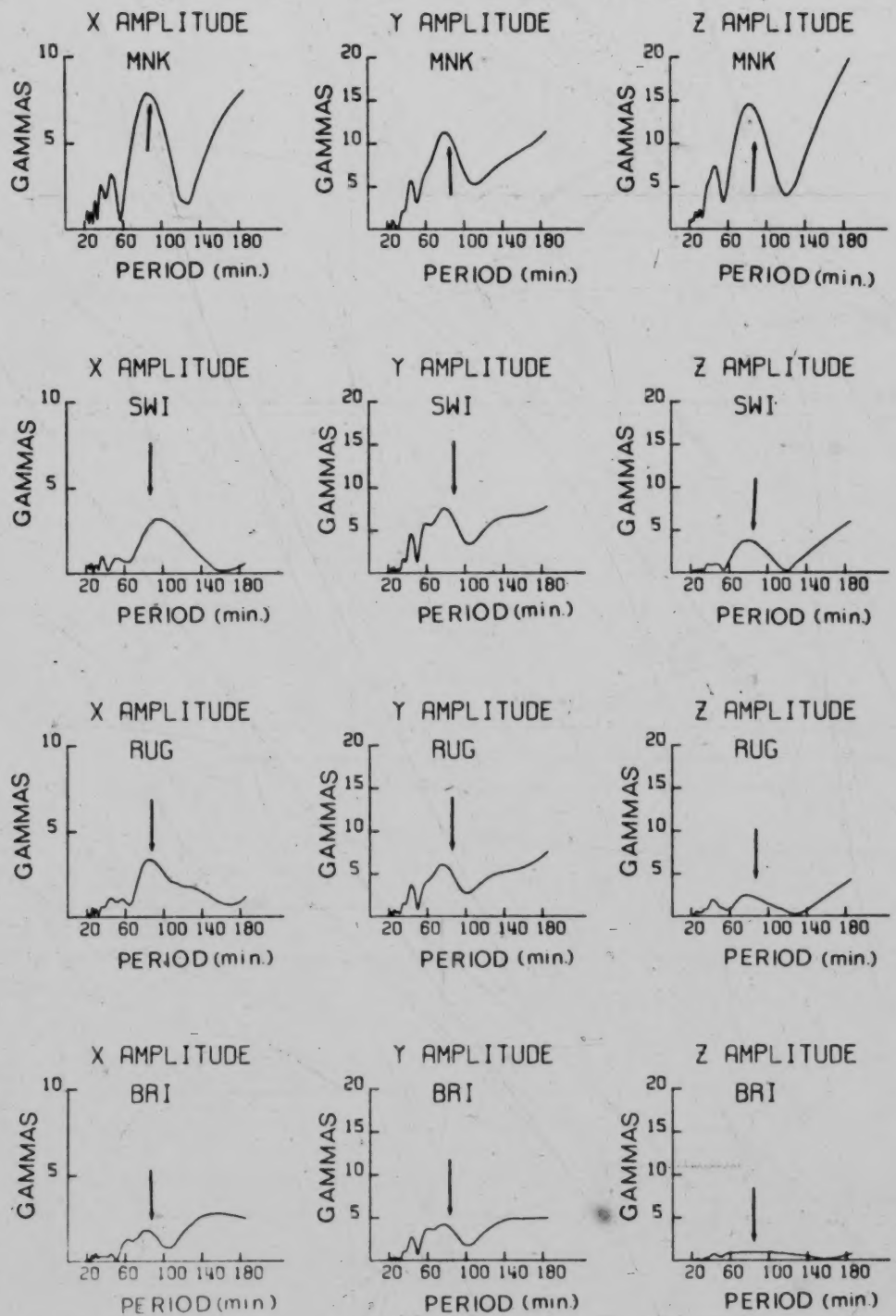
X AMPLITUDE
MNK
Y AMPLITUDE
MNK
Z AMPLITUDE
MNK
X AMPLITUDE
SWI
Y AMPLITUDE
SWI
Z AMPLITUDE
SWI
X AMPLITUDE
RUG
Y AMPLITUDE
RUG
Z AMPLITUDE
RUG
X AMPLITUDE
BRI
Y AMPLITUDE
BRI
Z AMPLITUDE
BRI
GAMMAS
PERIOD (min.)
20 60 100 140 180

Fig. 4.11 Fourier amplitude spectra in the period range 20-120 minutes for the event of September 13 1972, for four normal stations. Arrows indicate periods 25.0 and 36.6 min. at which this event shows peaks in energy.

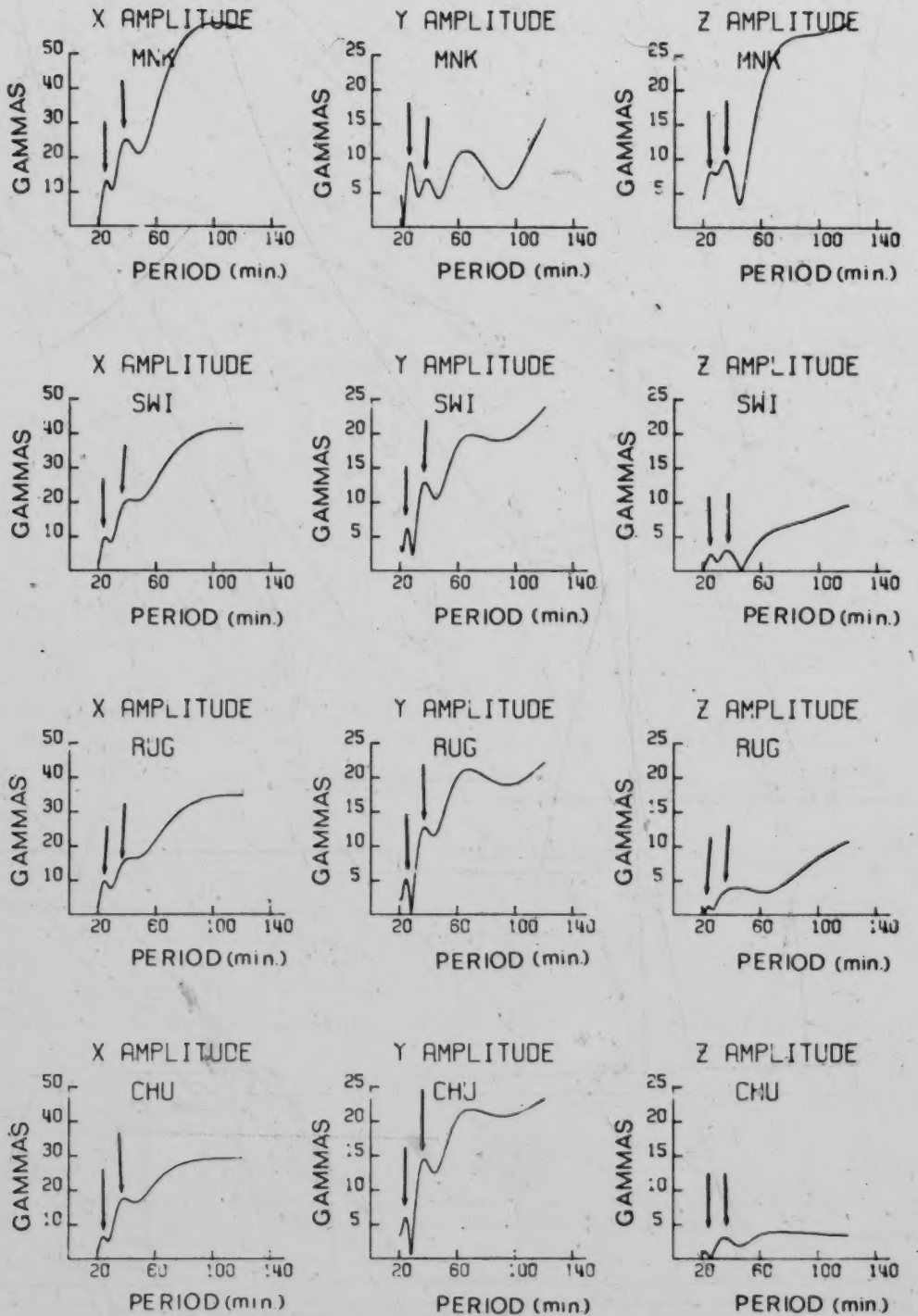
X AMPLITUDE
MNK
Y AMPLITUDE
MNK
Z AMPLITUDE
MNK
X AMPLITUDE
SWI
Y AMPLITUDE
SWI
Z AMPLITUDE
SWI
X AMPLITUDE
RUG
Y AMPLITUDE
RUG
Z AMPLITUDE
RUG
X AMPLITUDE
CHU
Y AMPLITUDE
CHU
Z AMPLITUDE
CHU
GAMMAS
PERIOD (min.)
20
60
100
140

at stations near the edges of the magnetometer array and as far as possible from the North American Central Plains anomaly. The positions of the stations are given in Fig. 4.1 and Table 4.2. The amplitude spectra are in general smooth with one or two major peaks. It may be noticed in Fig. 4.9 that the maxima do not often occur at the same period for both X and Y components even at the same station. The choice of periods at which the event has sufficient energy for both X and Y requires some personal judgement and compromise. The substorm events in general possess negligible energy at periods below 20 minutes while amplitudes at periods longer than 180 minutes are probably fictitious and may be due to the remnant long period trend which was not removed. The pulsation event of September 08 analyzed in this study possesses a significantly large peak around 13 minutes period. The double substorm of August 31 possesses a peak energy near 170 minute period. For the six events, periods at which the horizontal field components have large amplitudes were chosen making use of the stations whose spectra are illustrated in Figs. 4.9 -11 or similar stations near the limits of the array. In Table 4.3, the periods of the spectral peaks for the six events are listed. Maps of Fourier parameters which are considered later in this chapter are drawn at these periods.

Figs. 4.9-11 demonstrate the southward attenuation of the fields over the array even more clearly than the magnetograms in the preceding section. Between MNK and BRI

TABLE 4.2.

The positions of the Stations whose amplitude spectra are illustrated in Figs. 4.9-11.

Station	Latitude Degree N	Longitude Degree W
MNK	54.6	113.3
SWI	50.3	107.8
RUG	48.4	100.0
BRI	41.7	103.2
CHU	41.8	104.9

TABLE 4.3.

Periods at which the Spectral Peaks for the events occur

Event Date	Period (mins)	Length of Time-series (mins)
August 28, 1972	68.3	180
August 30, 1972	78.8	300
August 31, 1972	170.7	360
September 08, 1972	13.3	120
	31.5	120
September 12, 1972	26.6	120
Septebmer 13, 1972	25.0	120
	36.6	120

or between MNK and CHU there is a north-south separation of about 1300 km. For the substorm events at periods of 68.3 minutes in Fig. 4.9 and 78.8 minutes in Fig. 4.10 the X-component suffers more than 66% reduction in amplitude, Z component more than 80% while Y has 50% or less reduction of amplitude. For more worldwide events reduction in the amplitude is in general less than 25% for X and Y components but considerably more for the Z component which is more affected by any slight difference in the conductivity distribution under the stations. Fig. 4.11 at periods 25.0 and 36.6 minutes is an example of this case. The north-south decline in the X and Z amplitudes is qualitatively in harmony with the expected effects of increased distance from the auroral zone. However, the Fourier maps presented later in this chapter demonstrate this feature much more clearly.

4.3.2. Polarization of the Horizontal Field

Polarization hodograms obtained from amplitude-time data of variation fields have been used for a long time in describing the directional properties or polarization states of the geomagnetic fields (for example by Fowler, Kotick and Elliot, 1967). Bennett and Lilley (1972) introduced the use of horizontal polarization parameters into the scheme of presentation of array data. The theoretical methods long used in optics (Born and Wolf, 1959) were adapted for this purpose. Consider an horizontal co-ordinate system x, y with x

(north positive) and y(east positive), and two horizontal field components X and Y which are quasi-monochromatic and which differ in phase by ϕ. The field components can be written as:

$$X = X_o \cos(\omega t + \phi) \tag{4.1}$$

$$Y = Y_o \cos(\omega t) \tag{4.2}$$

In the array data presentation the parameters of interest are the semi-principal axes 'a' and 'b' and the angle ψ which the major axis makes with the geographic east (anticlockwise positive). When an angle α ($0 \leq \alpha \leq \pi/2$) is defined by

$$\tan \alpha = \frac{X_o}{Y_o} \tag{4.3}$$

Lilley and Bennett (1972) gave parameters by the relations

$$a^2 + b^2 = X_o^2 + Y_o^2 \tag{4.4}$$

$$\tan \psi = (\tan \alpha) \cos \phi \tag{4.5}$$

$$\sin 2\chi = (\sin 2\alpha) \sin \phi \tag{4.6}$$

where χ ($-\pi/4 \leq \chi \leq \pi/4$) an auxiliary angle which describes the shape of the ellipse is given by:

$$\tan \chi = \frac{b}{a} \tag{4.7}$$

If $\sin \phi < 0$ the ellipse is described in the clockwise sense, if $\sin \phi > 0$ anticlockwise and when $\sin \phi = 0$, the

ellipse degenerates to a line.

In array studies in Australia by Lilley and Bennett (1972) and by Gough, McElhinny and Lilley (1974) the horizontal field polarizations were considered in relation to the Fourier transform anomaly maps. Lilley and Bennett (1972) secured a better understanding of one of the Fourier phase maps only when the horizontal field observed over the array had been resolved along the directions of the major and minor axes of the field polarization ellipse. Gough et al., (1974) found that the knowledge of the horizontal polarization helped in the interpretation of the Z amplitude anomalies caused in a curved conductor or in 'crossed conductors'. For such purposes it suffices to obtain polarization parameters at a single station or a group of stations far from any internal or source anomalies.

In the present investigation the distribution of polarization ellipses for a long array is undertaken for different source fields. Effects of internal anomalies on polarization must exist but have not been previously used in studying the induced currents. From the Fourier coefficients at eight periods listed in Table 4.3, polarization ellipses were computed and plotted by Dr. Camfield according to the relations given in equations 4.1 - 4.7. The results are shown in Figs. 4.12 and 4.13.

The polarization of substorm events (Fig. 4.12) show a systematic north-south change in shape (ellipticity) and size.

Fig. 4.12. The horizontal polarization ellipses for the polar magnetic substorms events of (a) August 28 (68.3 min.) (b) August 30 (78.8 min.) (c) August 31 (170.7 min.) (d) September 12 (26.6 min.).

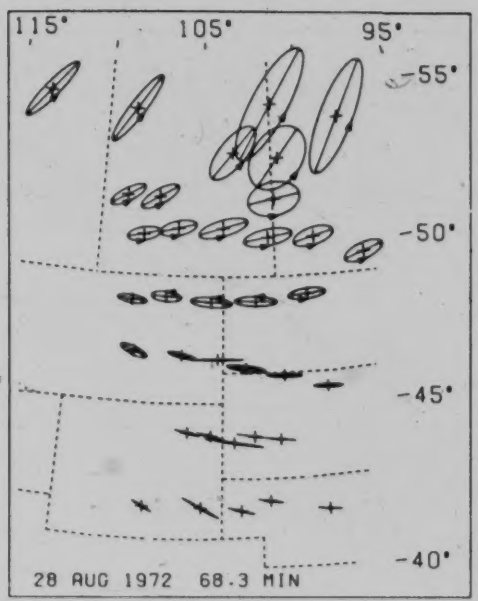
115°
105°
95°
-55°
-50°
-45°
-40°
28 AUG 1972 68.3 MIN

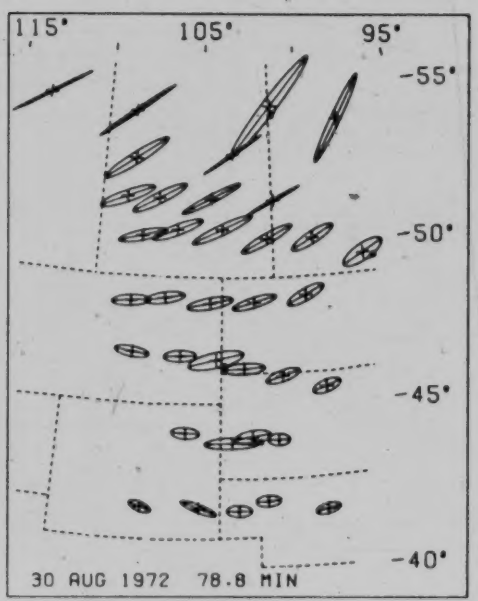
115°
105°
95°
-55°
-50°
-45°
-40°
30 AUG 1972 78.8 MIN

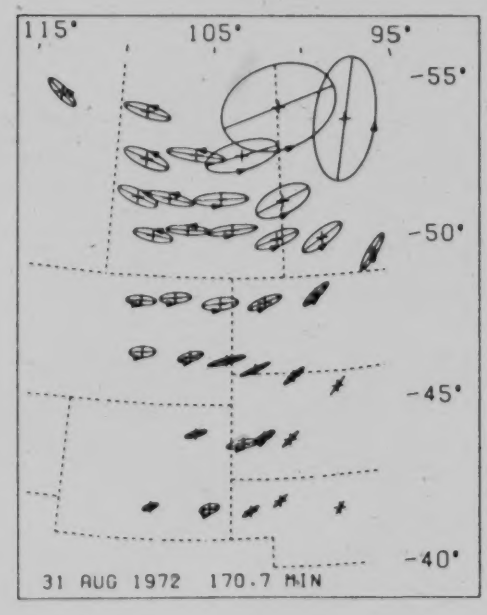
115°
105°
95°
-55°
-50°
-45°
-40°
31 AUG 1972 170.7 MIN

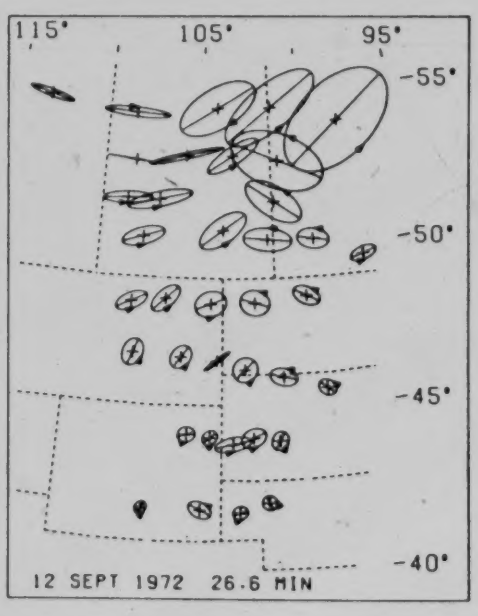
115°
105°
95°
-55°
-50°
-45°
-40°
12 SEPT 1972 26.6 MIN

Fig. 4.13 The horizontal polarization ellipses for the world-wide magnetic disturbances of (a) September 08 (13.3 min.) (b) September 08 (31.5 min.) (c) September 13 (25.0 min.) (d) September 13 (36.6 min.).

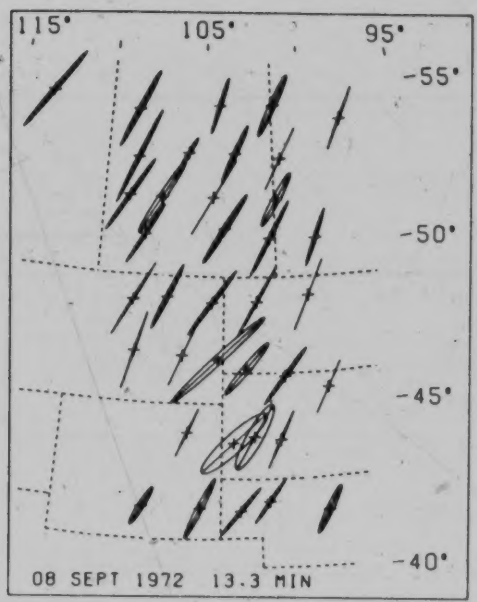
115°
105°
95°
-55°
-50°
-45°
-40°
08 SEPT 1972 13.3 MIN

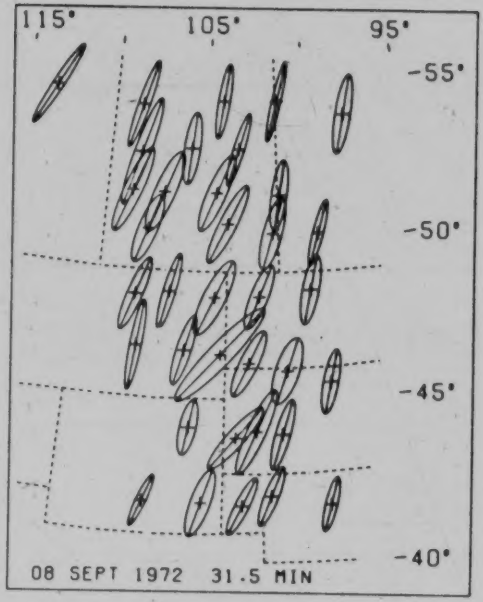
115°
105°
95°
-55°
-50°
-45°
-40°
08 SEPT 1972 31.5 MIN

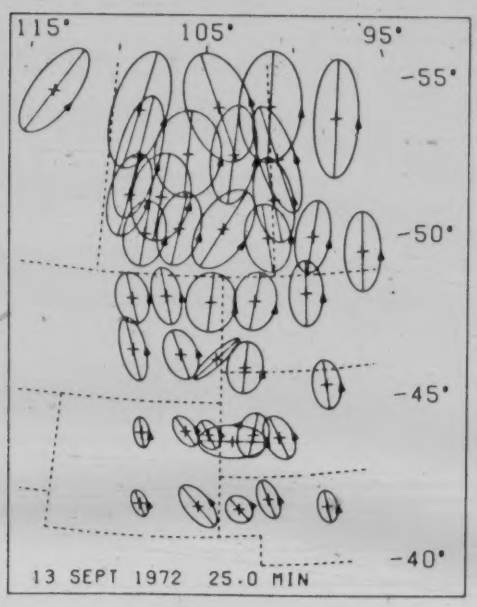
115°
105°
95°
-55°
-50°
-45°
-40°
13 SEPT 1972 25.0 MIN

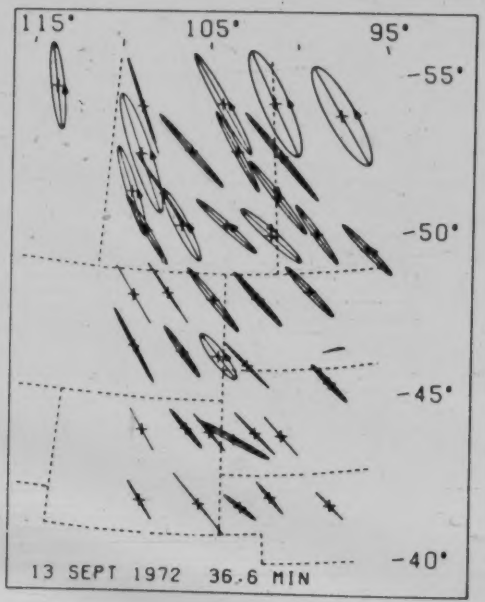
115°
105°
95°
-55°
-50°
-45°
-40°
13 SEPT 1972 36.6 MIN

The fields of substorms which are usually elliptically polarized in the northern region of the array become almost linearly polarized in the south. For some of the substorm events however (for example, Fig. 4.12b), the shape of the ellipse changes little but the size diminishes. The effect of the conductive body on the polarization ellipses is superimposed upon a pattern characteristic of the source field itself. Without detailed knowledge of the source field morphology maps like those in Figs. 4.12 and 4.13 are difficult to interpret. Nevertheless, the polarization pattern is interesting. The effect of the narrow conductive body under the Black Hills is to elongate the major axis and turn it east-west. This is best seen in Fig. 4.12a.

Worldwide events such as those of September 08 (Fig. 4.12a,b) and September 12 (Fig. 4.13c,d) show less north-south variability in the polarization ellipses. The major axes are nearer the north-south direction than for the substorms. As before the effect of the anomaly is to elongate the major axes and turn them east-west.

Porath et al., (1971) pointed out that the North American Central Plains anomaly has a strong period dependence with maximum response near 50 minutes (Fig. 2, their paper). It is worthy of note that the anomaly shows most strongly at periods 68.3 min (Fig. 4.12a) in the maps of polarization ellipses.

4.3.3. Fourier Transform Maps

Contoured maps of Fourier transform parameters at various periods provide semi-quantitative information on induction processes over different depth ranges. The depth of penetration of the fields increases with period approximately as the skin-depth. For this array Fourier maps are drawn at eight periods (listed in Table 4.3) at which the incident fields possess maximum energy. The maps were initially contoured in the computer, and final versions were hand-drawn from the machine-produced drafts.

The Fourier coefficients and the coordinates of the irregularly spaced stations were input to the computer contouring programmes. Polynomial fits of the data were made to produce surface approximations which were then plotted in the form of contour maps by means of a Calcomp plotter. As our group had not used these programmes before six hand-drawn Fourier maps were compared with those produced by the computer from the same data. The agreement was excellent. Probably because our stations were too few the machine-produced maps generally needed adjustment by hand. All possible precautions were taken to prevent the introduction of bias in these adjustments, by limiting the adjustment to linear interpolation between stations to add to, delete from or alter the directions of the contour lines drawn by machine.

Two versions of contouring programmes were available to our groups, the University of Alberta and the Earth Physics

Branch (EPB) versions. Both versions yielded identical results for the same data. At each period a set of six maps was produced, three for amplitudes and three for the phases. The eight sets of maps shown in Figs. 4.14-4.21 were produced by Dr. Camfield using the EPB contouring programme. Each map is based on at least 36 data values. Crosses indicate the stations which contributed information to the contour map on which they appear.

It must be remembered that Fourier transform maps are different from other geophysical anomaly maps in showing the combined effects due to source field and the earth's response to it. The amplitude maps are in units of gamma (nanotesla) while the phases are in minutes. For each set of maps the same contouring intervals for amplitudes and for phases are maintained.

The most interesting feature found in the Fourier maps is that relating to the North American Central Plains internal structure. Before considering this it is useful to consider the general features related to the source fields. In the amplitude and phase maps of substorm events especially above latitude 50°N, the overwhelming effects of the source fields dominate the picture with closely spaced contour lines with roughly northeast-southwest gradient. The substorm-field maps shown in Figs. 4.14-4.17 illustrate this. The presence of a conductive structure can be camouflaged by such source effects. In the worldwide disturbance events of September 08 and 13, 1972

Fig. 4.14 Fourier amplitude (in gammas) and phases (in minutes) at period 26.6 minutes from the magnetic polar substorm of September 12 1972. The contour intervals are 1 γ for the amplitudes and 1 minute for the phases. For polarization of the horizontal fields see Fig. 4.12.

12 Sept 1972 T = 26.6 min

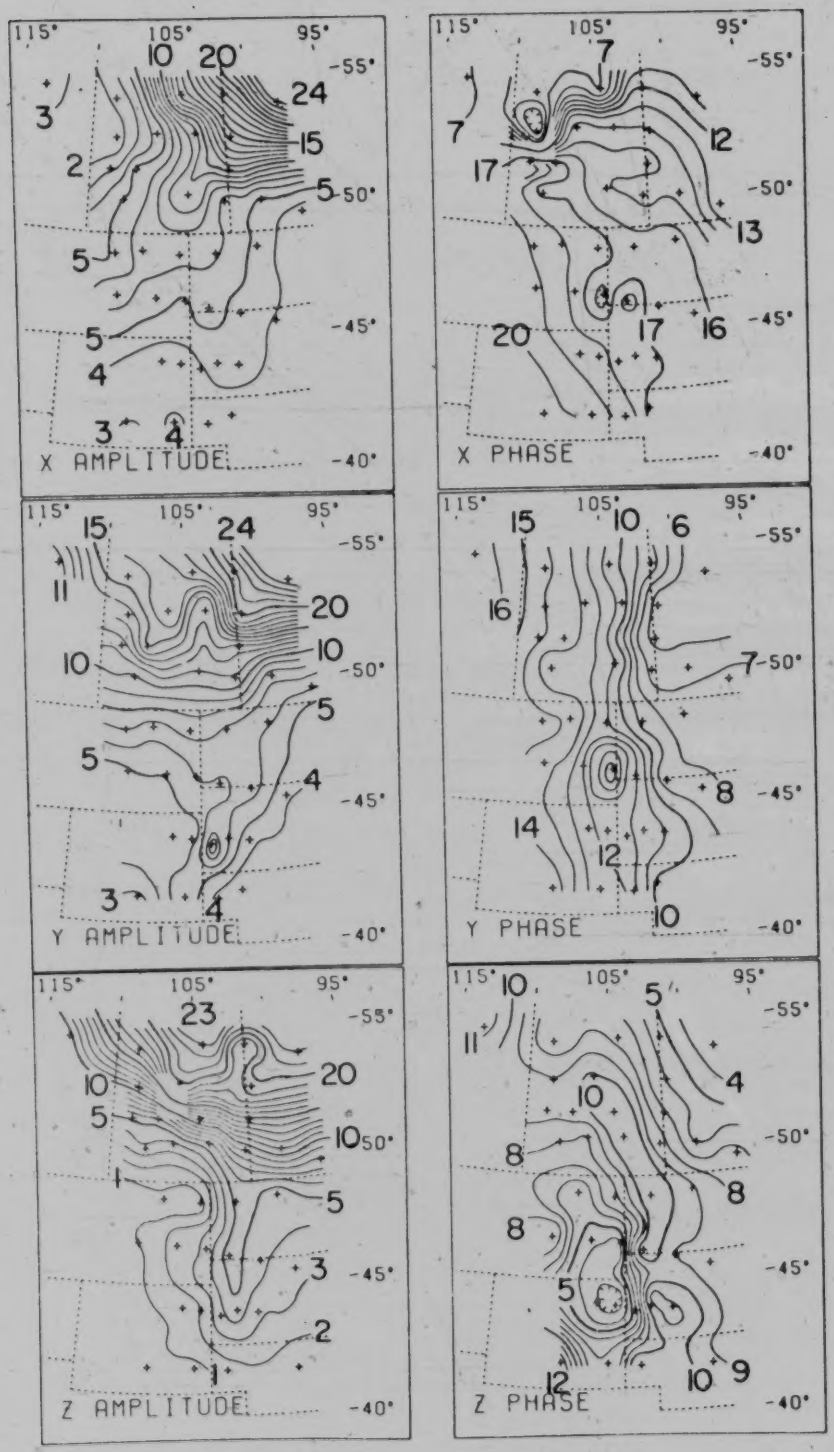

Fig. 4.15 Fourier amplitudes (in gammas) and phases (in minutes) at period 68.3 minutes from the magnetic polar substorm of August 28, 1972. The contour intervals are 1 γ for the amplitudes and 2 minutes for the phases. For polarization of the horizontal fields see Fig. 4.12.

28 August 1972 T = 68.3 min

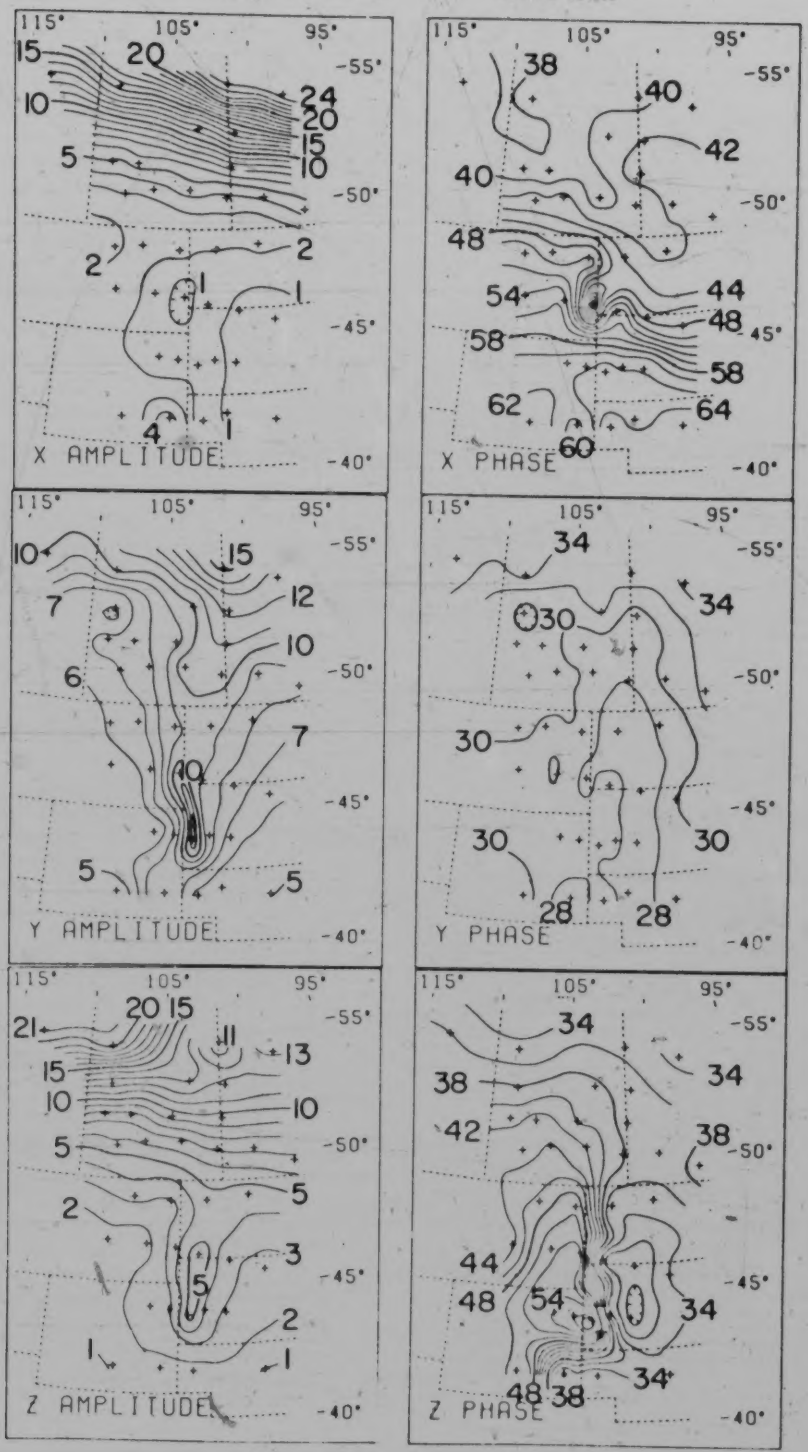

Fig. 4.16 Fourier amplitudes (in gammas) and phases (in minutes) at period 78.8 minutes from the magnetic polar substorm of August 30, 1972. The contour intervals are 1 γ for the amplitudes and 2 minutes for the phases. For polarization of the horizontal fields see Fig. 4.12.

30 August 1972 T = 78.8 min

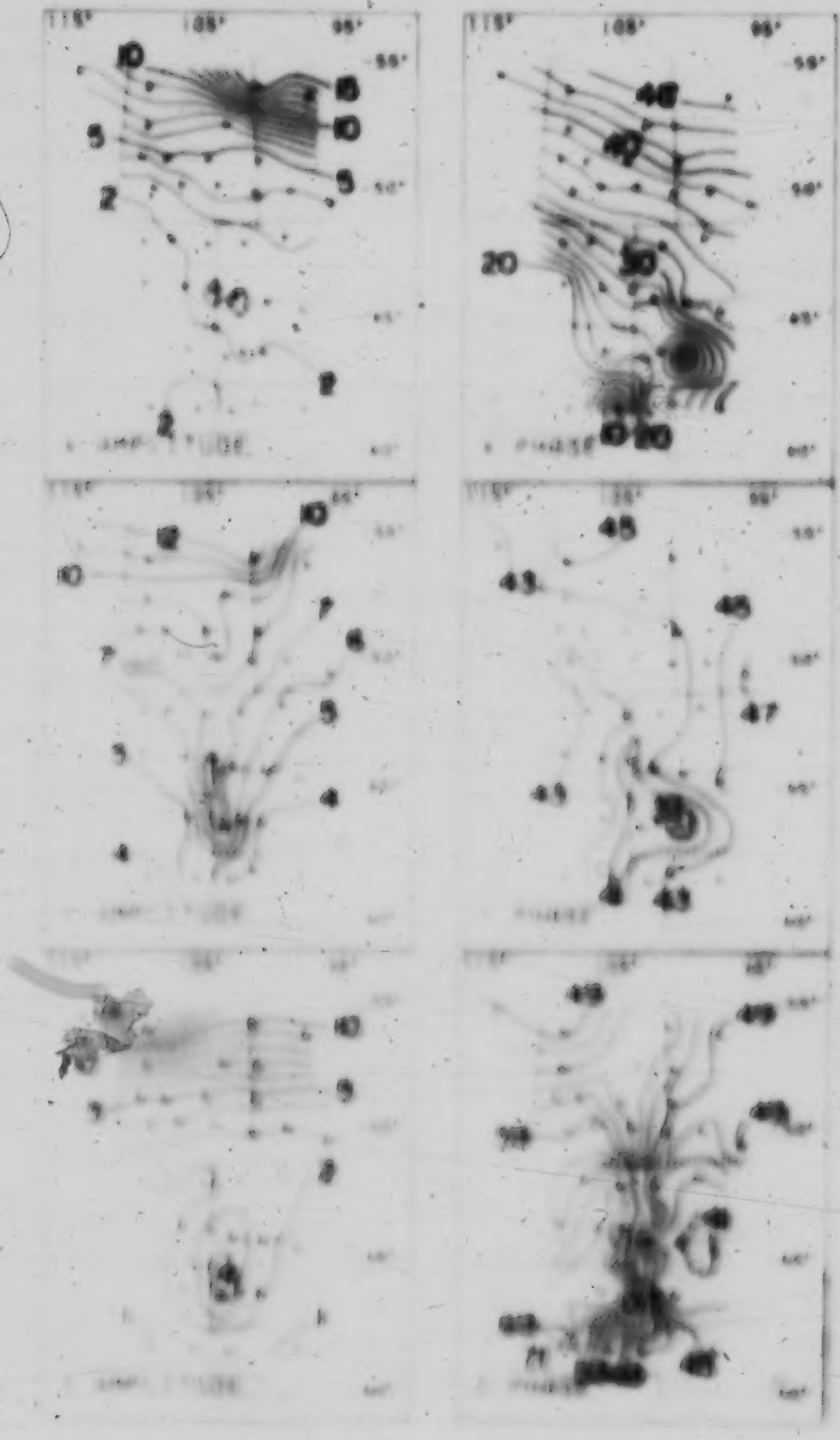

Fig. 8.17 Fourier amplitudes (in gammas) and phases (in minutes) at period 179.7 minutes from the magnetic polar substorm of August 11, 1972. The contour intervals are 1 γ for the amplitudes and 3 minutes for the phases. For polarization of the horizontal fields see Fig. 8.18.

31 August 1972 T • 170.7 min

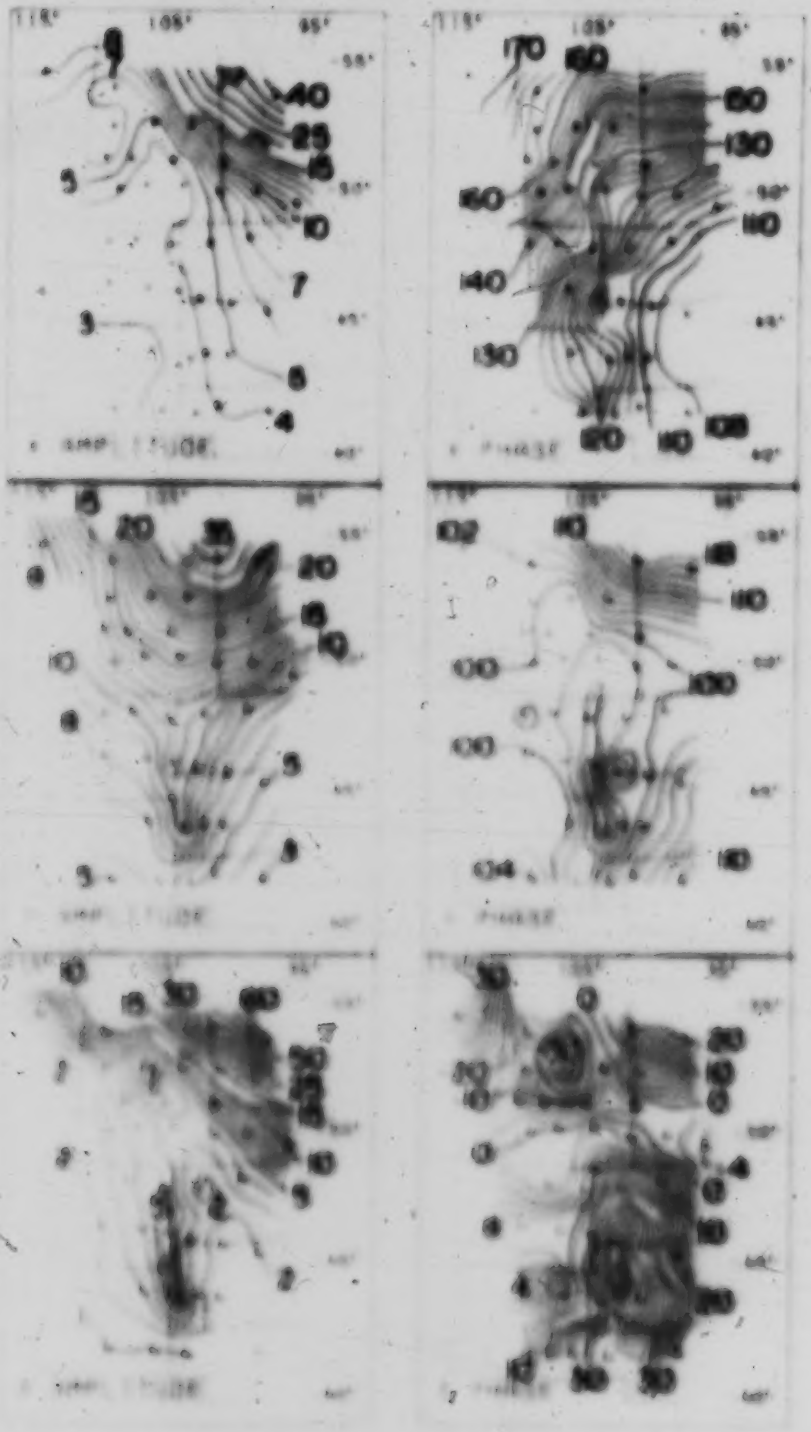

Fig. 4.10 Fourier amplitudes (in cm-sec) and phases (in minutes) at period 13.1 minutes from the polarization event of September 10, 1972. The contour intervals are 0.2 for the amplitudes and 1 minute for the phases. For polarization of the horizontal fields see Fig. 4.11

8 Sept 1972 T + 13.3 min

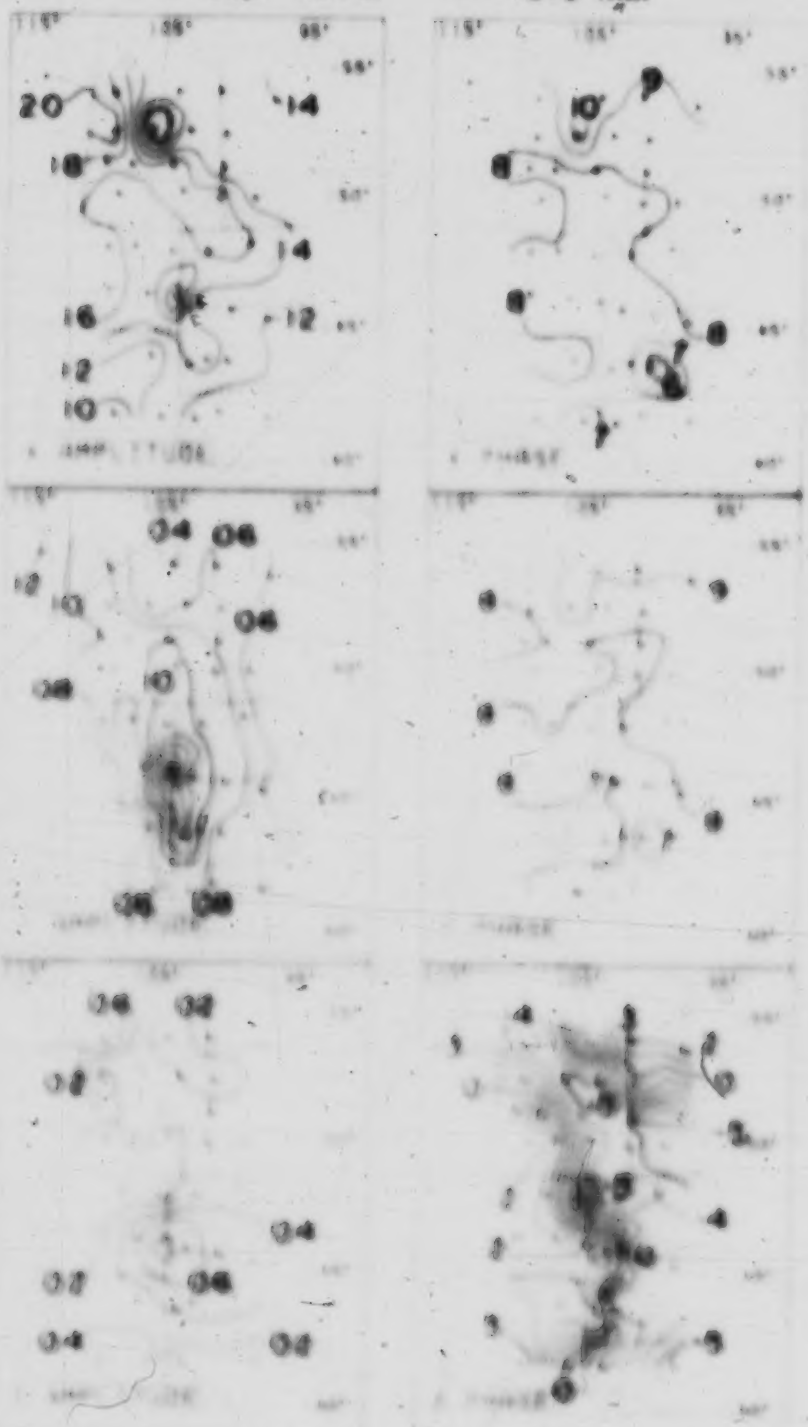

Fig. 8.10 Fourier amplitudes (in gammas) and phases (in minutes) at period 29.0 minutes from the disturbance event of September 13, 1972. The contour intervals are 1 γ for the amplitudes and 1 minutes for the phases. For polarization of the horizontal fields see Fig. 8.11.

13 Sept 1972 T = 25.0 min

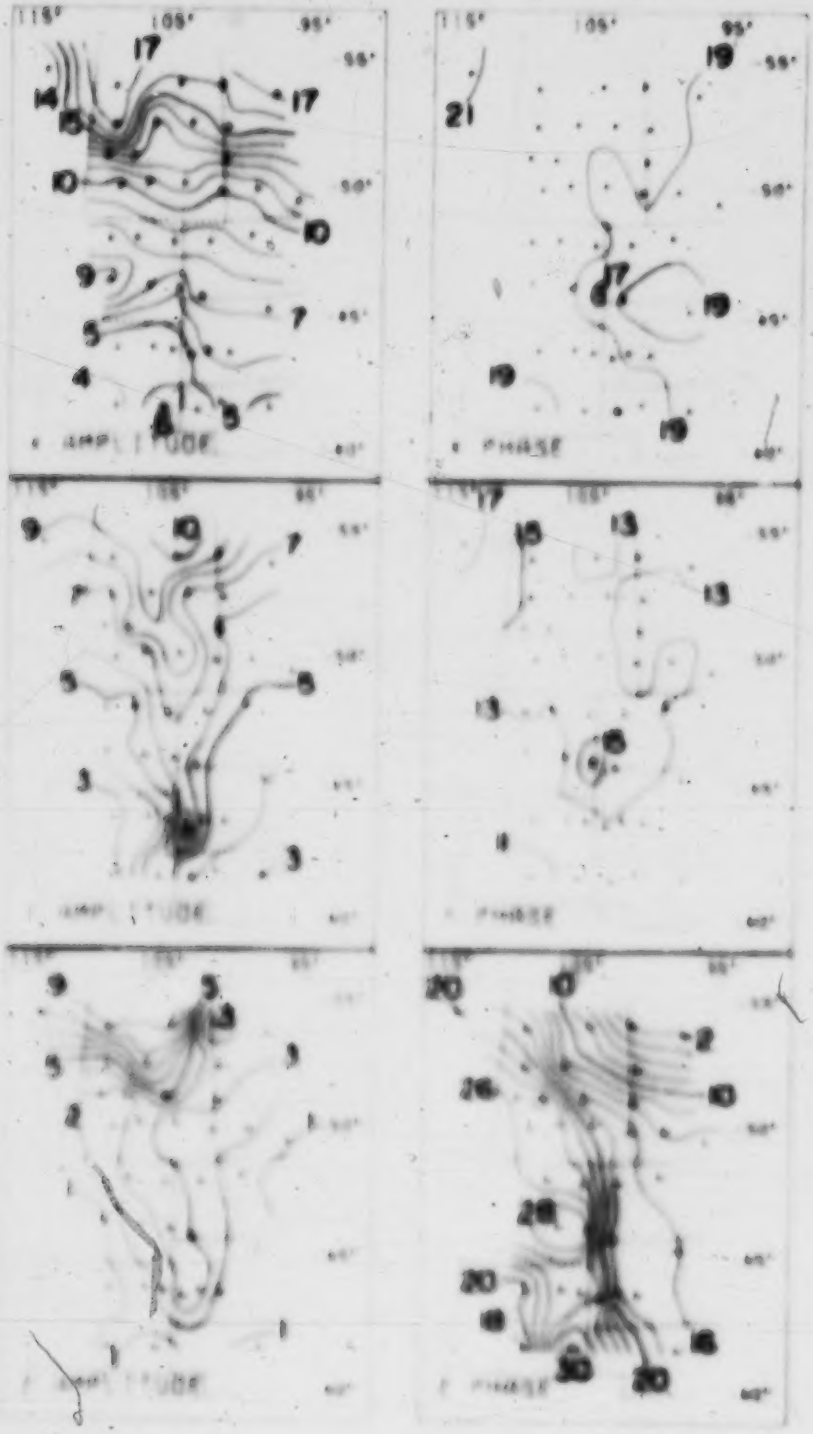

Fig. 4.10 Fourier amplitudes (in gammas) and phases (in minutes) at period 11.9 minutes from the pulsation event of September 08, 1972. The contour intervals are 0.2 γ for amplitudes and 1 minutes for the phases. For polarization of the horizontal fields see Fig. 4.11.

8 Sept 1972 T = 31.8 min

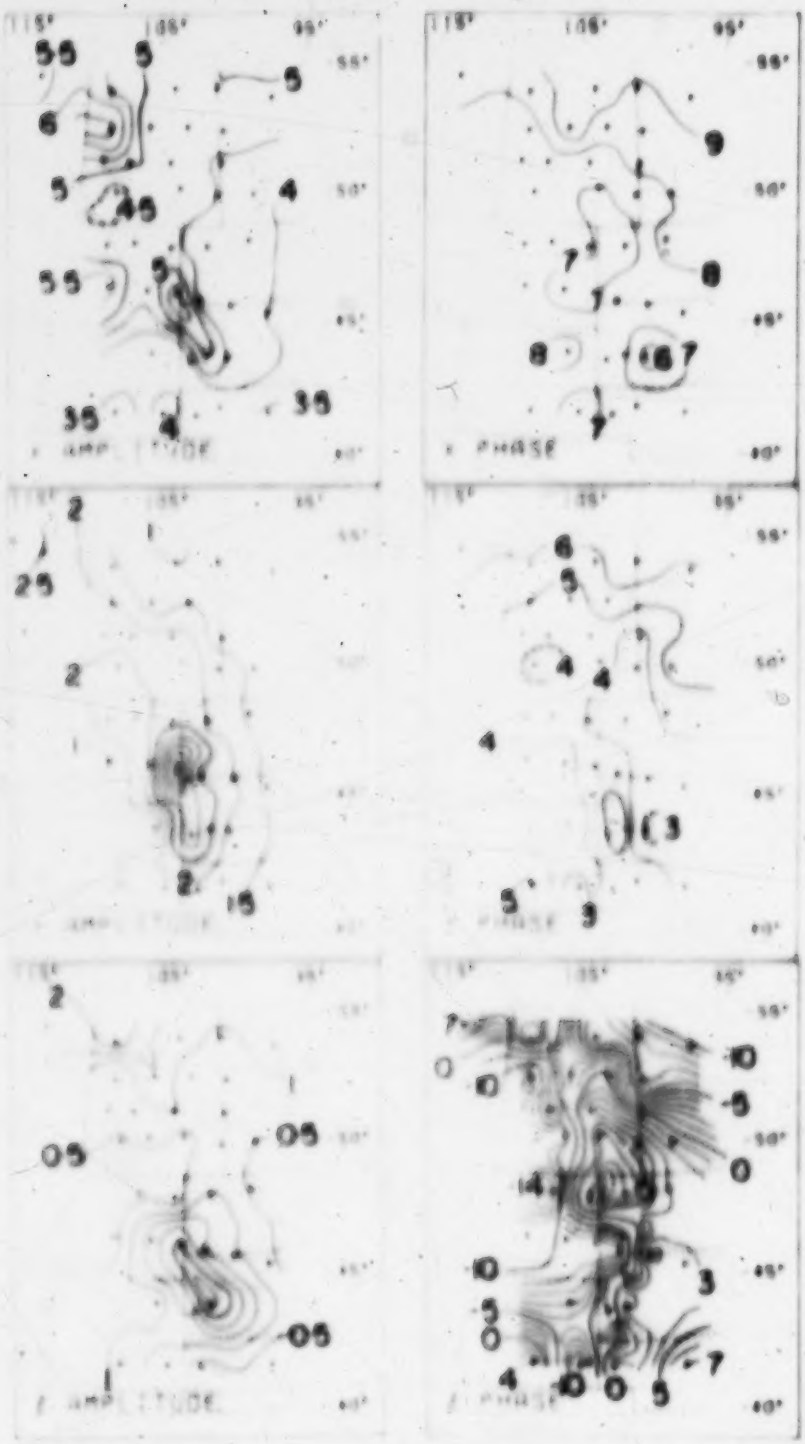

Fig. 4.21 Fourier amplitudes (in gammas) and phases (in minutes) at period 16.6 minutes from the disturbance event of September 13, 1972. The contour intervals are 1 γ for amplitudes and 2 minutes for the phases. For polarization of the horizontal fields see Fig. 4.13.

13 Sept 1972 T = 36.6 min

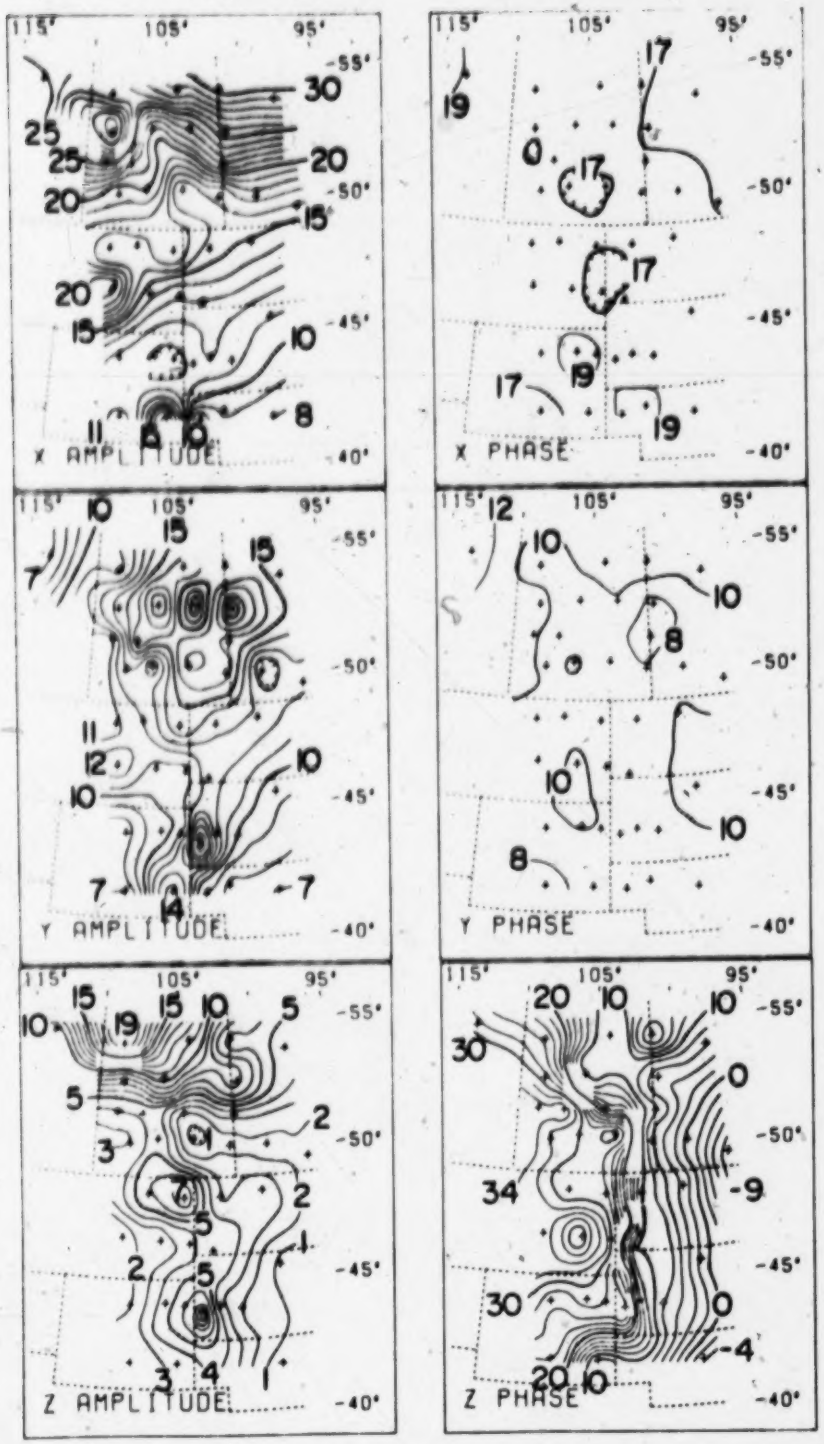

(maps shown in Figs. 4.19 through 4.21) the source fields do not produce such large gradients. In some amplitude maps it is possible to resolve the feature connected with the internal structure from the general trend well to the north of latitude 50°N. On some X phase maps a local minimum is superimposed on the more or less east-west phase increase trend (Figs. 4.14, 4.15 and 4.17) around BKR (46°N; 105°N; see Fig. 4.1). This is possibly related to the conductive body passing under this station. In the interpretation of phase maps it must be borne in mind that a change in sign from one map to another even for the same components may not have any significant physical meaning, because the absolute phase depends on the time interval chosen for the Fourier integral. The phase changes within each map are the significant results.

As earlier mentioned the most interesting feature found on the maps is the Central Plains anomaly. The Y and Z amplitude maps and Z phase maps contain abundant information on this. Throughout the period range of 13 to 170 minutes the anomaly persists. Camfield et al., (1971) discussed the anomaly in the period range 25-102 minutes. The X amplitude maps are in general less informative on the anomaly. Where they exhibit a local minimum or maximum except at the southern limit of the array, this is usually displaced from the axis of the current. Examples are seen in Figs. 4.20-21 and Fig. 4.15. These may be related to minor conductivity variations in the upper crust. Source-field variations may

also contribute. To the extent that the anomalous conductor strikes north-south, currents flowing in it will not produce anomalies in X. Two X amplitude maps (Figs. 4.19 and 4.21) show local maximum near CHU on line 8 (see location in Fig. 4.1). This indicates a downgoing current south of the Black Hills crustal conductivity anomaly into the deeper upper mantle conductive structure under the Southern Rockies. As earlier indicated a vertical current east of CHU would give enhanced X at CHU. The local maximum in the X phase maps (Fig. 4.16) is probably an expression of the downgoing current east of CHU.

The Y amplitude maps show the anomaly in variable manner as regards strike and extent. On the simple assumption that the axis of maximum conductivity is located under the Y maximum the conductor clearly passes under the Black Hills uplift in all maps (Figs. 4.14-4.21). Northward it bends slightly west of north to the intersection of the three state boundaries where some maps show a maximum in Y larger than that at the Black Hills (Figs. 4.18 and 4.20). The conductor then continues due north along the Montana-North Dakota boundary and into Saskatchewan, until it is lost in the source field of each event.

Very consistently in all maps the axis of the Y amplitude maximum swings to the southwest south of the Black Hills, to merge with Southern Rockies anomaly.

When the Z amplitude map is interpreted along with the Z phase maps, midpoint between the peaks in the Z amplitude is indicative of the axis of a linear conductive body. This gives a second method of locating the trend of the North American Central Plains conductor. When this is done the results are not always in harmony with the trends given by the maximum in Y amplitude.

For instance the Z maps in Fig. 4.20 indicate a strike more west of north than the Y maps show. In some cases, the line of Z cross-over is shifted several kilometers east or west of the axis of the Y anomaly, as for example in Fig. 4.14. The belt of crowded contour lines in Z-phase maps, however agree remarkably closely with strike of the anomaly as given by the Y amplitude maps in all the eight sets. The bend south of the Black Hills to the Southern Rockies is specially clear in the phase of Z.

4.3.4. Residual Fourier Coefficient Maps

The source field dominates the northern part of the maps of the last section. It is a standard practice in gravity and static magnetic field studies to separate anomalies of interest from regional fields by removing a general trend from the observed fields. The residual maps resulting from the process are usually more informative on the small-scale structures of interest. In the present study a similar approach has been tried to produce residual maps. The first

approach was to remove normal fields computed from a model of the auroral electrojet due to Summers and Weaver (1972). This yields smaller field gradients than the observed normal field gradients for X and Y components. The normal Y-field could not be adequately approximated probably because of the effects of field-aligned Birkeland currents (Appendix B). Next a simple approach was tried.

In each line of stations the mean of the sine and cosine coefficient data at the end stations was deducted from the coefficients at all the stations on the line. This assumes that the end stations represent the normal source field. Residual Fourier coefficients so obtained at periods 26.6, 68.3 and 170.7 minutes were contoured. Figs. 4.22-4.24 show the residual Fourier maps at the three periods for the horizontal field components X and Y.

It must be remembered that the sign of the coefficient maps and the distribution between sine and cosine coefficients depend on the transform window employed in computing the Fourier coefficients and have no physical significance. Thus, the anomaly can appear as features in cosine or sine maps or in both, and with either sign. In Fig. 4.22 it is interesting to note that the anomaly near the three-state intersection of the borders between the Dakotas and Montana appears in the sine coefficients, while that at the Black Hills is in the cosine map both with negative signs. This implies a phase difference of $\pi/2$ or 6.5 minutes at period 26 minutes, which

Fig. 4.22 Residual Fourier coefficient maps at period 26.6 min. The coefficients are in gammas and the contouring interval is 1 gamma for all components.

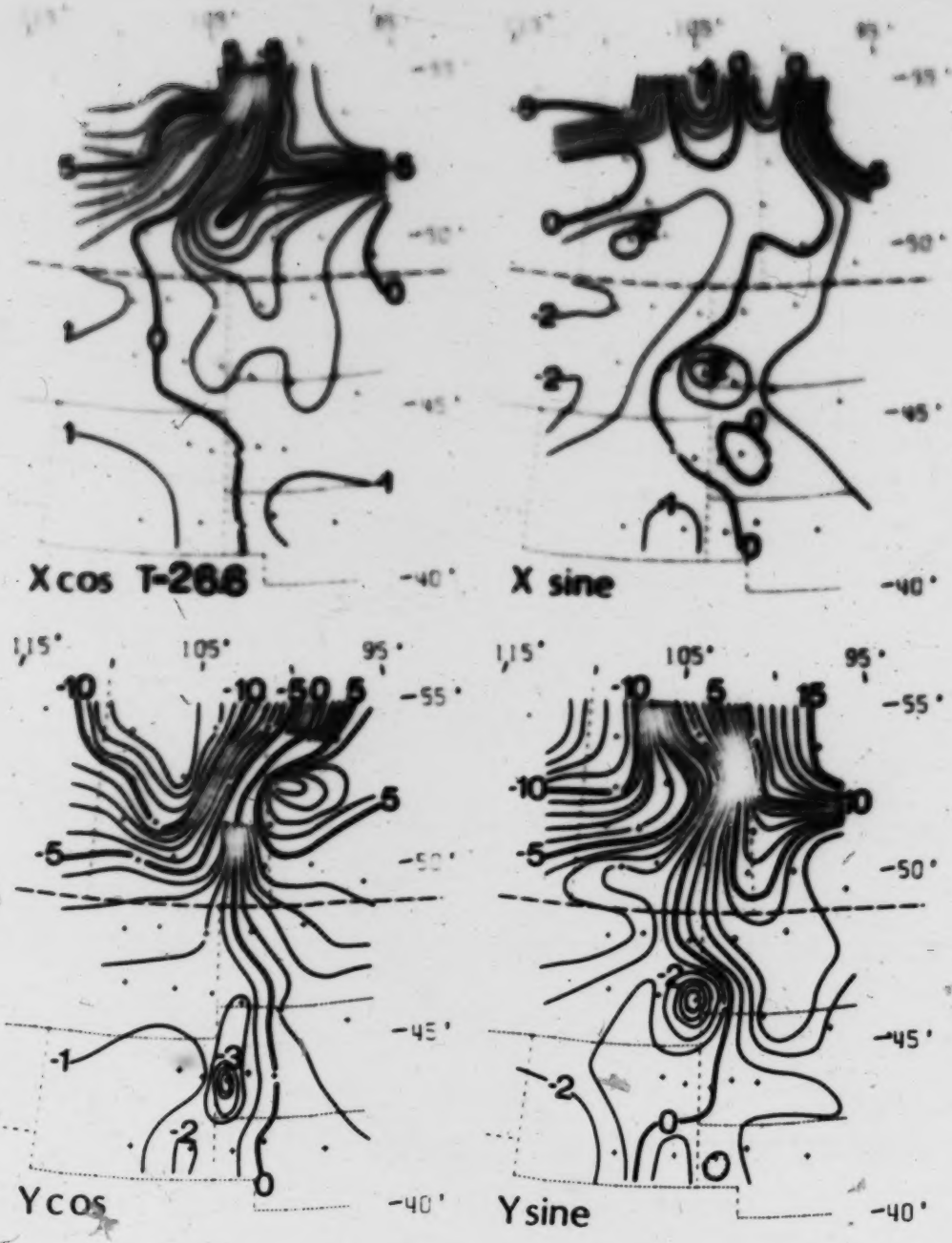
Xcos T-28.6
X sine
Ycos
Ysine
115°
105°
95°
-55°
-50°
-45°
-40°

Fig. 4.23 Residual Fourier coefficient maps at period 68.3 min. The coefficients are in gammas and the contouring interval is 1 gamma for all components.

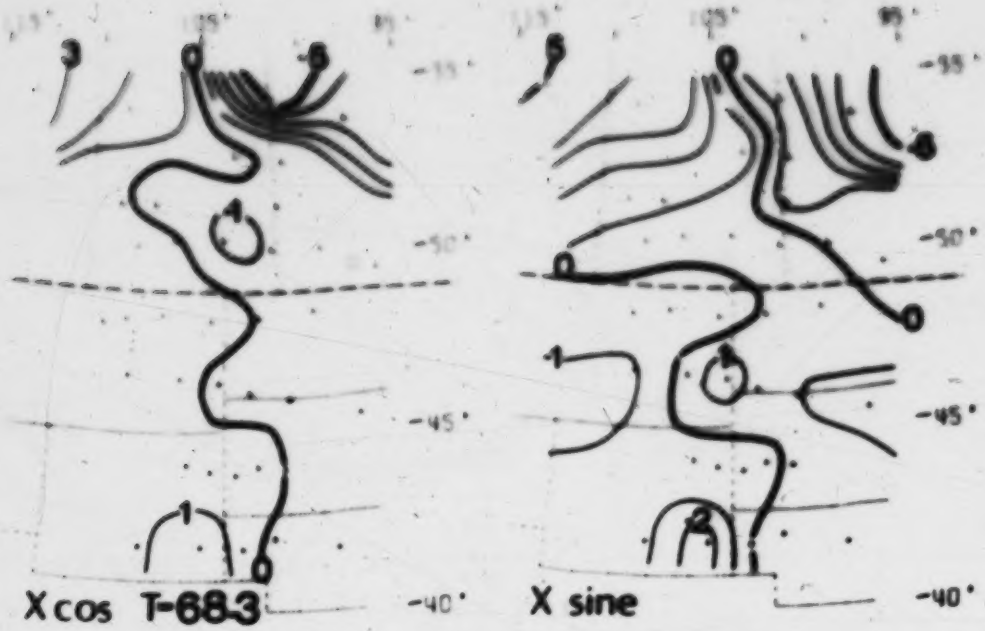
115°
105°
95°
-55°
-50°
-45°
-40°
Xcos T-683
X sine

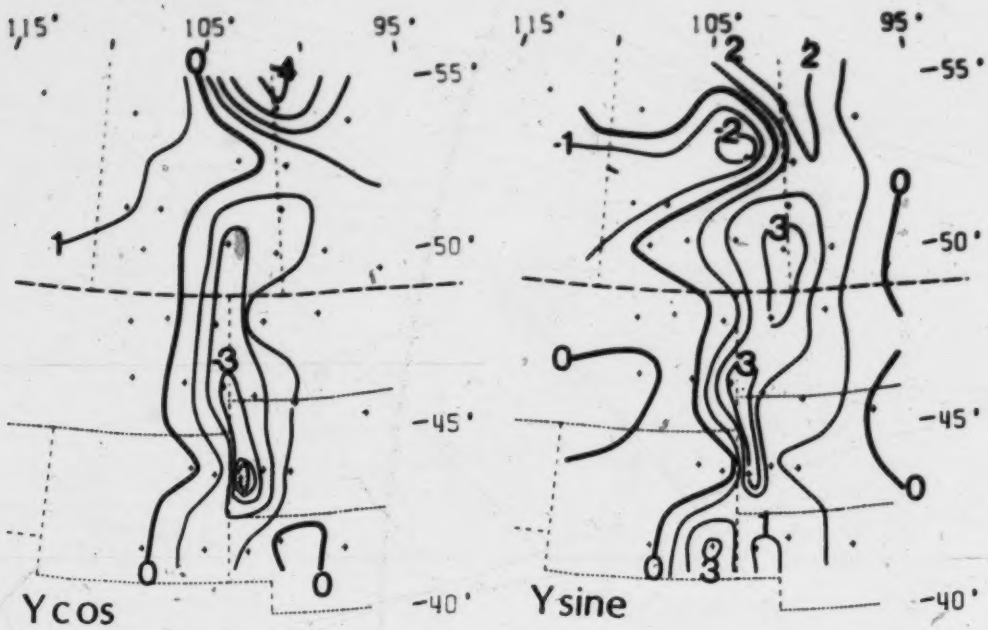
115°
105°
95°
-55°
-50°
-45°
-40°
Ycos
Ysine

Fig. 4.24 Residual Fourier coefficients maps at period 170.7 min. The coefficients are in gammas and the contouring interval is 1 gamma for all components.

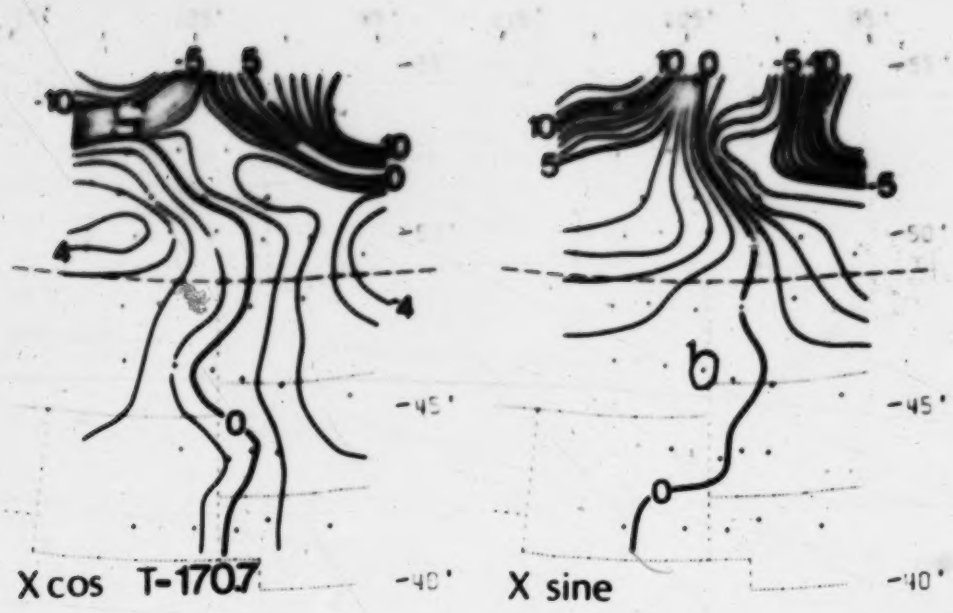
X cos T-1707
X sine
-40°
-45°
-50°

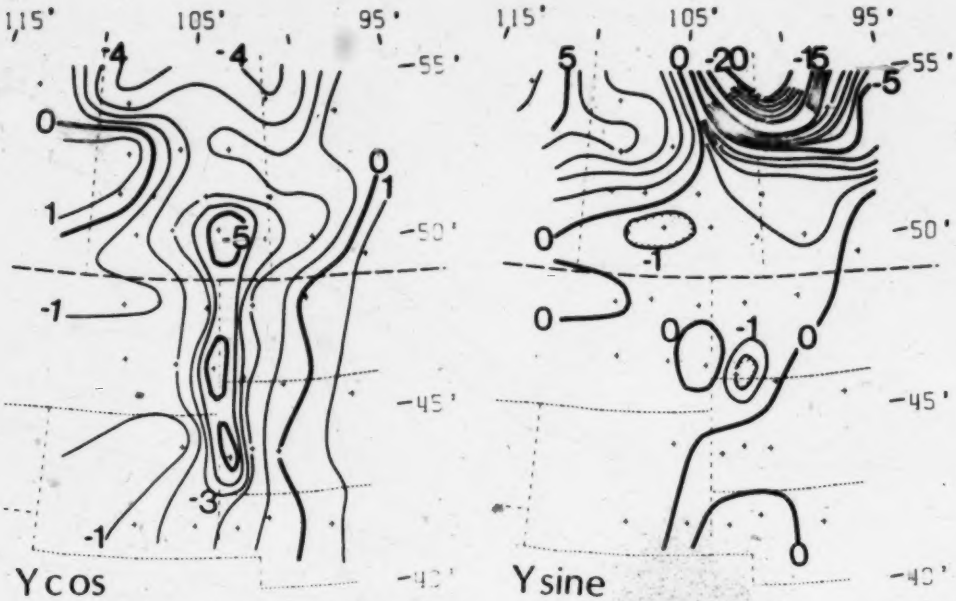
115°
105°
95°
-55°
-50°
-45°
-40°
Y cos
Y sine

agrees with Y phase map in Fig. 4.14. At period 68.3 minutes, near the maximum in the frequency response of the anomaly (Porath et al., 1971), the anomaly in Y appears over the latitude range 41° to 52°N, in both sine and cosine coefficient maps. At T = 170.7 min. (Fig. 4.24) it happens that the anomaly appears in the cosine map only.

Comparision of Figs. 4.23 and 4.15 shows that the rather simple approach to production of a residual map succeeds surprisingly wellin extending the closed contours to about 52°N at period 68.3 minutes. At 170.7 minutes (Figs. 4.24 and 4.17) the improvement is even greater. It is particular reassuring to observe the close resemblance between the residual anomalies of Figs. 4.23 and 4.24, derived from two different substorm events at very different periods. These maps indicate a conductor extending north to about 52°N, and either plunging to lower-crustal depth or broadening or both, in Canada.

The residual Fourier Y maps, the Y amplitude and Z phase maps allow the conductive body to be located with much better precision than was possible from the magnetograms. In Fig. 4.25, the location of the conductive zone in the North American Central Plains based on those Fourier maps is presented. In general, it is in agreement with the previous sketch in Fig. 4.8.

Fig. 4.25 The location of N.A.C.P. conductive body based on residual Y amplitude and Z phase anomaly maps of section 4.3.

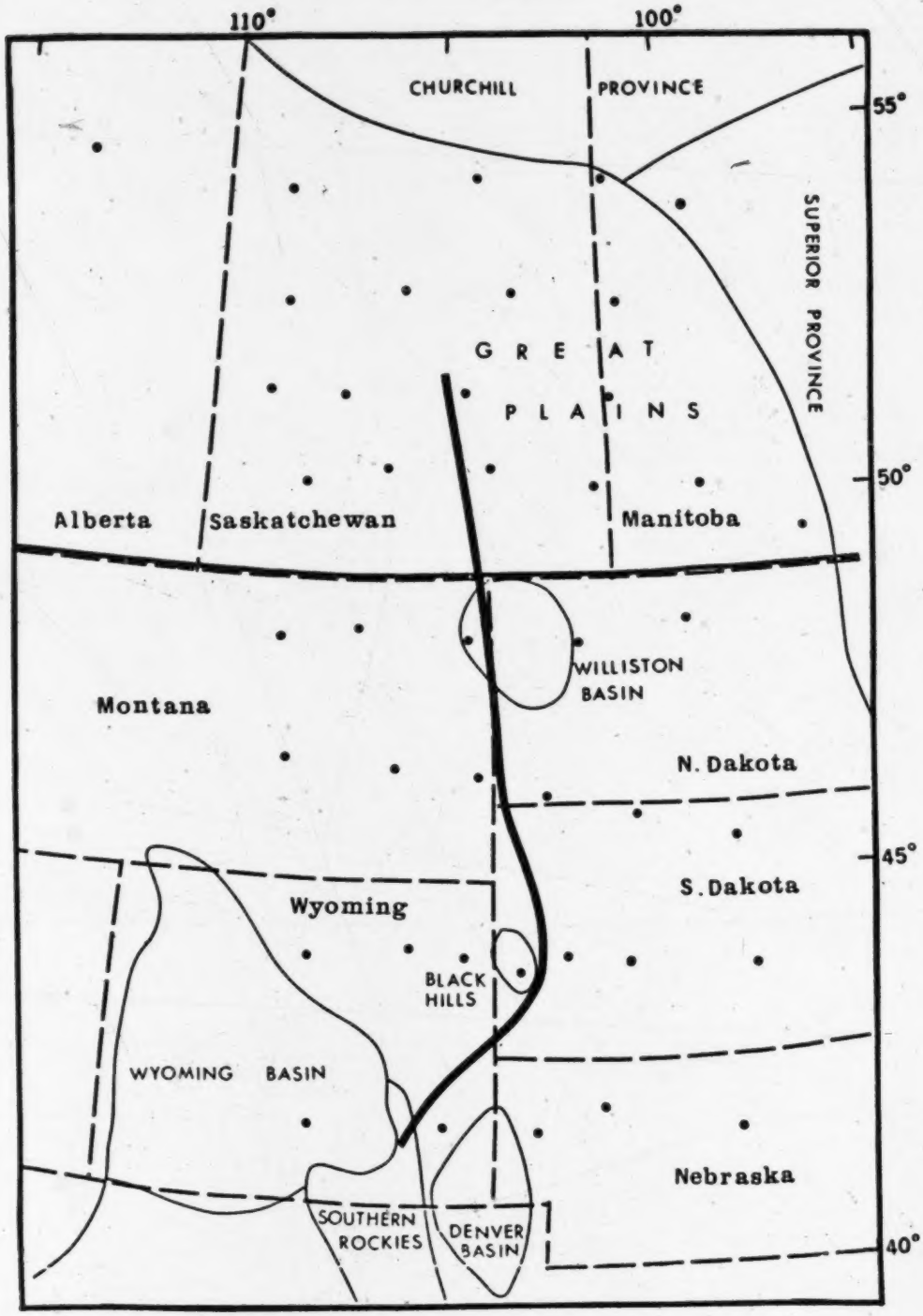
110°
100°
CHURCHILL
PROVINCE
55°
SUPERIOR PROVINCE
GREAT
PLAINS
50°
Alberta
Saskatchewan
Manitoba
WILLISTON
BASIN
Montana
N. Dakota
45°
S. Dakota
Wyoming
BLACK
HILLS
WYOMING BASIN
Nebraska
SOUTHERN
ROCKIES
DENVER
BASIN
40°

4.4. Transfer Functions

Transfer function and associated induction arrows provide another method of estimating the position of an induced current and hence of conductive structure. The theory of the method was outlined in Chapter I. In computing the transfer functions it was assumed that the normal Z field was negligible and hence that the observed Z field is totally anomalous. The mean of the horizontal fields at the end stations on each profile was taken as representing the normal horizontal field. Both assumptions are known to be poor approximations for this array, both because it is near the auroral zone and because the North American Central Plains anomaly is of current-concentration type. Equations (1.56a) and (1.56b) were used in calculating the transfer functions Z_x and Z_y from the Fourier transforms at periods 31.5, 36.6, 68.3 and 78.8 minutes. Six events of length ranging from 120 to 360 minutes were used. The transfer functions were computed only at stations where five or six events had been recorded. The induction arrows were reversed so that both the in-phase and the quadrature phase arrows point toward a good conductor. Most of the events were polar substorm type and possess peak-energy around 60 minutes but small around 30 minutes. Further, there is evidence that the anomaly has peak response near a period of one hour. It was found that the induction arrows at 68.3 and 78.8 minutes display a pattern, and these are shown in Figs. 4.26 and 4.27. The shorter period arrows

Fig. 4.26 The induction arrows at period 68.3 min. plotted as in-phase and quadrature phase components.

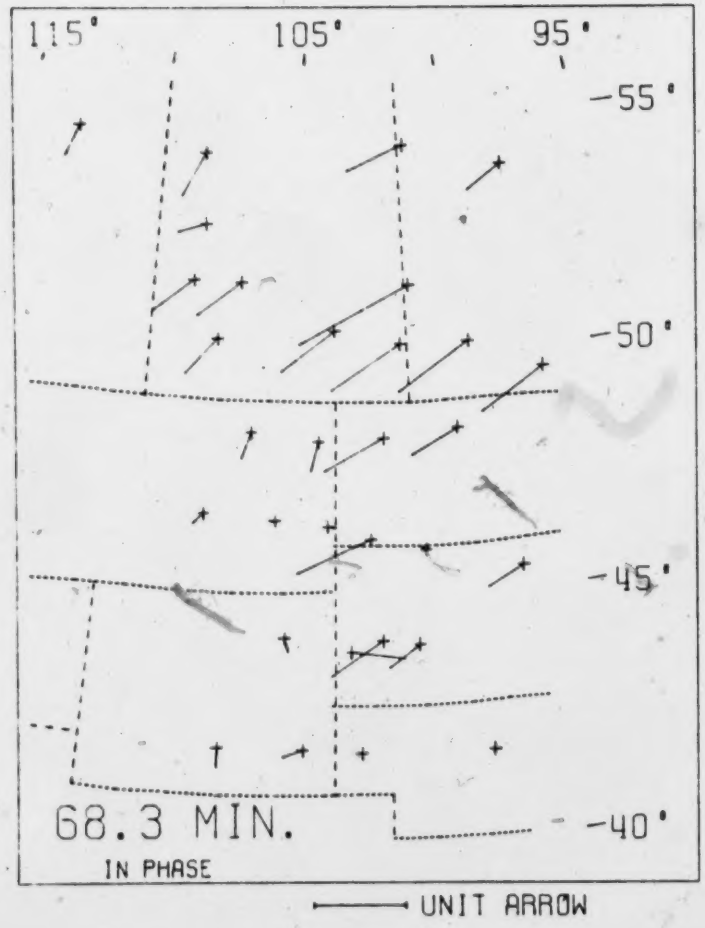
115°
105°
95°
-55°
-50°
-45°
-40°
68.3 MIN.
IN PHASE
UNIT ARROW

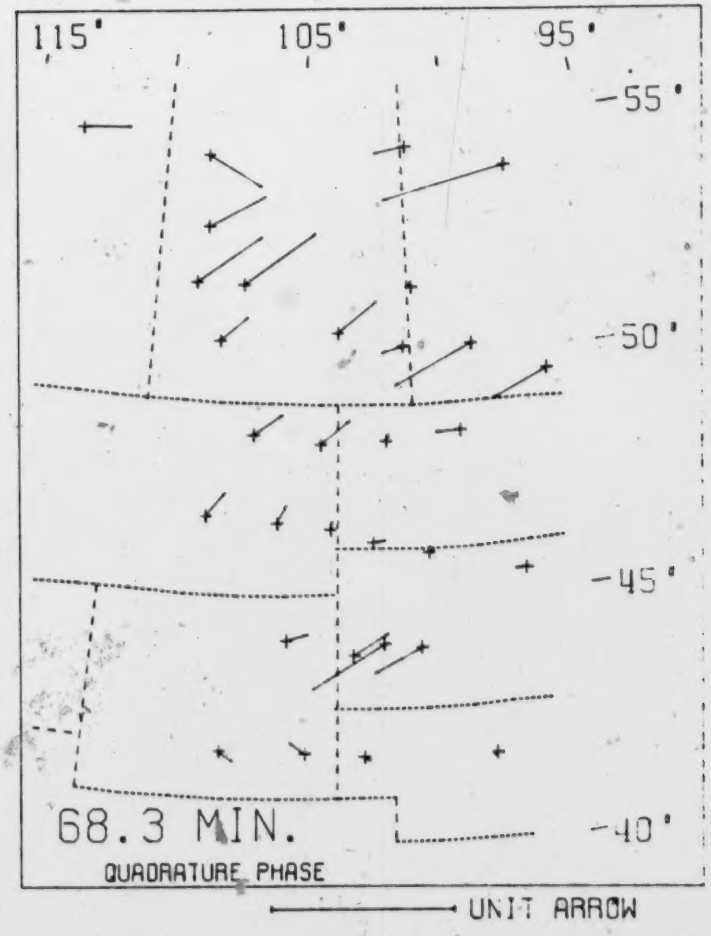
115°
105°
95°
-55°
-50°
-45°
-40°
68.3 MIN.
QUADRATURE PHASE
UNIT ARROW

Fig. 4.27 The induction arrows at period 78.8 min. plotted as in-phase and quadrature phase components.

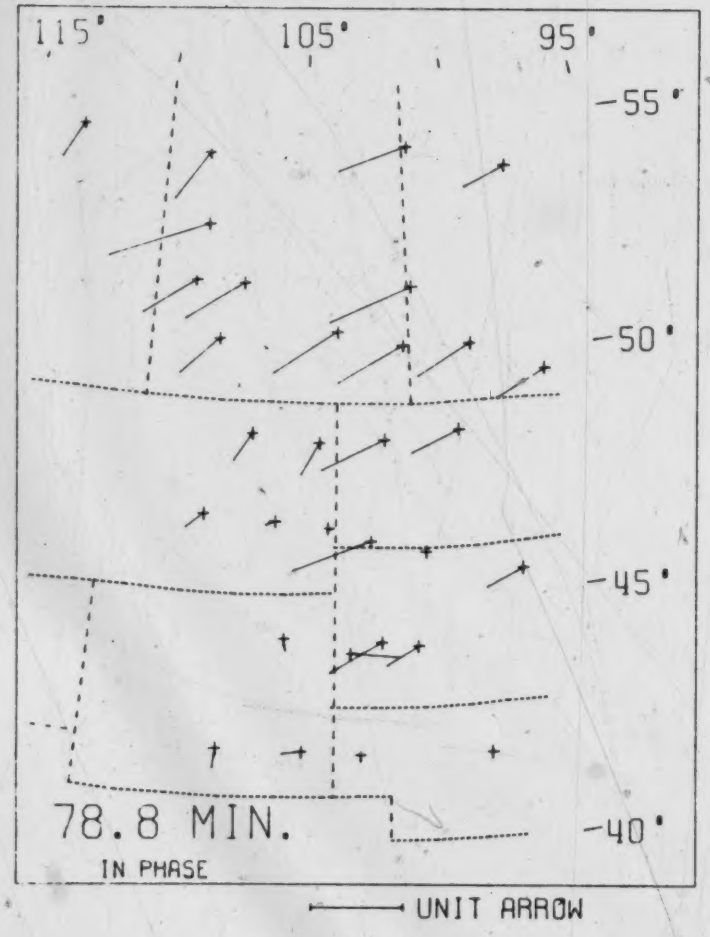
115°
105°
95°
-55°
-50°
-45°
-40°
78.8 MIN.
IN PHASE
UNIT ARROW

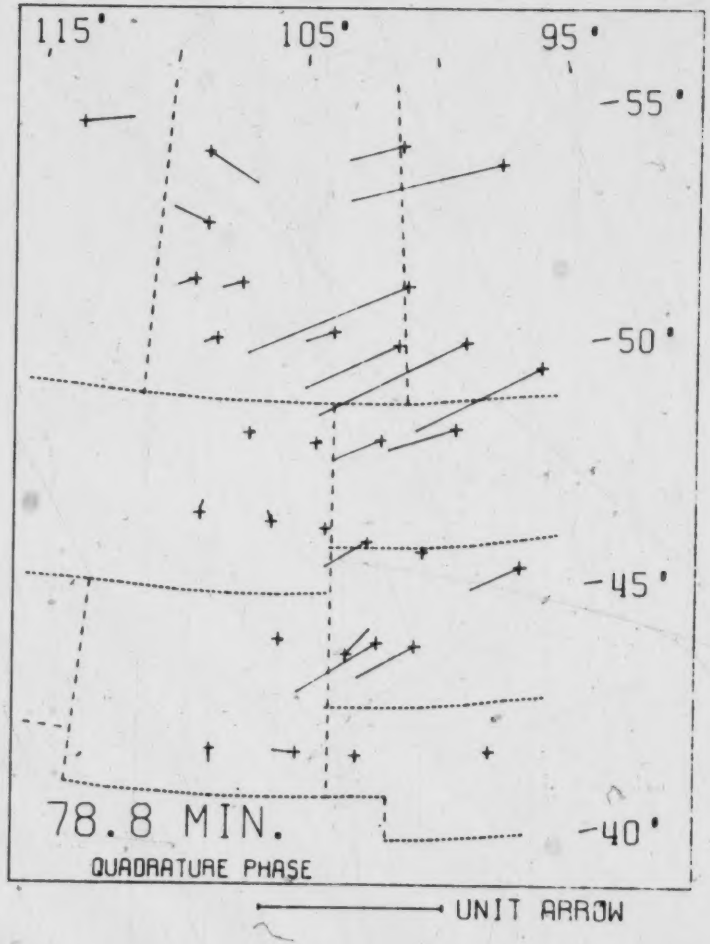
115°
105°
95°
-55°
-50°
-45°
-40°
78.8 MIN.
QUADRATURE PHASE
UNIT ARROW

convey little of interest. It should be noted that the quadrature-phase arrows are doubled in length compared with in-phase arrows.

The in-phase arrows at both periods and the quadrature-phase arrows at 78.8 minutes indicate the presence of the N.A.C.P. conductive body by a change of length of the induction arrows. Stations east of the conductor have long arrows directed west-southwest. Stations west of the conductor have short arrows in scattered directions. Only at CUS just west of the Black Hills does this induction arrow point east and locate the conductor under the Black Hills. The quadrature-phase arrows of Fig. 4.26 are much more interesting, pointing toward the conductor from both sides. Their reversal locates the conductor and confirms its presence through the whole north-south length of the array.

The following explanation is offered for the somewhat unexpected success of the quadrature-phase transfer-functions at 68.3 minutes. Normal Z is mainly in-phase with X and Y so the in-phase contain largely information about the normal field. At period 68.3 minutes the response of the conductive system is near maximum, and in quadrature-phase the normal field makes a relatively small contribution to Z_x and Z_y. The assumptions adopted in calculating these functions are therefore more nearly valid and the induction effects stand out.

It is encouraging that the residual Y amplitude and Z phase anomaly maps of the last section, and the induction

arrows of Figs. 4.26, agree as to the location of the conductive structure.

CHAPTER V

THE NATURE OF THE CONDUCTIVE ZONE UNDER THE NORTH AMERICAN CENTRAL PLAINS

5.1. Depth Estimates for the Conducting Zone Under the Central Plains

Examination of the magnetograms, the Fourier transform maps and the induction arrows presented in the last chapter provide evidence for a narrow conductive zone extending between latitudes 41.8°N and 54°N and possibly further north. An estimate of the depth to the conductor can be made from a line-current approximation. If a line-current I amp flows at a depth d metre the magnetic fields at the horizontal distance y metre from the axis are given by:

$$\text{Eastward:} \quad Y = \frac{200\ I\ d}{(y^2 + d^2)}\ \gamma \qquad (5.1)$$

$$\text{Vertical:} \quad Z = \frac{200\ I\ y}{(y^2 + d^2)}\ \gamma \qquad (5.2)$$

Y has a maximum of 200I/d at y = 0 (on the current axis). At a distance d on either side of the axis Y assumes the value 100I/d. Thus, the halfwidth of the Y amplitude profiles is twice the depth of the line current. Also, at $y = \pm d$ equation (5.2) assumes extremal values $\pm$ 100I/d. The separation between the positive and negative peaks in Z is twice the depth to the linear current. The current axis must

be under the point where cross-over (Z = 0) is observed.

To use the line current approximation in estimating the depth of the conductor the anomalous component of the observed field must be separated from the normal field. The normal fields Y_n and Z_n are estimated as the means of the observations at the two end stations on each east-west profile. From the Fourier maps and the Fourier parameter data profiles of normalized eastward field (Y_a/Y_n) and vertical field (Z_a/Y_n) have been extracted using the relations:

$$\frac{Y_a}{Y_n} = \frac{Y - Y_n}{Y_n} \qquad (5.3)$$

$$\frac{Z_a}{Y_n} = \frac{Z - Z_n}{Y_n} \qquad (5.4)$$

where Y and Z refer to the observed fields. Figs. 5.1-4 illustrate the profiles at different periods and latitudes.

It is known that the induced horizontal (Y_a say) over a perfectly conducting half-space is in the limit equal to the normal field (Y_n) (Price, 1950). A finite conductive body must therefore cause an anomalous field Y_a much less than the normal Y_n. In the amplitude profiles of Y_a/Y_n (Figs. 5.1-5.4) peaks of Y_a/Y_n often exceed unity. This demands the current channelling effect as pointed out by Camfield et al., (1971) under the Central Plains anomaly.

The separations between Z peaks yield more consistent estimates of the depth estimates than the Y halfwidths. The

Fig. 5.1 Normalized eastward (Y_a/Y_n) and vertical (Z_a/Y_n) amplitude profiles at latitude 43.8°N for periods 13.3, 36.6, 68.3 and 170.7 minutes.

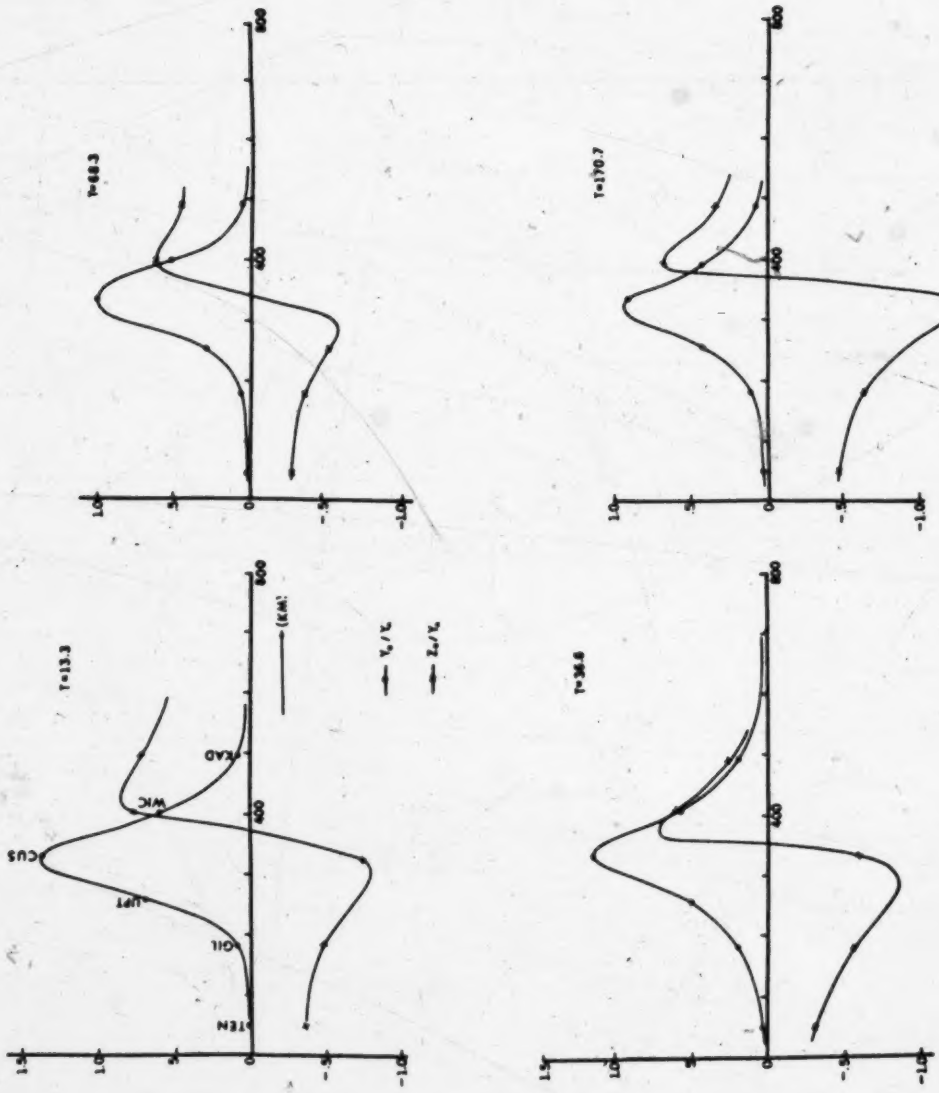
T=88.3
T=170.7
T=13.3
T=36.8
(KM)
Y_1/Y_0
Y_2/Y_0
READ
WIC
CUS
UPT
OIL
TEN
800
400
0
-400
-800
1.0
.5
-.5
-1.0

Fig. 5.2 Normalized anomalous eastward (Y_a/Y_n) and vertical (Z_a/Y_n) amplitude profiles at latitude 46.4°N for periods 13.3 and 170.7 minutes.

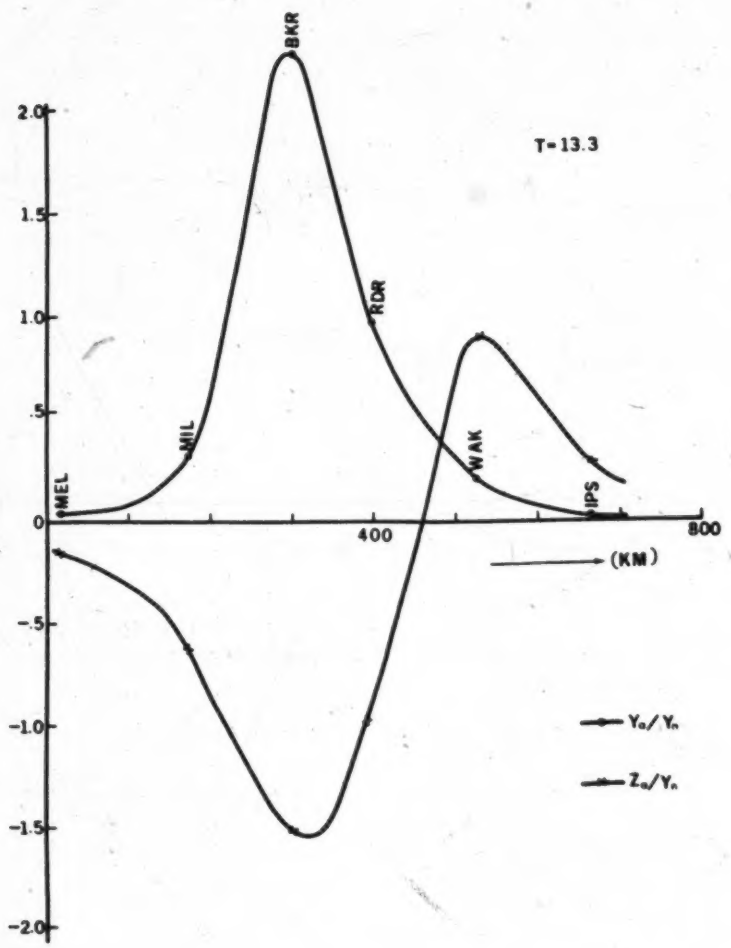
BKR
T=13.3
RDR
MIL
WAK
MEL
IPS
2.0
1.5
1.0
.5
0
-.5
-1.0
-1.5
-2.0
400
800
(KM)
Y_o/Y_n
Z_o/Y_n

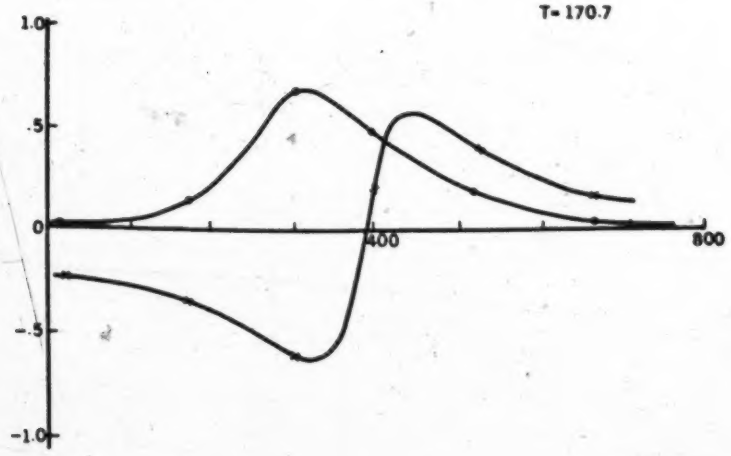
T=170.7
1.0
.5
0
-.5
-1.0
400
800

Fig. 5.3 Normalized anomalous eastward (Y_a/Y_n) and vertical (Z_a/Y_n) amplitude profiles at latitude 41.8°N for period 36.6 minutes.

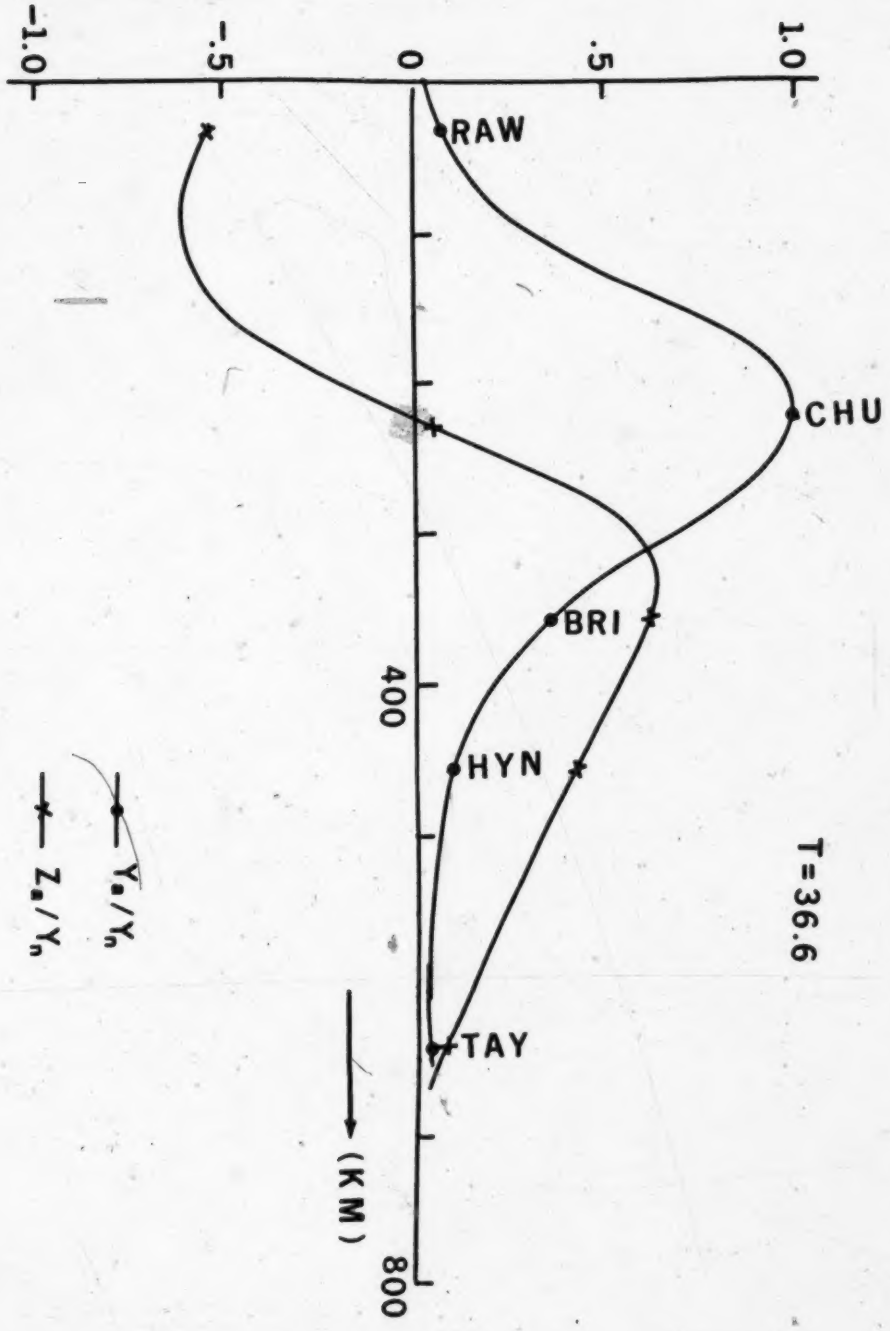
-1.0
-.5
0
.5
1.0
RAW
CHU
BRI
400
HYN
TAY
800
(KM)
T=36.6
Y_a/Y_n
Z_a/Y_n

Fig. 5.4 Normalized anomalous eastward (Y_a/Y_n) and vertical (Z_a/Y_n) amplitude profiles at latitude 48°N for period 170.7 minutes.

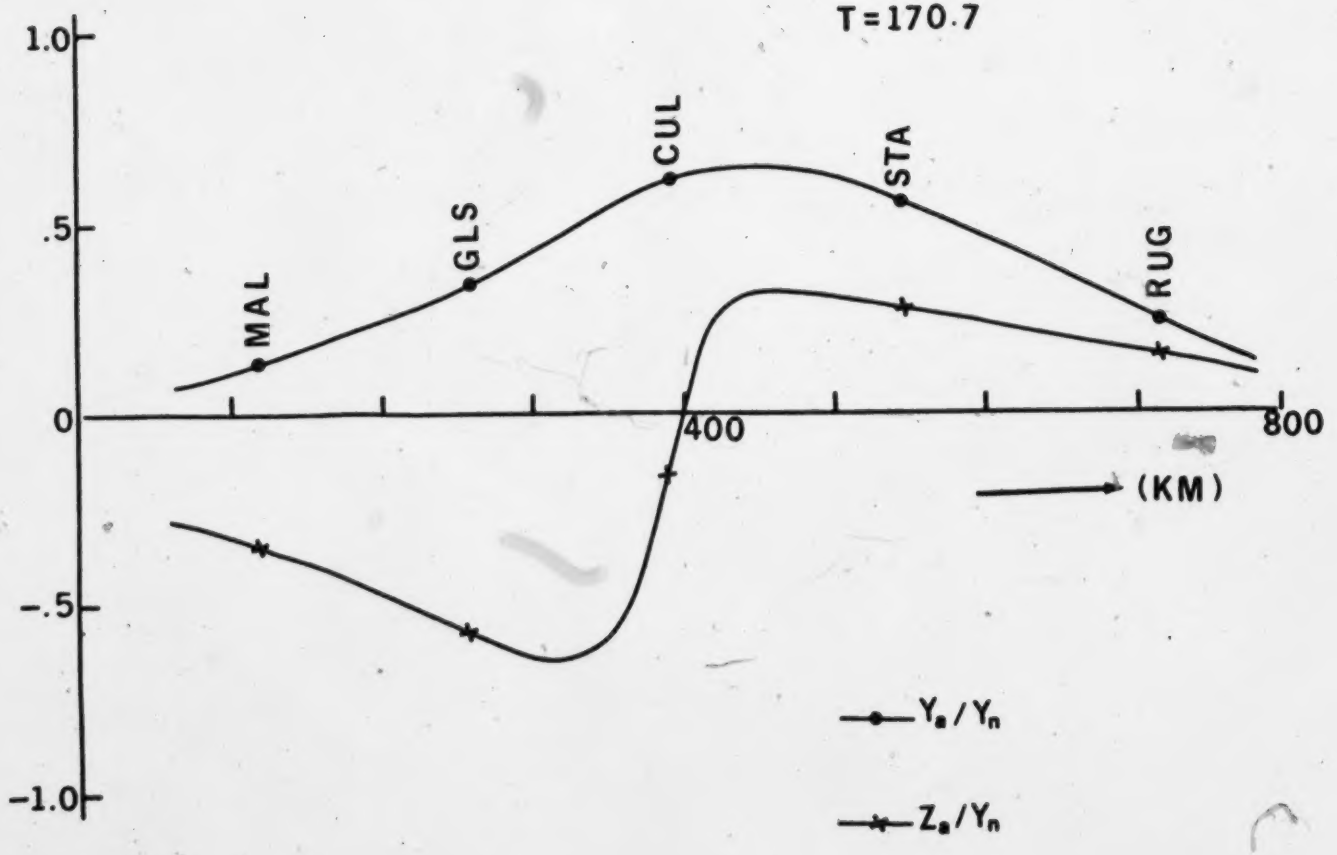
T=170.7
1.0
.5
0
-.5
-1.0
MAL
GLS
CUL
STA
RUG
400
800
(KM)
Y_a / Y_n
Z_a / Y_n

results of depth estimates to the conductor are given in column 3 of Table 5.1. From the location of Y maximum and Z cross-over the axis of the internal current is also determined. Results are given in columns four and five of Table 5.1. It is noticed that the Z-cross-over is often displaced several tens of kilometers east of Y-maximum. This probably indicates that the current is not a simple line current. Large station spacing can also be a contributor to this effect. Also, the Z_a/Y_n profiles are in general asymmetric, this feature was also found by Porath et al., (1971) in Z_a/Y_n profiles across the Black Hills uplifts (See Fig. 3.6). It is either due to deviation of the current from being simple line current or to large station spacing or to both. From Table 5.1 it is seen that the depth to the line current is between 37 and 75 km. between latitudes 43.8° and 48.0°N, but 120 km at the southernmost profile (latitude 41.8°N). These depth estimates further support the dipping of the crustal current somewhere south of the Black Hills to link with the deep current in the upper mantle under the Southern Rockies.

Camfield (1973) gives a sketch originally due to Gough (unpublished) of a network of conductors which could produce the anomaly (see Fig. 5.3; Camfield, 1973). A narrow conductor in the crust joins two large undefined conductive regions possibly in the crust. A return current is allowed to flow in connecting conductors possibly in the crust or upper mantle which link the two undefined regions. The conductivity of the narrow

TABLE 5.1.

Maximum depths to the line current and the locations of its axis at various latitudes

Latitudes °N	Period (Minutes)	Maximum Depth (km)	Location of Axis (degree W)	
			From Y Maximum	From Z cross-over
41.8	36.6	120	104.9	104.8
43.8	13.3	43	103.5	103.2
	36.6	37	103.5	103.3
	68.3	60	103.4	103.3
	170.7	45	103.4	103.4
46.4	13.3	75	104.1	102.4
	170.7	65	104.1	101.9
48.0	170.7	55	104.8	104.6

conductor is higher by 2 orders of magnitude than the conductivity of the surrounding region. The unknown regions in the Gough-Camfield model inevitably remain undefined in the present array, since they are outside its limits.

In this thesis the emphasis is on detailed mapping of the anomalous conductor. Models of conductive bodies that may provide more quantitative knowledge of the structure are not attempted. In Chapter III the unsuccessful effort of Porath et al., (1971) to model the anomaly by induction in a two dimensional body was mentioned. It appears that three-dimensional numerical modelling is a possible resort. The Gough-Camfield type of structure is, of course, three-dimensional. At the moment the cost of modelling three-dimensional bodies is almost prohibitive for a University research grant. For crustal anomalies Russian workers (Rokityanskiy et al., 1969) have employed diffraction of plane waves by a conducting cylinder immersed in a non-conducting medium to derive simple relations for interpreting geomagnetic depth sounding and magnetotelluric data. As geomagnetic induction theory involves the diffusion equation the use of plane waves is obviously questionable. The Alert anomaly in Ellesmere Island of the Canadian arctic has been well studied for several years (Whitham, 1964; Niblett and Whitham, 1970; and Praus et al., 1971).

This anomaly involves a reversal in Z accompanied by an enhancement in the horizontal field within a short distance. This is similar to the North Central Plains anomaly although it is of smaller magnitude. In modelling this anomaly, Rikitake and Whitham (1964) found that a conducting cylinder at a depth 25-30 km coupled to a more conducting mantle could adequately account for the observed field variations. When this model failed to account for the magnetotelluric observations of Whitham and Anderson (1965), Dyck and Garland (1969) produced analogue model of the current channelling effect to explain the puzzling features. Thus, the interpretation of a current channelling anomaly in terms of conductive body is very difficult and may remain unapplied for some time to come. In computing three-dimensional models of conductive structures, data from the undefined regions connected by the conducting zone are a necessity for meaningful interpretation. Securing such data is fraught with vast difficulties of logistics and is at present impossible.

5.2. Possible Association of N.A.C.P. Anomaly With Other Geophysical Observations

The 1972 array is in the region termed the stable Central Plains by King (1959). The region is composed of Precambrian basement mantled by a veneer of Paleozoic and later sediments. Since the Precambrian time, the Central Plains have been subjected to only mild tectonic disturbances. Bordering the array to the north is the Canadian shield where Precambrian

basement has been exposed. The shield has been divided into structural provinces on the basis of potassium-argon dating by Stockwell (1962).

The conductive body mapped in this study is not correlated with any major tectonic features except at its southern end where it disappears into the Southern Rockies (See Fig. 4.1). Sedimentary rocks do not usually contain highly conductive regions such as are required to generate the large anomalies observed in the variation fields. In Germany for example, thick sedimentary structures at the edge of more resistive regions were found attractive in the explanation of the anomalies observed in geomagnetic and telluric variation fields by Vozoff and Swift (1968). In the North American Central Plains however there is no reason to expect very conductive sediments, still less their concentration in a narrow linear strip.

The Black Hills uplifts are a geothermal region. The heat flow of 2.2 HFU observed in the region is anomalously higher than the 1.4 HFU generally found in the Central Plains (Blackwell, 1969; Sass et al., 1971; Combs and Simmons, 1973). A narrow anomaly in the crust solely due to heat flow will require a high temperature (> 1000°C) at this shallow depth. This is unreasonable for this depth (Tozer, 1959).

Seismic travel times of P- and S- body waves show regional variation in the upper mantle structure in North America (Herrin and Taggart, 1968; Hales and Herrin, 1972).

A narrow structure of the type encountered in N.A.C.P. is very unlikely to be detected by seismic methods. An examination of the gravity anomaly maps of Canada (see Map 38 of Buck, 1968; as an example) yields no clear evidence of density variation related to the anomaly.

Camfield et al., (1971) suggested that a belt of graphite schist might be responsible for the anomalous conductive zone under the Central Plains. Independent evidence by Lidiak (1971) confirms the presence of metamorphic rocks in sufficient abundance in the basement exactly in the position of the conductive structure (Gough and Camfield, 1972). Camfield et al., (1971) mapped the anomaly between latitudes 44° and 48°N. Magnetotelluric work by Vozoff et al., (1969) in eastern Montana had shown the existence of conductive bodies in the region of the present anomaly. Recently, Rankin and Reddy (1973) presented results from magnetotelluric sounding at three sites in and around the Black Hills uplifts. The computed tensor apparent resistivity led them to suggest that the anomaly is confined to the central region of the Black Hills, and to be due to migration of hydrated subcrustal melts into the upper crust. Their restricted frequency range effectively confines their observations to the crust.

If the line of the anomaly axis is continued northward to the shield it coincides with a linear fault zone in the Churchill province (see Fig. 1 of Byers, 1962). This led the writer to suspect a connection of this anomaly with faults in

the lower crust. The high conductivity could be related to a belt of metamorphic rocks preserved between the faults in which case Liadiak's metamorphic belt would be fault-bounded. Alternatively the high conductivity could be related to serpentinized sub-crustal rocks which had invaded the fault zone. Here the suggestion of Hyndman and Hyndman (1968) that hydrated sub-crustal minerals could be highly conductive is relevant. A suggestive piece of independent evidence supports the existence of a fault near the conductive zone in the Williston Basin (see Fig. 4.1 and 4.8).

The epicentres of an earthquake of moderate magnitude which occurred on July 26, 1972 at Bengough, Saskatchewan lies on the axis of the conductor at 49.68°N, 104.88°W (Horner et al., 1973). Two other earthquakes are known to have occurred at approximately the same location. The Avonlea earthquake of May 15, 1909 (Agarwal, 1962) has its epicentre located at 50°N, 105°N. Another earthquake has been located approximately 50 km northeast of Bengough; this occurred on October 11, 1968. Fig. 5.5 is a sketch map of Saskatchewan showing the conductive body and the epicentres. Earthquakes are rare in Saskatchewan (see Milne; 1967). It has been proposed (Bishop, 1956) that the earthquakes were related to collapse of top structure over a cavity left by dissolved Prairie evaporite (salt) beds. While this remains a valid possibility, arguments in favour of deep-faulting have also been put forward (for example by Haites, 1959). The location

Fig. 5.5 Map of Saskatchewan showing the N.A.C.P. conductive body and the epicentres of the 3 earthquakes recorded in this region.

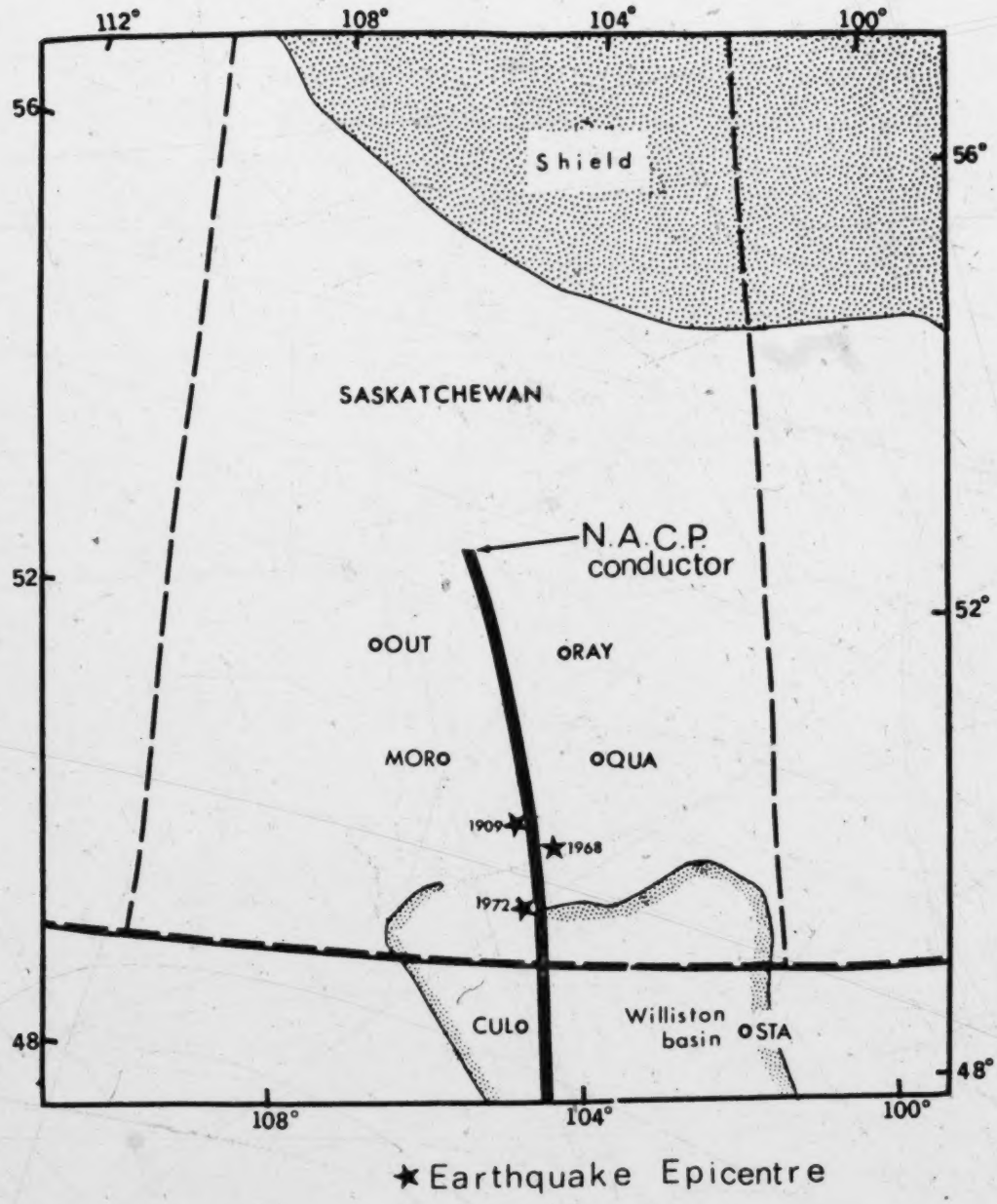
112°
108°
104°
100°
56
56°
Shield
SASKATCHEWAN
N.A.C.P.
conductor
52
52°
OOUT
ORAY
MORO
OQUA
1909
1968
1972
48
48°
CULO
Williston
basin
OSTA
108°
104°
100°
★ Earthquake Epicentre

of the epicentres near the conductive body suggests that alternatively the basement faults may still be active.

In the Ukranian shield Rokityanskiy et al., (1969) and Rokityanskiy and Logvinov (1972) have discovered elongated crustal conductive zones along fault zones.

Whether or not a metamorphic belt extends along the whole length of the North American Central Plains anomaly, it is very probable that graphite schists contribute to the high conductivity under the Black Hills. A similar belt of graphite schists has been proposed to account for the variation field anomalies in west Hungary (Adam, 1973).

From the interpretation of the magnetograms and Fourier maps, it has been suggested that the crustal anomaly of North American Central Plains makes an almost vertical link with the conductive zone in the upper mantle under the Southern Rockies. The alternative is that the two currents overhap at their different levels and each fans out one in the crust and the other in the upper mantle. This would be a strange coincidence and is unlikely. For an almost vertical link an almost vertical conductor perhaps in the form of rising magma columns is required.

5.3 Suggestions for Future Array Studies

The present study has mapped the conductive zone in the North American Central Plains to a latitude 54°N although

with poor lateral definition beyond 52°N. A future array study could be designed to define the lateral extent of conductor from latitude 52°N and beyond. In such residual anomalies obtained by deducting the fields of a three-dimensional current system over a layered earth from the observed fields might isolate the induced fields better.

A dense array to the south of the Black Hills might further elucidate the relationship between the North American Central Plains crustal conductor and the Southern Rockies upper-mantle conductor.

REFERENCES

REFERENCES

Adam, A. (1973) Two kinds of characteristic ΔZ conductivity anomaly in West Hungary and their appearance in R.T.F.S. and M.T.S.; Phys. Earth Planet. Interiors, 7, 486-490.

Anderson, C. W. (1970) Geomagnetic depth sounding and the upper mantle in the western United States; Ph.D. Thesis, Department of Physics, University of Alberta, Edmonton, Canada.

Anderson, D. L. (1967) Phase changes in the upper mantle; Science, 157, 1165-1173.

Agarwal, R. G. (1962) Earthquake of May 15, 1909; J. Alberta Soc. Pet. Geol., 10, 198-202.

Bennett, D. J. and F.E.M. Lilley (1972) Horizontal polarization in array studies of anomalous geomagnetic variations; Nature Phys. Sci., 237, 8-9.

Bishop, R. A. (1956) Explanation of the Avonlea fault block in southern Saskatchewan; J. Alberta Soc. Petrol. Geol., 4, 10, 235-236.

Blackman, R. B. and J. W. Tukey (1959): The Measurement of Power Spectra; Dove, New York, N.Y.

Blackwell, D. D. (1969) Heat flow determination in the northwestern United States; J. Geophs. Res., 74, 992-1007.

Bonnevier, B., R. Bostrom and G. Rostoker (1970) A three-dimensional model current system for polar magnetic substorms; J. Geophys. Res., 75, 107-122.

Born, M. and E. Wolf (1959) Principles of Optics; Pergamon Press Inc., New York.

Buck, R. J. (1968) The Gravity Anomaly Field in western Canada with maps Part II; Pub. Dom. Obs. Canada.

Byers, A. R. (1962) Major faults in western part of Canadian shield with special Reference to Saskatchewan; The Tectonics of the Canadian Shield, Roy. Soc. Canada, Special Pub., 4, 40-59.

Camfield, P. A. (1973) Studies with a two-dimensional magnetometer array in northwestern United States and southwestern Canada; Ph.D. Thesis, Department of Physics, University of Alberta, Edmonton, Canada.

Camfield, P. A., D. I. Gough and H. Porath (1971). Magnetometer array studies in the northwestern United States and southwestern Canada; Geophys. J. R. astr. Soc., 22, 201-221.

Caner, B., W. H. Cannon and C. E. Livingstone (1967) Geomagnetic depth sounding and upper mantle structure in the cordillera region of western North America; J. Geophys. Res., 72, 6335-6351.

Chan, T., E. Nyland and D. I. Gough (1973) Partial Melting and conductivity anomalies in the upper mantle; Nature, 244, 1366, 89-91.

Chapman, S. and A. T. Price (1930) The electric and magnetic state of the interior of the earth as inferred from terrestial magnetic variations; Phil. Trans. Roy. Soc., A 229, 427-482.

Chapman, S. and T. T. Whitehead (1923) The influence of electrically conducting material within the earth on various phenomena of terrestrial magnetism; Trans. Cambridge Phil. Soc., 22, 463-482.

Cochrane, N. A. and R. D. Hyndman (1970) A new analysis of geomagnetic depth-sounding data from western Canada; Can. J. Earth Sci., 7, 1208-1218.

Coggan, J. H. (1971) Electromagnetic and electrical modelling by finite element method; Geophys., 36, 132-155.

Combs, J. and G. Simmons (1973) Terrestrial Heat Flow Determination in the North Central United States; J. Geophys. Res., 78, 441-461.

d'Erceville, I. and G. Kunetz (1962) The effect of a dyke fault on the earth's natural electromagnetic field; Geophys., 27, 651-665.

Dosso, H. W. (1966) Analogue model measurements for electromagnetic variations near vertical faults and dykes; Can. J. Earth Sci., 3, 287-303.

Dosso, H. W. and J. A. Jacobs (1968) Analogue model measurement of electromagnetic variations in the near field of an oscillating line current; Can. J. Earth Sci., 5, 23-29.

Dyck, A. V. and G. D. Garland (1969) A conductivity model for certain features of the Alert anomaly in geomagnetic variations; Can. J. Earth Sci., 6, 513-516.

Everett, J. E. and R. D. Hyndman (1967) Geomagnetic variations and electrical conductivity structures in southwestern Australia; Phys. Earth Planet. Interiors, 1, 24-34.

Fowler, R. A., B. J. Kotick and R. D. Elliot (1967) Polarization analysis of natural and artifically induced geomagnetic micropulsations; J. Geophys. Res., 72, 2871-2883.

Gough, D. I. (1973) The geophysical significance of geomagnetic variation anomalies; Phys. Earth Planet. Interiors, 7, 379-388.

Gough, D. I. (1974) Electrical conductivity under western North America in relation to heat flow seismology and structure; J. Geomag. Geoelect. (in press).

Gough, D. I. and P. A. Camfield (1972) Convergent geophysical evidence of a metamorphic belt through the Black Hills of South Dakota; J. Gephys. Res., 77, 3168-3170.

Gough, D. I., J. H. de Beer and J.S.V. van Zijl (1973) A magnetometer array study in South Africa; Geophys. J. R. astr. Soc., 34, 421-433.

Gough, D. I., F. E. M. Lilley and M. W. McElhinny (1972) A poralization sensitive magnetic variation anomaly in South Australia; Nature 239, 88-89.

Gough, D. I., M. W. McElhinny and F. E. M. Lilley (1974) A magnetometer array study in southern Australia, Geophys. J., 36, 345-362.

Gough, D. I. and H. Porath (1970) Long-lived thermal structure under the Southern Rocky Mountains; Nature, 226, 837-839.

Gough, D. I. and J. S. Reitzel (1967) A portable three-component magnetic variometer; J. Geomag. Geoelect., 19, 203-215.

Gough, D. I. and J. S. Reitzel (1969) Magnetic deep sounding and local conductivity anomalies; The Application of Modern Physics to the Earth and Planetary Interiors, ed. S.K. Runcorn, Wiley-Interscience, London, 139-153.

Haites, T. T. (1959) Avonlea and its significance; J. Alberta Soc. Pet. Geol., 7, 167-176.

Hales, A. L. and E. Herrin (1972) Travel times of seismic waves; The Nature of the Solid Earth; McGraw-Hill, New York.

Hermance, J. F. (1968) Model studies of the coast effects on geomagnetic variations; Can. J. Earth Sci., 5, 515-522.

Herrin, E. and J. Taggart (1968) Regional variation in P travel times; Bull. Seismol. Soc. Am., 58, 1325-1337.

Horner, R. B., A. E. Stevens and H. S. Hasegawa (1973) The Bengough, Saskatchewan, Earthquake of July 26, 1972; Can. J. Earth Sci., 10, 1805-1821.

Hutton, R. (1969) Electromagnetic in the earth by the equitorial electrojet; Nature, 222, 363-364.

Hyndman, R. D. and D. W. Hyndman (1968) Water saturation and high electrical conductivity in the lower continental crust; Earth Planet. Sci. Letters, 4, 427-432.

Jacobs, J. A. (1970) Geomagnetic Micropulsations Physics and Chemistry in Space, 1, Springer-Verlag, New York.

Jones, F. W. and L. J. Pascoe (1972) The perturbation of alternating geomagnetic fields by three-dimensional conductivity inhomogeneities, Geophys. J. R. Astr. Soc., 27, 479-485.

Jones, F. W. and A. T. Price (1970) The perturbation of alternating geomagnetic fields by conductivity anomalies, Geophys. J. R. astr. Soc., 20, 317-334.

King, P. B. (1959) The Evolution of North America; Princeton Press, Princeton U.

Kisabeth, J. L. and G. Rostoker (1971) Development of the polar electrojet during polar magnetic substorms; J. Geophys. Res., 76, 6815-6825.

Kisabeth, J. L. and G. Rostoker (1973) Current flow in auroral loops and surges inferred from ground-based magnetic observations; J. Geophys. Res., 78, 5573-5584.

Lahiri, B. N. and A. T. Price (1939) Electromagnetic induction in non-uniform conductors and the determination of the conductivity of the earth from terrestrial magnetic variations; Phil. Trans. Roy. Soc.; A237, 509-540.

Likiak, E. G. (1971) Buried Pre-Cambrian rocks of South Dakota; Bull. Geol. Soc. Amer,; 82, 1411-1420.

Lilley, F. E. M. and D. J. Bennett (1972) An array experiment with magnetic variometers near the coasts of South-east Australia; Geophys. J. Roy. Astr. Soc., 29, 49-64.

Lilley, F. E. M. and D. J. Bennett (1973) Linear relationships in Geomagnetic variation studies; Phys. Earth Planet. Interiors, 7, 9-14.

Lines, L. R. and F. W. Jones (1973) The perturbation of alternating geomagnetic fields by three-dimensional island structures; Geophys. J. Roy. ast. Soc., 32, 133-154.

Madden, T. R. and C. M. Swift (1969) Magnetotelluric studies of the electrical conductivity structure of the crust and upper mantle; The Earth Crust and Upper Mantle. ed. P. J. Hart; Geophysical Monograph 13, A. G. U., Washington D. C. 469-479.

Mathisrud, G. C. and J. S. Sumner (1967) Underground induced polarization surveying at Homestake Mine; Mining Congress Journal; 53, (3), 66-69.

Milne, W. G. (1967) Earthquake epicentres and strain releases in Canada; Can. J. Earth Sci., 4, 797-814.

Niblett, E. R. and K. Whitham (1970) Multidisciplinary studies of geomagnetic variation anomalies in the Canadian arctic; J. Geomagn. Geoelec, 22, 99-111.

Oldenburg, D. W. (1969) Separation of magnetic substorm fields for mantle conductivity studies in the western United States; M. Sc. Thesis, Department of Physics, University of Alberta, Edmonton, Canada.

Oni, E. and A. O. Alabi (1972) Preliminary results of the upper mantle conductivity structure in Nigeria; Phys. Earth Planet. Interiors, 5, 179-183.

Parkinson, W. D. (1959) Direction of rapid geomagnetic fluctuation; Geophys. J. Roy. astr. Soc., 2, 1-4.

Parkinson, W. D. (1962) The influence of continents and oceans on geomagentic variations; Geophys. J. Roy. astr. Soc., 6, 441-449.

Peltier, W. R. and J. F. Hermance (1971) Magnetotelluric fields of a Gaussian electrojet; Can. J. Earth Sci., 8, 338-346.

Porath, H. (1971) Magnetic variation anomalies and seismic low-velocity zone in the western United States; J. Geophys. Res., 76, 2643-2648.

Porath, H. and A. Dziewonski (1971) Crustal electrical conductivity anomalies in the Great Plains province of the United States; Geophys., 36, 382-395.

Porath, H., D. I. Gough and P. A. Camfield (1971) Conductive structures in the northwestern United States and Southwest Canada; Geophys. J. Roy. astr. Soc., 23, 387-398.

Porath, H., D. W. Oldenburg and D. I. Gough (1970) Separation of magnetic variation fields and conductive structures in the western United States; Geophys. J. R. astr. Soc., 19, 237-260.

Praus, O., J. M. De Laurier and L. K. Law (1971) The extension of the Alert geomagnetic anomaly through northern Ellesmere island Canada; Can. J. Earth Sc., 8, 50-64.

Presnall, D. G., C. L. Simmons and H. Porath (1972) Changes in electrical conducvitiy of a synthetic basalt during melting; J. Geophys. Res., 77, 5665-5672.

Price, A. T. (1950) Electromagnetic induction in a semi-infinite conductor with a plane boundary; Quart. J. Mech. Appl. Math., 2, 283-310.

Price, A. T. (1962) The theory of magnetotelluric fields when the source field is considered; J. Geophys. Res., 67, 1907-1918.

Rankin, D. (1962) The magnetotelluric effect on a dike; Geophys., 27, 666-676.

Rankin, D. and I. K. Reddy (1973) Crustal conductivity anomaly under the Black Hills: A magnetotelluric study; Earth and Planet. Sci. Letters, 20, 275-279.

Reitzel, J. S., D. I. Gough, H. Porath and C. W. Anderson (1970) Geomagnetic Deep Sounding and upper mantle structure in the western United States; Geophys. J. R. astr. Soc., 19, 213-235.

Rikitake, T. (1950a) Electromagnetic induction within the Earth and its relation to the electrical state of the Earth's interior part I; Bull. Earthq. Res. Inst. Tokyo, 28, 45-100.

Rikitake, T. (1950b) Electromagnetic induction within the Earth and its relation to the electrical state of the Earth's interior part II; Bull. Earthq. Res. Inst. Tokyo, 28, 219-262.

Rikitake, T. (1966) Electromagnetism and the Earth's Interior; Elesvier, Amsterdam.

Rikitake, T. and Y. Honkura (1973) Recent Japanese studies on conductivity anomalies; Phys. Earth Planet. Interiors; 7, 203-213.

Rikitake T. and K. Whitham (1964) Interpretation of the Alert anomaly in geomagentic variations; Can. J. Earth Sci., 1, 35-62.

Rokityanskiy, I. I. and I. M. Logvinov (1972) An electrical conductivity anomaly on the Kirovograd block of the Ukranian Shield; Izv. Physics. of Solid Earth, 6, 104-110.

Rokityanskiy, I. I., I. M. Logvinov and N. A. Luginina (1969) Magnetovariational profiling of the Ukranian shield: Izv. Physics, of Solid Earth, 3, 196-199.

Rostoker, G. (1972) Polar magnetic substorms: Rev. Geophys. Space Phys.; 10, 157-211.

Roy, R. F., D. D. Blackwell and E. R. Decker (1972) Continental heat flow; The Nature of Solid Earth, ed. E. C. Robertson, McGraw-Hill, 506-543.

Sass, J. H., A. H. Lachenbruch, R. J. Munroe, G. W. Green and T. H. Moses, Jr.; Heat flow in the western United States, J. Geophys. Res., 76, 6376-6413.

Schmucker, U. (1964) Anomalies of geomagnetic variations in the southwestern United States; J. Geomag. Geoelect.; 15, 193-221.

Schmucker, U. (1970) Anomalies of geomagnetic variations in the southwestern United States; Bull. Scripps Inst. Oceanography, 13, 1-165, Univ. California, San Diego.

Schmucker, U., S. E. Forbush, O. Hartmann, A. A. Giesecke, M. Casaverde, J. Castillo, R. Salgueiro and S. del Pozo (1967) Electrical conducticity anomaly under the Andes. Annual Report Dept. Terrestrial Magn., Carnegie Inst. of Washington, 11-28.

Schuster, A. (1889) The diurnal variation of the terrestrial magnetism; Phil. Trans. Roy. Soc., A180, 467-518.

Stockwell, C. H. (1962) A tectonic map of the Canadian shield; Roy. Soc. Can. Special Publ., 4, 6-15.

Summers, D. M. and J. T. Weaver (1973) Electromagnetic induction in stratified conducting Half-Space by an Arbitrary Periodic Source; Can. J. Phys., 51, 1064-1074.

Tozer, D. C. (1959) The electrical properties of the earth's interior; in: L. H. Ahrens, F. Press, K. Rankama and S. K. Runcorn (Editors), Physics and Chemistry of the Earth, Pergamon, London, 3, 414-436.

Vozoff, K., A. Orange and H. S. Lahman (1969) Magnetotelluric deep earth resistivity at eight U. S. "type locations"; Final Report for contract Nonr. 4900(06) N.R. 081-25/3-23-65, Goescience Inc., Cambridge, Mass.

Vozoff, K. and C. M. Swift (1968) Magnetotelluric measurements in the North German basin; Geophys. Prospect., 16, 454-473.

Weaver, J. T. (1963) The electromagnetic field within a discontinuous conductor with reference to geomagnetic micropulsations near a coastline, Can. J. Phys., 41, 484-495.

Weaver, J. T. (1973) Induction in a layered plane-earth by uniform and non-uniform souce fields; Phys. Earth Planet. Interiors, 7, 266-281.

Weaver, J. T. and D. J. Thomson (1972) Induction in a non-uniform conducting half-space by an external line current; Geophys. J. R. astr. Soc., 28, 163-185.

Wiens, R. G. and G. Rostoker (1973); Ground based magnetic signatures of the phases of magnetospheric substorms - a reconciliation; EOS, Trans. Amer. Geophys. Union, 54, 412.

Wiese, H. (1962) Geomagtische Tiefentellurik Teil II: Die Streichrichtung der Utergrundstrukturen des electrischen Widerstandes, erschlossen aus geomagnetischen variationen; Geofisica pura e applicate; 52, 83-103.

Whitham, K. (1964) Anomalies in geomagnetic variations in the arctic archipelago of Canada; J. Geomag. Geoelect., 15, 227-240.

Whitham, K, and F. Andersen (1965) Magnetotelluric experiments in northern Elesmere island; Gephys. J., 4, 317-345.

Wright, J. A. (1969) The magnetotelluric and geomagnetic response of two dimensional structures; GAMMA (Inst. Geophysik Meteorogic Tech. Univ. Braunschweig) 7, 102 pp.

APPENDICES

APPENDIX A

Locations and the names of the magnetometer stations. The magnetic declinations of these stations are also given.

Line	Station Code Name	Station Name	Latitude Degree N	Longitude Degree W	Magnetic Declination Degree E
1	NWY	Norway House	54.0	97.8	10.2
1	CRN	Cranberry	54.5	101.4	14.3
1	BIG	Big Sandy	54.4	104.2	17.2
1	MEA	Meadow Lake	54.2	108.5	20.3
1	MNK	Meanook	54.6	113.3	23.6
2	MAF	Mafeking	52.7	101.1	13.5
2	MIS	Mistatim	52.9	103.4	15.8
2	STL	St. Louis	52.9	105.8	17.8
2	BAT	Battleford	52.7	108.4	19.5
3	ROB	Roblin	51.4	101.4	13.4
3	RAY	Raymore	51.5	104.5	16.2
3	OUT	Outlook	51.5	107.1	18.0
3	BRC	Brock	51.5	108.7	19.1
4	WPG	Winnipeg	49.6	97.1	8.7
4	NEE	Neepawa	50.2	99.5	11.3

Line	Station Code Name	Station Name	Latitude Degree N	Longitude Degree W	Magnetic Declination Degree E
4	MOO	Moosomi	50.2	101.7	13.2
4	QUA	Quappelle	50.5	103.9	15.2
4	MOR	Mortlach	50.5	106.1	16.8
4	SWI	Swift Current	50.3	107.8	18.3
5	RUG	Rugby	48.4	100.0	10.2
5	STA	Stanley	48.2	102.4	13.4
5	CUL	Curlbertson	48.2	104.5	14.9
5	GLS	Glasgow	48.3	106.6	16.3
5	MAL	Malta	48.2	108.2	17.1
6	IPS	Ipswich	45.5	99.3	10.2
6	WAK	Walker	45.9	101.2	12.0
6	RDR	Reeder	46.1	102.9	13.2
6	BKR	Baker	46.4	104.2	14.1
6	MIL	Miles City	46.5	105.8	15.0
6	MEL	Melstones	46.6	108.0	16.5

Line	Station Code Name	Name	Latitude Degree N	Longitude Degree W	Magnetic Declination Degree E
7	PUK	Pukwana	43.8	99.1	10.2
7	KAD	Kadoka	43.9	101.5	11.8
7	WIC	Wicksville	44.0	102.6	12.6
7	CUS	Custer	43.8	103.5	13.1
7	UPT	Upton	44.0	104.5	13.6
7	GIL	Gillette	44.1	105.5	14.2
7	TEN	Ten Sleep	44.0	107.4	15.2
8	TAY	Taylor	41.7	99.6	10.3
8	HYN	Hyannis	42.0	102.0	11.8
8	BRI	Bridge Port	41.7	103.2	12.5
8	CHU	Chugwater	41.8	104.9	13.3
8	RAW	Rawlings	41.8	107.3	14.5

APPENDIX B

The Source of Polar Magnetic Substorm Fields

THE SOURCE OF POLAR MAGNETIC SUBSTORM FIELDS

Polar substorm events are large amplitude magnetic disturbances associated with three-dimensional current systems that flow in association with complicated processes involving solar wind-magnetosphere interactions. The current flows down along the magnetic field lines from the magnetotail in the equatorial plane to the ionosphere at the latitudes of the auroral zone and back up the field lines into the magnetotail. (Bonnevier, Bostrom and Rostoker, 1970). A model of a three-dimensional current system is illustrated in Fig. B-1. The field aligned (Birkeland) parts of the current are almost vertical and give rise mainly to assymmetric D-field (Rostoker, 1972). The ionospheric part of the current (electrojet) usually flows westward in the midnight sector to produce $-\Delta H$ on the ground. At times strong eastward electrojet flows in a region further west of the westward electrojet (in the post-noon and evening sectors) to produce $+\Delta H$. Usually both the eastward and westward electrojets co-exist with the eastward jet being considerably weaker (Kisabeth and Rostoker, 1973).

The location of the axis of the electrojet is obtained as the locus of points along which the Z variation field is zero with Z being positive to the north and negative south of the axis. The longitudinal extent of the electrojet can be

Fig. B-1 An illustration of a three-dimensional current system responsible for polar magnetic substorm fields. (Dr. G. Rostoker's permission to reproduce this diagram is acknowledged with thanks).

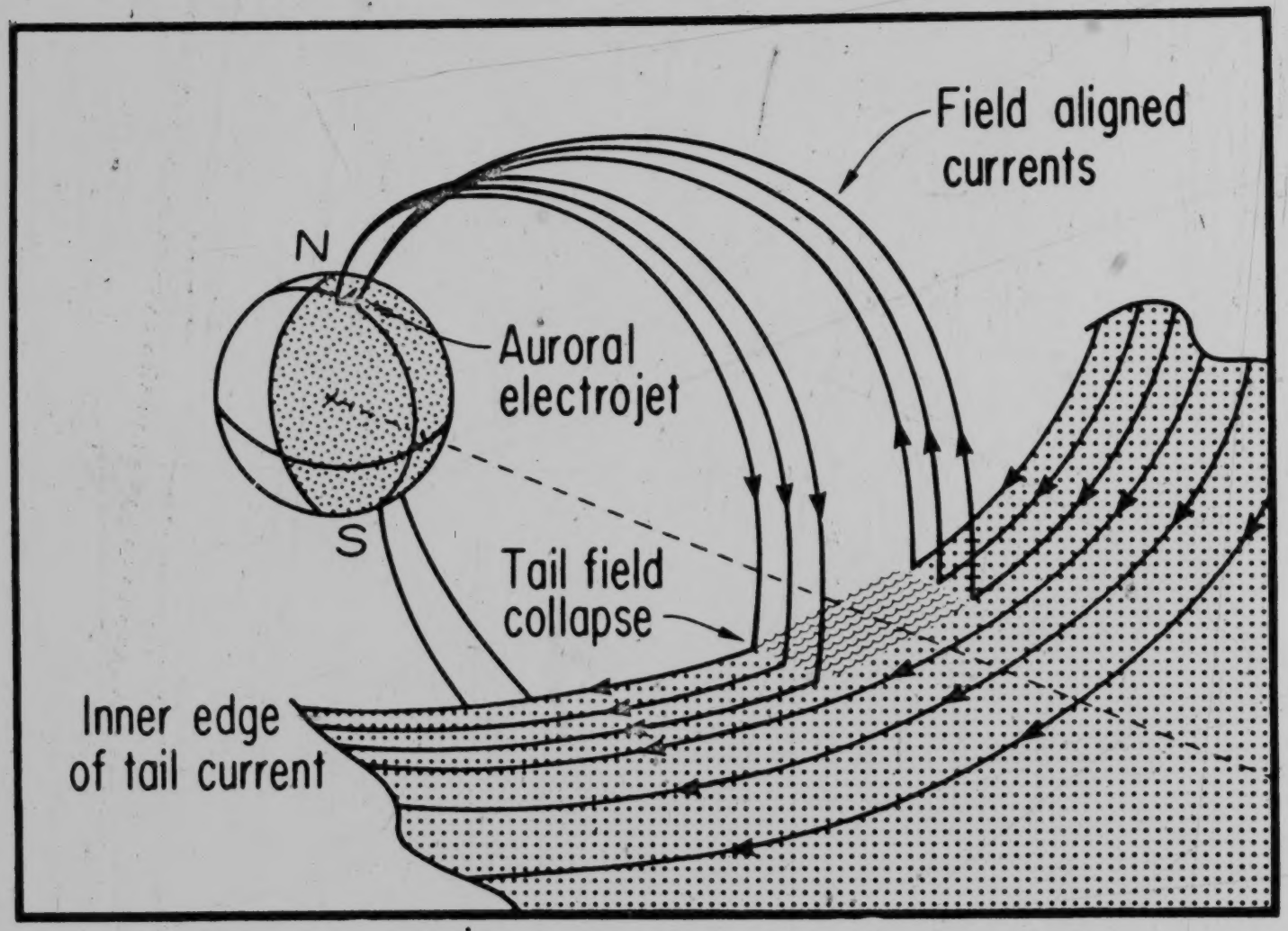
Field aligned
currents
N
Auroral
electrojet
S
Tail field
collapse
Inner edge
of tail current

determined from the D variation field which takes opposite signs near either end of the current system. The H and Z components of the substorm current system have considerable north-south spatial gradient while the D has less north-south spatial gradient.

On the account of improved coverage of ground observation with magnetometers, the recent picture of the substorm current systems is more complicated than the simplified version given above. For example, it is now believed that a sequence of current systems are usually developed at the northern edge of a pre-existing one (Kisabeth and Rostoker, 1971; Wiens and Rostoker, 1973). Thus, the substorm events may now be attributed to a sequence of three-dimensional current systems. In geomagnetic induction work in a region close to the auroral zone, the investigator is mainly concerned with approximate location of the current axis and Birkeland currents, and with the length of the electrojet. Close to the ionospheric-magnetospheric source currents, many irregularities are observed in the magnetograms of the variation fields.

In this study, magnetograms collected from a world-wide network of standard observatories by Space Physics workers of the University of Alberta were examined to locate the axis and the length of the electrojet for the substorm events analyzed. The classification of the events into types was also based on this examination. Fig. B-2 shows the locations of the stations whose magnetograms were examined.

Fig. B-2 The standard observatories whose magnetograms were examined for classification of the events analyzed in this thesis and for the parameters of the electrojet currents that are responsible for the substorms events.

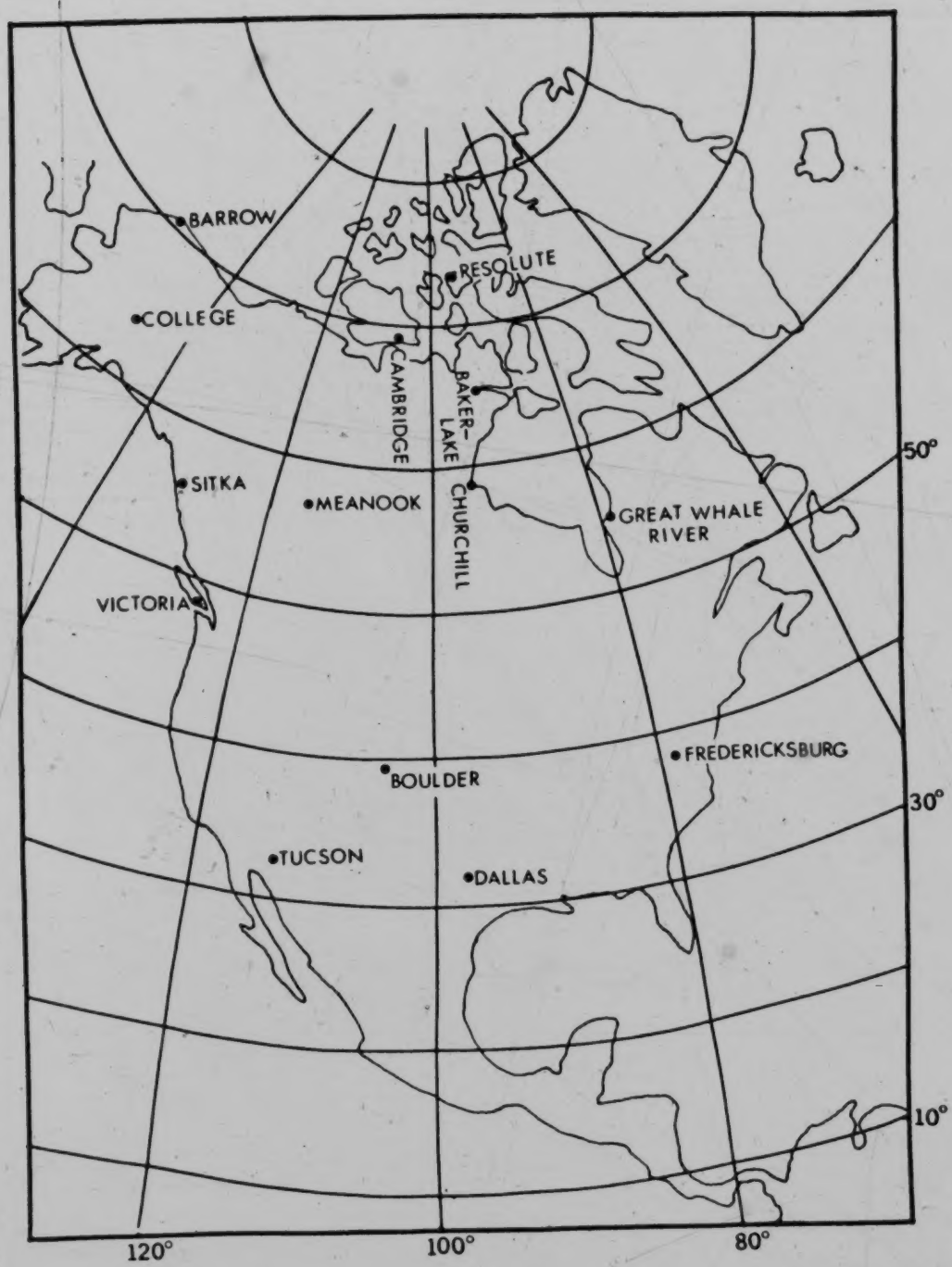
BARROW
RESOLUTE
COLLEGE
CAMBRIDGE
BAKER-LAKE
SITKA
MEANOOK
CHURCHILL
GREAT WHALE RIVER
VICTORIA
FREDERICKSBURG
BOULDER
TUCSON
DALLAS
50°
30°
10°
120°
100°
80°

Low latitude stations of GUAM (15°N, 144°E) HONOLULU (21.3°N, 158°W) and SAN JUAN (31°S, 69°W) not shown in Fig. B-2 were also among the observatories whose magnetograms were studied. The sparse distribution of the stations gives only semi-qualitative information about the source fields.